

NATIONAL ADVISORY COMMITTEE FOR AERONAUTICS

LNACA
CONFERENCE ON THE TURBOJET ENGINE FOR SUPERSONIC
AIRCRAFT PROPULSION

(A COMPILATION OF THE PAPERS PRESENTED)

Lewis Flight Propulsion Laboratory
Cleveland, Ohio

CLASSIFICATION CHANGED
UNCLASSIFIED

TO _____ July 11, 1951

By Authority of Automatic Date 2-2-65

Downgrading Stamp

GROUP 4
Downgraded at 5 year
intervals; declassified
after 12 years



N 66-16280

GPO PRICE \$ _____

CFSTI PRICE(S) \$ _____

(ACCESSION NUMBER)

(PAGES)

(NASA CR OR TMX OR AD NUMBER)

(THRU)

(CODE)

(CATEGORY)

Hard copy (HC) 5.00

Microfiche (MF) 1.00

ff 653 July 65

TMX#

1

DECLASSIFIED
[REDACTED]

NACA CONFERENCE
ON
THE TURBOJET ENGINE FOR SUPERSONIC
AIRCRAFT PROPULSION
A COMPILATION OF THE PAPERS PRESENTED

Lewis Flight Propulsion Laboratory
Cleveland, Ohio

July 11, 1951

GROUP 4
Downgraded at 3 year
intervals; declassified
after 12 years

[REDACTED]



LIST OF CONFEREES

The following conferees were registered at the NACA conference on The Turbojet Engine for Supersonic Aircraft Propulsion, Lewis Flight Propulsion Laboratory, Cleveland, Ohio, July 11, 1951:

Abbott, I. H.	NACA - Washington
Ahern, R. I.	Wright Air Development Center
Alford, J. S.	General Electric
Angell, P. T.	Thompson Products
Arnold, J. E.	Consolidated Vultee
Barfield, Capt. H.	Wright Air Development Center
Barnard, D. P.	Standard Oil of Indiana
Bartlett, P. M.	Bureau of Aeronautics
Bell, E. B.	Wright Air Development Center
Blose, D. H.	Wright Air Development Center
Bowman, R. G.	Republic Aviation
Brown, W. J.	Wright Air Development Center
Buhler, R. D.	University of California
Bullock, R. O.	NACA - Lewis
Campbell, K.	Wright Aeronautical
Canavan, Lt. Cmdr. D.	Dept. of Navy
Carhart, T. P.	Wright Air Development Center
Carmichael, R. P.	Wright Air Development Center
Carr, D. E.	Phillips Petroleum
Cesaro, R. S.	NACA - Washington
Cetrone, V. C.	Sperry Gyroscope
Chamberlin, R. B.	Wright Air Development Center
Chandler, M. E.	Niles-Bement-Pond
Chenoweth, O.	Wright Air Development Center
Clark, D. B.	Wright Aeronautical
Collins, J. H.	NACA - Lewis
Collins, W.	Continental Aviation
Comenzo, R.	NACA - Langley
Condra, Capt. E. M.	Bureau of Aeronautics
Conrad, E. W.	NACA - Lewis
Cortright, E. M.	NACA - Lewis
Crowley, J. W.	NACA - Washington
Cummings, R. E.	Thompson Products
Curry, W. H.	Los Alamos Scientific Lab.
Dale, J. R.	Strategic Air Command
Daley, J. A.	NAMC - Philadelphia
Davis, F. W.	Consolidated Vultee
Davis, W. F.	NACA - Ames



DECLASSIFIED

INTRODUCTION

This volume contains copies of the technical papers presented at the NACA conference on The Turbojet Engine for Supersonic Aircraft Propulsion on July 11, 1951 at the Lewis Flight Propulsion Laboratory. A list of the conferees, who are members of the aircraft industry and the military services, is included.

The original presentation and this record are considered supplementary to, rather than substitutes for, the Committee's system of complete and formal reports.

NATIONAL ADVISORY COMMITTEE
FOR AERONAUTICS

DECLASSIFIED
CONTENTS

INTRODUCTION

LIST OF CONFEREES

TECHNICAL DISCUSSIONS:

I - ENGINE CHARACTERISTICS

1. INTRODUCTION AND COMMENTS Ia
By Bruce T. Lundin
2. ANALYSIS OF TURBOJET-ENGINE CHARACTERISTICS FOR
SUPERSONIC PROPULSION
By David S. Gabriel
3. COMMENTS Ib
4. TURBOJET THRUST AUGMENTATION FOR SUPERSONIC PROPULSION
By William A. Fleming and E. William Conrad
5. COMMENTS Ic
6. SOME NOTES ON ENGINE-COMPONENT RESEARCH
By Robert O. Bullock
7. COMMENTS Id
8. TURBOJET-ENGINE CONTROL SYSTEMS IN SUPERSONIC FLIGHT
By John C. Sanders

II - ENGINE INSTALLATION

9. INTRODUCTION AND COMMENTS IIa
By Demarquis D. Wyatt
10. EFFECT OF BOUNDARY-LAYER CONTROL ON PERFORMANCE OF SIDE
INLETS AT SUPERSONIC SPEEDS
By Edgar M. Cortright
11. COMMENTS IIb
12. EFFECTS OF INLET DESIGN ON PERFORMANCE OF TURBOJET-ENGINE
INSTALLATIONS
By Roger W. Luidens and Fred T. Esenwein
13. COMMENTS IIc
14. THRUST CHARACTERISTICS OF AN EJECTOR PUMP
By H. Dean Wilsted

03:11:45:30

Degutis, A. J.	Wright Air Development Center
DeRoze, L.	Air Technical Intelligence Center
Diehl, Capt. W. S.	NACA - Subcommittee
Dietz, R. O.	ARO, Inc.
Drell, H.	Lockheed Aircraft
Dryden, Dr. H. L.	NACA - Washington
DuBois, Capt. J. M.	NACA Liaison Office
Duncan, Cmdr. R. L.	Office of Naval Research
Dunham, S. W.	Wright Air Development Center
Ellis, C. B.	Oak Ridge National Laboratory
Ellisman, C.	NAMTC, Point Mugu
Enders, W. H.	Massachusetts Inst. of Technology
Erwin, J. R.	NACA - Langley
Esenwein, F. T.	NACA - Lewis
Evvard, J. C.	NACA - Lewis
Faget, M. A.	NACA - Langley
Fennema, F.	Offutt Air Force Base
Findley, H.	Eaton Manufacturing
Fischer, L. J.	General Electric
Flader, D. F.	Fredric Flader
Flader, F.	Fredric Flader
Fleming, W. A.	NACA - Lewis
Forry, J. E.	Bureau of Aeronautics
Foster, R. B.	Bell Aircraft
Fraas, A. P.	Oak Ridge National Laboratory
Franks, R.	Union Carbide & Carbon
Gabriel, D. S.	NACA - Lewis
Garner, Capt. C.	Wright Air Development Center
Glaus, R.	Minneapolis-Honeywell
Glodeck, E.	Research & Development Board
Green, A. W. F.	Allison
Greenstreet, M. E.	Battelle Memorial Inst.
Gregory, A. T.	Ranger Aircraft
Grenoble, H. E.	General Electric
Guttmann, K.	Research & Development Board
Haaser, Capt. W. L.	Wright Air Development Center
Hadfield, Lt. Col. E. S.	Wright Air Development Center
Hall, Lt. Col. E. N.	Wright Air Development Center
Hall, J.	NACA - Lewis
Hall, R. S.	General Electric
Hardgrave, E. J.	Johns-Hopkins
Hasert, C.	USAF - Washington
Haugen, Col. D. R.	USAF - Washington
Hazen, R. M.	Allison

DECLASSIFIED

Heaton, Lt. Col. D. H.	USAF, ARDC - Baltimore
Hedrick, W. S.	Sverdrup & Parcel
Herald, J. M.	Wright Air Development Center
Holaday, W. M.	Socony-Vacuum
Hrebec, Capt. G. M.	Strategic Air Command
Hunter, W. H.	NACA - Lewis
Hurley, W. V.	General Electric
Jarrett, A. L.	Chance-Vought
Jonas, J.	Northrop Aircraft
Jordan, D. J.	Pratt & Whitney
Karanik, J.	Grumman Aircraft
Kartveli, A. A.	Republic Aviation
Keating, T. J.	Wright Air Development Center
Kelso, Capt. W. R.	Edwards Air Force Base
Kemper, C.	NACA - Lewis
Kinney, R. W.	Wright Air Development Center
Klein, E. L.	Research & Development Board
Klepinger, R. H.	Wright Air Development Center
Kotcher, Lt. Col. E.	Wright Air Development Center
Kuhrt, W. A.	United Aircraft
Lamar, W. E.	Wright Air Development Center
Lancaster, O. E.	Bureau of Aeronautics
Larsen, H.	AAF Institute of Technology
Laucher, R. G.	McDonnell Aircraft
Lawrence, W. C.	American Airlines
Lawson, G. W.	General Electric
Lazar, J.	NACA - Washington
Lee, J. G.	United Aircraft
Lewis, R. B.	Wright Aeronautical
Littell, R. E.	NACA - Washington
Long, M. E.	David Taylor Model Basin
Louden, F. A.	Bureau of Aeronautics
Luidens, R. W.	NACA - Lewis
Lundin, B. T.	NACA - Lewis
Luskin, H.	Douglas Aircraft
McCarthy, J. S.	McDonnell Aircraft
Maloney, J. G.	Consolidated Vultee
Maloney, R. E.	Wright Air Development Center
Manganiello, E. J.	NACA - Lewis
Marwood, R. M.	Solar Aircraft
Maske, E. B.	Consolidated Vultee
Matzdorf, R. E.	Consolidated Vultee
Meehan, D. L.	Douglas Aircraft

CONFIDENTIAL

Melrose, G.	Bell Aircraft
Mercer, J.	United Aircraft
Michaels, C. M.	Wright Air Development Center
Miller, H.	ARO, Inc.
Mock, F. C.	Bendix Aviation
Mullaney, R.	Grumman Aircraft
Myers, D. D.	North American Aviation
Nay, Col. P. F.	Wright Air Development Center
Neill, T. T.	NACA - Washington
Nichols, M. R.	NACA - Langley
Niewald, R. J.	NACA - Washington
Norman, Col. H. H.	USAF - Langley
Oates, C.	Chance-Vought
Olmsted, P. B.	Bureau of Aeronautics
Olson, W. T.	NACA - Lewis
Parke, D. B.	McDonnell Aircraft
Parkins, W. A.	Pratt & Whitney
Pierce, E. F.	Wright Aeronautical
Pierce, E. W.	Douglas Aircraft
Pinkel, B.	NACA - Lewis
Pinnes, R. W.	Bureau of Aeronautics
Powell, J. L.	Bureau of Aeronautics
Prachar, O. P.	Allison
Pratt, P. W.	Pratt & Whitney
Prouty, Maj. R. V.	USAF - Langley
Retz, R. H.	Wright Air Development Center
Robbins, Maj. H. W.	NACA Liaison Officer - Cleveland
Rock, E. A.	Boeing Airplane
Rogers, Milton	Naval Ord.
Ross, Lt. Col. D. M.	Wright Air Development Center
Rothrock, A. M.	NACA - Washington
Rubert, K. F.	NACA - Langley
Samaras, D. G.	Wright Air Development Center
Sanders, J. C.	NACA - Lewis
Sanders, N. D.	NACA - Lewis
Savage, C. A.	Consolidated Vultee
Schey, O. W.	NACA - Lewis
Schiller, E.	Glenn L. Martin
Schloesser, V. V.	Westinghouse
Schumaker, W. A.	Wright Air Development Center
Scott, R. L.	NAMC - Philadelphia
Sea, A. L.	Wright Air Development Center
Sens, W. H.	Pratt & Whitney
Sharp, E. R.	NACA - Lewis

CONFIDENTIAL

DECLASSIFIED

Shine, A. J.	AAF Institute of Technology
Shore, D.	Wright Air Development Center
Silverstein, A.	NACA - Lewis
Simpson, Capt. E. C.	Wright Air Development Center
Smith, Maj. R. O.	Wright Air Development Center
Smith, N. D.	NACA - Langley
Sorgen, C. C.	Bureau of Aeronautics
Steinhoff, E. A.	Holloman Air Force Base
Stirgwalt, T.	General Electric
Stranges, P.	Air Technical Intelligence Center
Sylvander, R. C.	Eclipse-Pioneer
Tanczas, F. T.	Nat. Military Establishment
Taylor, E. S.	Massachusetts Inst. of Technology
Taylor, B. L.	North American Aviation
Taylor, Maj. J. E.	Wright Air Development Center
Towle, H.	Republic Aviation
Tuzen, Maj. J. B.	Wright Air Development Center
Ullman, G.	NACA - Washington
Underwood, W. J.	NACA Liaison Officer - Dayton
Van Valkenburgh, L. D.	Fairchild
Wascher, W. L.	Wright Air Development Center
Wasielewski, E. W.	NACA - Lewis
Watson, Col. H. E.	Air Technical Intelligence Center
Wein, K. L.	Wright Air Development Center
Weitzen, W.	USAF - Washington
Wetzler, J. M.	Allison
Wheelahan, Lt. Cmdr. J. E.	Bureau of Aeronautics
White, R. S.	CAA - Washington
Williams, Lt. Col. F. W.	Sverdrup & Parcel
Wilson, R. G.	North American Aviation
Wilsted, H. D.	NACA - Lewis
Wiseman, H. E.	Offutt Air Force Base
Wislicenus, G. F.	Johns-Hopkins
Woeste, W. J.	Wright Air Development Center
Woodworth, L. R.	Rand Corp.
Wyatt, D. D.	NACA - Lewis
Young, M. H.	Wright Aeronautical
Young, R. W.	Reaction Motors


DECLASSIFIED

1. INTRODUCTION AND COMMENTS Ia

By Bruce T. Lundin



SECRET

1. - INTRODUCTION AND COMMENTS Ia

By Bruce T. Lundin

2235
The first paper summarizes the results of an analytical investigation that had as its objective the establishment of the most suitable design characteristics of a turbojet engine for supersonic propulsion. This analysis, which will indicate the type or kind of components required in the engine and determine their optimum operating conditions, will thus serve as a general basis for review of the research investigations to be presented in subsequent papers.

The suitability or merit of any aircraft power plant is, of course, highly dependent upon the characteristics of the airplane in which it is installed and on the particular propulsion requirements of that airplane. Any analysis of aircraft propulsion systems must, therefore, be properly and completely integrated both with the type or configuration of airplane and with the particular flight plan of the airplane if significant results are to be obtained. This close alliance or interrelation among the characteristics of the propulsion system, the aircraft type, and the flight plan not only precludes perfect generality of results but also necessitates the selection of particular cases for investigation. The various airplane configurations and flight plans selected for the present analysis are not considered necessarily optimum but were chosen after some study in a manner that is believed to be fairly representative of some current practices and that will provide a useful and realistic evaluation of at least the trends and relative importance of the various propulsion system variables.

Two different types of aircraft were considered, a high-altitude interceptor and a bomber. The particular flight plan selected for the interceptor aircraft is illustrated in figure 1. As indicated in this figure, two different combat flight speeds at an altitude of 50,000 feet were selected, one at a Mach number of 1.35 and the other at a Mach number of 1.80. Both aircraft were considered as reaching this combat flight condition by acceleration to a Mach number of 0.8 at low altitude, climb to 35,000 feet at this Mach number, and then acceleration to full design speed at 35,000 feet. Climb to the combat altitude is then made at the design Mach number, either 1.35 or 1.80. It was further required that both aircraft be capable of sustaining continuously a 2-g maneuver at the combat condition without loss in speed or altitude. A pay load of 3000 pounds was assumed, and, based on a preliminary study of the effects of gross weight, a take-off gross weight of 40,000 pounds was chosen.

For the supersonic bomber the exact flight path varied somewhat depending on the characteristics of the propulsion system under study, but all bombers were assumed to have a supersonic flight radius of

SECRET



03:19:15:00:30

500 miles at a Mach number of 1.5, with the bomb drop occurring at an altitude of 50,000 feet. The flight speed beyond the 500-mile supersonic radius of action was at a Mach number of 0.9. The bomber has an initial gross weight of 150,000 pounds and carries a pay load of 10,000 pounds.

Evaluation of the various propulsion systems for the bomber aircraft is made on the basis of the total flight range. For the fixed-flight plan of the interceptor aircraft, the various airplane performance factors such as take-off distance, rate of climb, time to combat, and combat endurance were evaluated and compared. It is to be noted that no loiter or hold time at low altitude is provided in this flight plan because the incorporation of such requirements would severely penalize the combat capabilities of the airplane. A loiter time may, however, be included at subsonic speeds and at moderate altitudes without appreciably altering the general trends and comparisons indicated by the analysis.

The configurations selected for the interceptor aircraft are representative of fairly conventional design. A model illustrating the general configuration of the airplane for a flight Mach number of 1.35 is shown in the photograph of figure 2 and the airplane for a flight Mach number of 1.80 is shown in figure 3. For both flight speeds, two types of engine installation were included, a submerged installation and a nacelle installation. For the submerged installation (figs. 2 and 3), the airplane was powered by a single engine installed in the aft part of the fuselage and for the nacelle installation, shown in figure 4 for a flight Mach number of 1.80, the airplane was powered by two engines installed in nacelles at the wing tips.

After the combat condition of each type of airplane was established according to the flight plan, the thrust required by the propulsion system was fixed. Various operating conditions and air-flow capacities of the components making up an engine capable of providing this thrust were then established, with due allowance for variations in weight and drag of the complete airplane, and the airplane performance over the complete flight plan was determined. The principal engine variables studies are as follows: the compressor pressure ratio, the compressor efficiency, the air flow per unit of frontal area, the turbine-inlet temperature, the afterburner discharge temperature, and the basic engine weight. Variations in each of these variables resulted, of course, in different sizes and weights of the power plants producing the required thrust that were integrated into the aerodynamic characteristics of the airplane. For example, variations in the pressure ratio of the compressor resulted in changes in engine weight and size that were associated with changes in engine drag, fuselage size, fuel load, wing loading, and so forth. The design point of the power plant was assumed to be the combat condition; each engine therefore operated at off-design conditions over different portions of the flight plan.



3
2235-1
DECLASSIFIED

INTERCEPTOR FLIGHT PLAN

2g COMBAT MANEUVERABILITY
40,000 LBS. T.O. GROSS WEIGHT

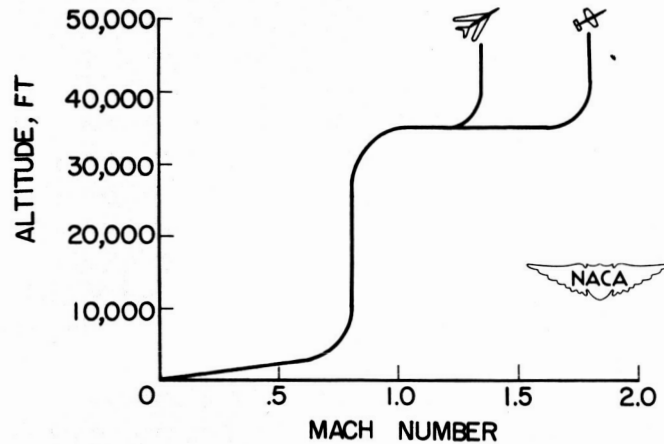


Figure 1

INTERCEPTOR AIRPLANE WITH SUBMERGED ENGINES FOR 1.35 FLIGHT MACH NUMBER

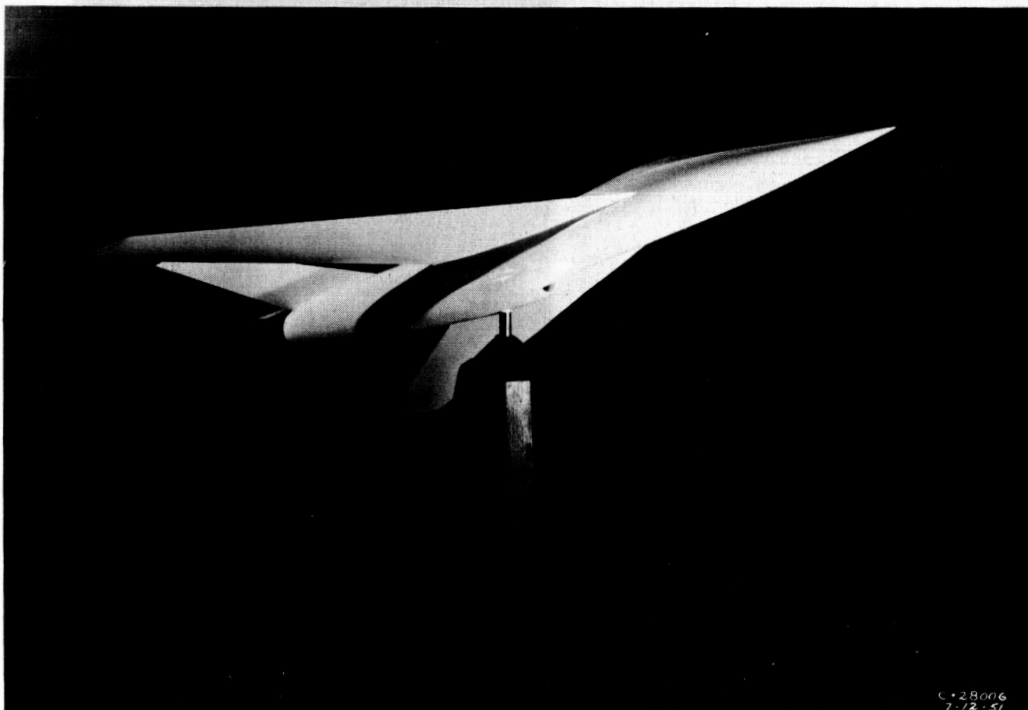


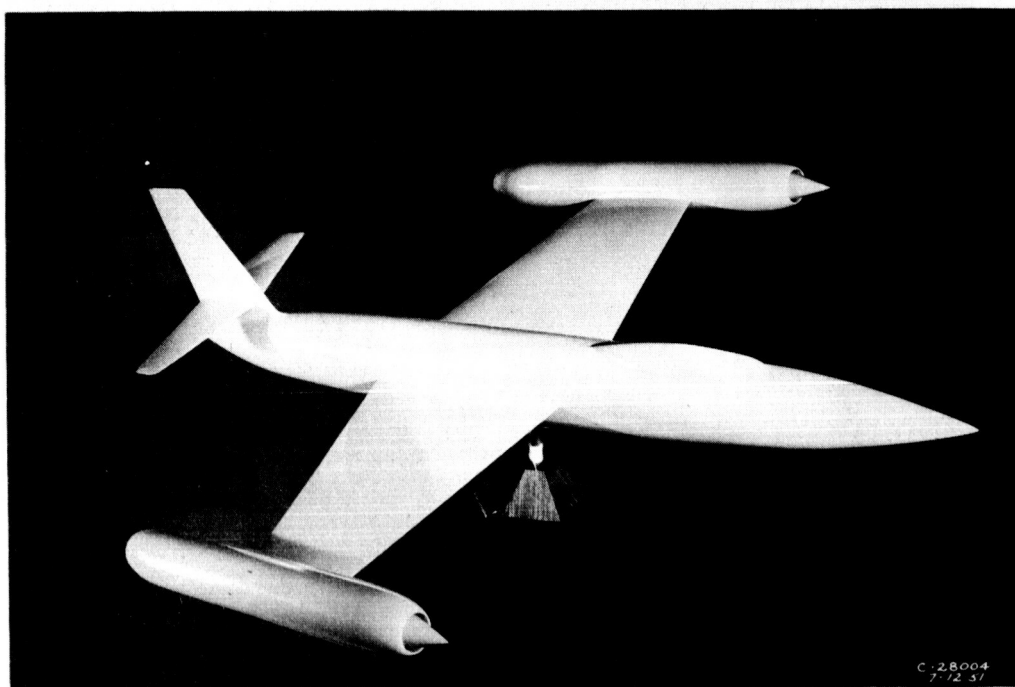
Figure 2

~~CONFIDENTIAL~~
INTERCEPTOR AIRPLANE WITH SUBMERGED ENGINES
FOR 1.80 FLIGHT MACH NUMBER



Figure 3

INTERCEPTOR AIRPLANE WITH NACELLE - INSTALLED
ENGINES FOR 1.80 FLIGHT MACH NUMBER



~~CONFIDENTIAL~~


DECLASSIFIED

2. ANALYSIS OF TURBOJET-ENGINE CHARACTERISTICS FOR
SUPERSONIC PROPULSION

By David S. Gabriel

SECRET

2. - ANALYSIS OF TURBOJET-ENGINE CHARACTERISTICS

FOR SUPERSONIC PROPULSION

By David S. Gabriel

The performance of the various interceptor airplanes was computed for each part of the flight plan as outlined in the INTRODUCTION and COMMENTS. The airplane-performance variables investigated for all the engine-design conditions considered in the analysis were: take-off distance, time to reach the combat condition, loitering fuel consumption, and combat time. Examination of the results showed that the take-off distance, loitering fuel consumption, and time to reach the combat, were uniformly good for all engine-design variables investigated; for example, for the 1.35 Mach number designed airplanes, take-off distance varied from 1000 to 3000 feet, loitering fuel consumption was approximately one-tenth the combat fuel consumption, and time to reach the combat condition was from 4 to 6 minutes. The combat time was therefore selected as the figure of merit for airplane performance. The combat times were computed for complete consumption of the available fuel.

In the analysis the effects on airplane performance of independently varying the engine design variables were first examined. No final conclusions can be drawn from these results because in actual engine designs, a change in one engine design results in associated changes in other variables. The result of these interrelated variations will be discussed later, but first some of the results of the general analysis will be shown:

The optimum amount of afterburning required for the interceptor was determined initially. Combat time for a nacelle-type airplane is shown in figure 1 as a function of the afterburner outlet temperature. The curves are for a design-flight Mach number of 1.35, a sea-level rated-compressor pressure ratio of 5.0, a peak compressor efficiency of 0.85, and an air flow per unit compressor-frontal area of 30 pounds per second per square foot. The rated pressure ratio is defined at sea level and flight Mach number of 0. The actual operating compressor pressure ratio varies with flight conditions. Curves are shown for specific engine weights (that is, the engine weight per unit of thrust without afterburning at sea level and flight Mach number of 0) of 0.3 and 0.4. For these conditions for a given engine weight, the combat time apparently optimizes at an afterburner temperature less than maximum temperature; for example, for an engine weight of 0.4 the afterburner temperature for optimum combat time is about 3100° R. The existence of this optimum may best be explained by tracing the engine and airplane changes as the afterburner outlet temperature increases. Starting at the condition for no afterburning, the engine has low specific fuel consumption but also has

SECRET

[REDACTED]

[REDACTED]

[REDACTED]

SECRET

2-3

effects are important because of the influence on the airplane performance in several ways. A decrease in efficiency reduces the thrust per pound of air flow and therefore a larger engine is required for a given flight condition. A larger engine means more drag and engine weight; hence, less fuel is available. At the same time specific fuel consumption increases. These three effects are all unfavorable and add up to large reductions in airplane performance.

An important element in the interacting effects of thrust per pound of air flow and specific fuel consumption was the pressure drop due to afterburning or momentum pressure drop. This pressure drop was directly related to the afterburner-inlet velocity, and in fact increased with approximately the square of the velocity. A large part of the reduction in combat time between pressure ratios of 5 and 3 was caused by the increased momentum pressure drop associated with the higher afterburner-inlet velocities at low pressure ratios. The velocities are illustrated in figure 4 over most of the range of pressure ratios the velocities encountered are considerably higher apparently than present afterburner-design practice permits. Afterburners investigated worked fairly well up to velocities of about 500 feet per second. The velocity at a pressure ratio of 5 was 540 feet per second and increased to over 700 feet per second at a pressure ratio of 3. Because of the increased turbine work required at low compressor efficiencies and the corresponding low tail-pipe pressures, the afterburner-inlet velocities for compressor efficiencies of 0.75 are higher than those for efficiencies of 0.85. The afterburner size for these calculations was chosen to fit in a nacelle of the same diameter as would accommodate the rest of the engine; in other words, the afterburner size was fixed by the compressor size. This size afterburner, apparently, resulted in excessively high velocities at the inlet. The high velocities could be reduced by making the nacelles and tail-pipe larger. The decreased velocities would improve the combustion and increase the thrust but, of course, at the same time the drag would be increased. The drag and thrust could be traded nearly equally until the velocities were reduced by 50 to 100 feet per second. If the nacelle diameter were increased further, however, excessive performance losses would result.

Another engine design variable that was considered was the compressor-air-flow handling capacity. The effect of air-handling capacity on optimum combat time is illustrated in figure 5. The optimum combat time is plotted as a function of air flow per unit compressor-frontal area for various rated pressure ratios. All of the curves are for a constant weight per unit compressor frontal area corresponding to the nominal dry weight of 0.3. Compressor air flows greater than 30 apparently do not appreciably improve performance, because of the high afterburner-inlet velocity. The limit on the air flow could be raised if larger afterburners were used. For larger afterburners the curves would increase approximately linearly.

0371: [REDACTED] 30

The performance shown so far has been for airplanes designed for a flight Mach number of 1.35. The analysis was extended to flight Mach numbers of 1.8. There was a surprising similarity between the results for the two flight speeds. The principal difference was that the combat time for the higher flight speed was about half the combat time for the low speeds. Some of the results of the analysis of the 1.8 Mach number airplanes will be shown in figures 6 to 15.

The combat time for the 1.8 Mach number design airplane is plotted against the afterburner-outlet temperature in figure 6. Combat time continuously increases up to maximum afterburner-outlet temperatures. The gains in combat time for increases in afterburner temperature above 3500° R were very small, however, and the increases would probably be outweighed by practical consideration of combustion efficiency and cooling difficulties. Engine weight effects indicated by the two lines for dry specific weights of 0.3 and 0.4 were similar to those for the 1.35 design Mach number.

The effect of pressure ratio at optimum afterburner-outlet temperature on combat time for the 1.8 Mach number design airplane is shown in figure 7. There is little choice between pressure ratios of 3 to 7 on a combat time basis. There are, however, significant gains to be made by maintaining high efficiency.

The important criterion for choice of compressor pressure ratio at this high flight speed is the afterburner-inlet velocity. The afterburner-inlet velocities are very high at low pressure ratios (fig. 8). As previously mentioned, velocities over 500 feet per second cannot be tolerated at the present time. The curves show that pressure ratios of about 5 are needed before afterburner-inlet velocities reach this level. For this design Mach number as well as for the lower flight speed, a decrease in afterburner-inlet velocity of 50 to 100 feet per second is possible without excessive performance loss by the increase of the nacelle diameter.

The trends of airplane combat time with compressor efficiency, pressure ratio, afterburner-outlet temperature, and air flow handling capacity are similar for both 1.35 and 1.8 design flight Mach numbers.

The possibilities of improving airplane performance by other engine design methods were also considered. Because of the large premium on thrust per pound of air flow, use of higher turbine-inlet temperatures looked attractive. The use of high turbine-inlet temperatures combined with turbine cooling to satisfy the material requirements was investigated.

Combat time for optimum afterburner temperature is plotted against pressure ratio for various turbine-inlet temperatures and a constant engine weight per unit of frontal area in figure 9. Although some

[REDACTED]

4

SECRET

afterburning was used at all turbine-inlet temperatures, the afterburner temperature rise for high values of turbine-inlet temperature was very small. The turbines were assumed to be air cooled and the cooling losses were incorporated in the calculations. A shift in optimum pressure ratios toward the higher pressure ratios was observed. The curves are very flat, however, and the gains in combat time for increases in pressure ratio above 5 are small. At a pressure ratio of 5, a gain in combat time of only 10 percent could be realized by increasing turbine-inlet temperature to 2500°R . If the turbine-inlet temperature were increased to 3000°R , a gain in combat time of 14 percent would result, provided the engines had the same weight. These effects are rather small.

The increased volume flow through the turbine for higher turbine-inlet temperatures results in higher afterburner-inlet velocities as shown in figure 10. Of course, the afterburner-inlet pressures and temperatures were also higher and these higher pressures and temperatures may possibly counterbalance the higher velocities so that the afterburner-design problem may be no more difficult than for the uncooled engines.

The figures 1 to 10 have been based on use of a variable-area convergent nozzle at the afterburner outlet. Turbojet engines operating at flight Mach numbers of 1.35 and 1.8 have exhaust-nozzle pressure ratios as high as 8:1. If a variable-area convergent-divergent exhaust nozzle or some similar device were used instead of a convergent nozzle, gain in thrust per pound of air flow would be apparent. This gain would permit the use of lighter and smaller engines and would result in decreased airplane drag. The airplane drag would decrease further because with a larger nozzle-exit area, the nacelle boattail drag would be less. These multiple effects combine to improve considerably airplane performance, as shown in figure 11. Combat time is plotted against afterburner temperature for the 1.8 Mach number design case. The rated pressure ratio is 5 and compressor efficiency is 0.85. Lines are shown for airplane performance with the convergent nozzle, as given in the previous charts, and for the convergent-divergent nozzle fully expanded in all cases. An increase in optimum combat time of about 24 percent was obtained. The optimum afterburner temperature is shifted from 4000°R to approximately 3100°R . Nozzle configuration, therefore, has a very large effect on performance.

In addition to the nacelle-type power-plant installations, the performance of airplanes with engines submerged in the fuselage was investigated for both design flight Mach numbers. In this investigation the space requirements in the fuselage for carrying payload, radar, pilot, fuel, and similar bulky necessities in addition to the engines were considered. For every practical case, the frontal area of the fuselage was necessarily considerably larger than the frontal area of the engine compressor. It was possible, therefore, to allow the tail-pipe area to be larger relative to the compressor flow area for the submerged installation

SECRET

CONFIDENTIAL

than for the nacelle installations. The favorable effects of utilization of this extra space are shown in figure 12. Combat time is plotted against rated pressure ratio for the 1.8 Mach number design. The curves are shown for a compressor air flow per unit frontal area of 30 pounds per second per square foot and for a dry specific engine weight of 0.3. Curves are shown for both the nacelle-type installation and the submerged installation. The performance of the airplane with submerged engine was only slightly better than the nacelle type at a pressure ratio of 5. At a pressure ratio of 3, however, there was a gain in combat time of over 25 percent when the engines are submerged. The cause for the large increase in combat time is due to the reduction of afterburner-inlet velocity. A reduction in afterburner-inlet velocity from 665 feet per second to about 500 feet per second was obtained by utilizing the additional space available for the afterburner in the submerged case. This reduction in velocity was accompanied by a corresponding decrease in afterburner-momentum pressure drop, hence the thrust per pound of air flow was increased and the engine weight and specific-fuel consumption were conserved. These savings in weight and fuel flow may be translated into performance improvement in the submerged installation and not in the nacelle installations because the drag penalties are less for small increases in fuselage diameter than for similar increases in nacelle diameter. These advantages exist only for high compressor air flows. If the air flow per unit frontal area of the compressor were reduced to about 25 pounds per second per square foot of frontal area thereby reducing the general level of the afterburner-inlet velocities, the differences in performance would become small.

The results presented in figures 11 and 12 are representative of numerous similar curves obtained in the general interceptor analysis. In this portion of the analysis, the engine design variables of compressor efficiency, air-flow handling capacity, compressor pressure ratio, and engine weight were varied independently. In actual engine design, of course, these variables are not completely independent; for instance, engine weight might be reduced but only at the expense of compressor efficiency. A study of the best possible combination of components for the conventional axial-flow compressor-turbojet engine was, therefore, made to determine the variation of efficiency weight and air-flow handling capacity that would probably be encountered for engines of various pressure ratios. When the schedule of weights, efficiencies, and pressure ratios were determined, the airplane performance for each design-pressure ratio could be obtained by simple interpolating in the more general analysis.

The airplane performance with the integrated schedule of engine design variables is presented in figure 13. Combat time is plotted against rated pressure ratio for both design Mach numbers and for both submerged and nacelle installed engines. The compressor air flow handling capacity of 25.8 is representative of good current design

practice. For the design flight Mach number of 1.35, the compressor pressure ratio of 5 is optimum for the nacelle installation. At this pressure ratio, the afterburner-inlet velocities are about 450 feet per second. For the submerged installation, however, pressure ratios from 3 to 5 may be used with little difference in combat time. The afterburner-inlet velocity for a pressure ratio of 3 in this case is about 500 feet per second and at a pressure ratio of 5 is 470 feet per second.

The curves shown in figure 13 are considerably flatter than those shown in preceding figures in which engine weight and efficiency were constant. These differences in slope are caused by the combined effects of changes in engine weight and efficiency with pressure ratio.

For the design flight Mach number of 1.8, little difference in combat time resulted from using pressure ratios of 3 or 5 for both the submerged and nacelle installations. From the standpoint of reliability and manufacturing simplicity, a selection of a pressure ratio of 3 in both cases is probably more desirable. The afterburner-inlet velocities, however, are 615 feet per second for the pressure ratio of 3 in a nacelle installation and only 460 feet per second for the pressure ratio of 5. These high burner-inlet velocities would probably introduce afterburner-combustion difficulties, and higher compressor-pressure ratios to reduce the burner-inlet velocities may be a necessity. In the submerged installation, however, the afterburner-inlet velocities are only 500 feet per second at a pressure ratio of 3. The design pressure ratio of 3, therefore, is practical for this condition.

Reasonable combat times evidently may be obtained in aircraft powered by conventional axial-flow compressor-type turbojet power plants. At a design flight Mach number of 1.35, combat times of about 34 minutes are possible, and at a design Mach number of 1.8, combat times of about 16 minutes may be obtained.

The supersonic bomber introduces somewhat different power-plant problems than the supersonic interceptor. The bomber is not required to fulfill the combat requirement of 2g maneuverability; as a result, the power loading for the bomber is considerably less than for the fighter and the airplane lift-drag ratios are appreciably higher. In other respects the aircraft are aerodynamically similar. It will be shown that these differences lead to greater premiums on specific fuel consumption and fewer benefits for increases in thrust per pound of air flow for the bomber-type airplane than for the interceptor.

The effect of afterburner-outlet temperature on relative range of the bomber airplane is presented in figure 14. The bomber had a 500-mile-radius Mach number of 1.5 and cruise Mach number of 0.9. The curves are for nominal dry specific weights of 0.3 and 0.4 for a rated pressure ratio

031710 000000

of 7, compressor efficiency of 0.85, and air flow per unit compressor frontal area of 30 pounds per second per square foot. For a constant engine weight, the optimum afterburner temperature is about 2600° R. The use of afterburning in the supersonic portion of the flight plan permits the installation of small engines with low specific fuel consumption and good off-design performance in the cruise region. It should be pointed out, however, that the effect of afterburner temperature is small and a reduction in engine weight of only 20 percent would be required for the nonafterburning case to obtain range equivalent to the optimums shown. Engine weight is important for the bomber although the effects are less than for the interceptor airplanes. Comparison of the two curves shows that an increase in engine weight of 25 percent results in a decrease in optimum range of 6 percent.

The relative range for optimum afterburner temperature is plotted against rated compressor pressure ratio for peak compressor efficiencies of 0.85 and 0.75 in figure 15. The optimum pressure ratios for the bomber are over 7 although the gains from pressure ratios of 7 to 9 are small. The paramount importance of compressor efficiency is obvious from comparison of the two lines. A loss in range of about 23 percent occurs when efficiency is reduced from 0.85 to 0.75. These results emphasize the importance of low specific fuel consumption for this application.

The effects of increasing turbine-inlet temperature for the bomber were also investigated. Because the off-design characteristics of engines with high turbine-inlet temperatures are poor, the use of these engines in airplanes having wide flight-speed variations, such as the bomber being considered, does not lead to immediately evident large gains in performance. It is possible, however, that the bomber performance could be improved by using high turbine-inlet temperatures, and thereby eliminating the necessity for afterburning. The resulting weight savings may lead to range improvements. The off-design performance of high-temperature engines could also be improved considerably by using variable-area turbine nozzles.

The results of introducing the schedule of weights and efficiencies for the conventional subsonic axial-flow compressor-type engine into the generalized bomber analysis are shown in figure 16. The relative range for optimum afterburner temperature is plotted against compressor-pressure ratio for the scheduled weights and efficiencies. Optimum pressure ratio is slightly over 7, but the gains in range for pressure ratios greater than 5 are very small. The conventionally designed engine for the bomber application should have a rated compressor pressure ratio of 5 or 7 and either no afterburning or afterburning to temperature of only about 2500° R.

In summary, a few of the important points indicated by the analysis will be reviewed. The interceptor analysis has shown that afterburner-

CONFIDENTIAL

2-9

outlet temperatures of 3100° to 3500° R are adequate to insure optimum or nearly optimum airplane performance. The airplane performance in general is insensitive to changes in compressor-pressure ratio or turbine-inlet temperature. Component efficiencies and engine weights, however, are design variables of first order importance. One of the principal problems in the design of engines for these applications is the high afterburner-inlet velocities encountered for most of the engine design conditions investigated. In many cases these inlet-velocity limits are the determining factor in engine compressor selection.

The use of a variable-area convergent-divergent nozzle appreciably improves airplane performance. Conventionally designed engines for the interceptors should have pressure ratios from 3 to 5.

A somewhat different type of engine is desirable for the supersonic bomber. This engine should have very little or no afterburning and compressor-pressure ratios in the range of 5 to 7. Efficiency should not be sacrificed for engine weight.

CONFIDENTIAL

EFFECT OF AFTERBURNER OUTLET TEMPERATURE ON COMBAT TIME

DESIGN $M_0 = 1.35$

$W_a/A_c = 30 \text{ LB/}(SEC)(SQ \text{ FT})$

$T_4 = 2000^\circ \text{R}$

$\eta_{c, \text{max.}} = .85$

$(P_3/P_2)_r = 5$

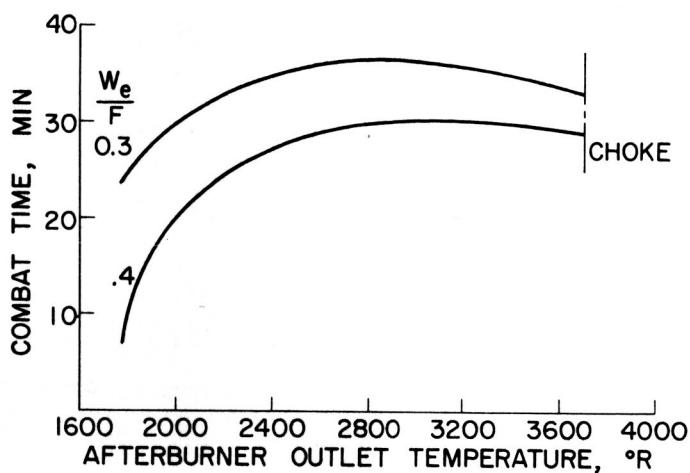


Figure 1

INTERCEPTOR AIRPLANE FOR FLIGHT MACH NUMBER OF 1.80 WITH NONAFTERBURNING TURBOJET ENGINES

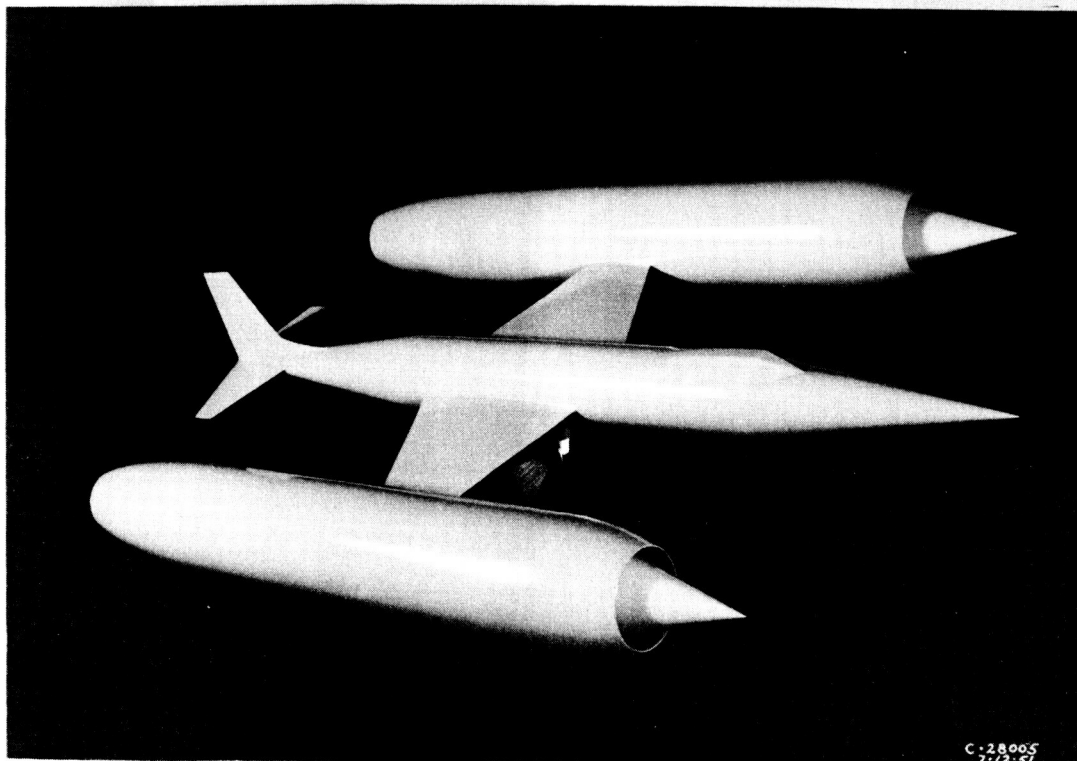


Figure 2

03715-00000

EFFECT OF COMPRESSOR EFFICIENCY AND PRESSURE RATIO ON COMBAT TIME

DESIGN $M_0 = 1.35$

$W_a/A_c = 30 \text{ LB/ (SEC) (SQ FT)}$

$T_4 = 2000^\circ \text{ R}$

W_e/F (at $P_3/P_2 = 5$ and $\eta_c = .85$) = 0.3

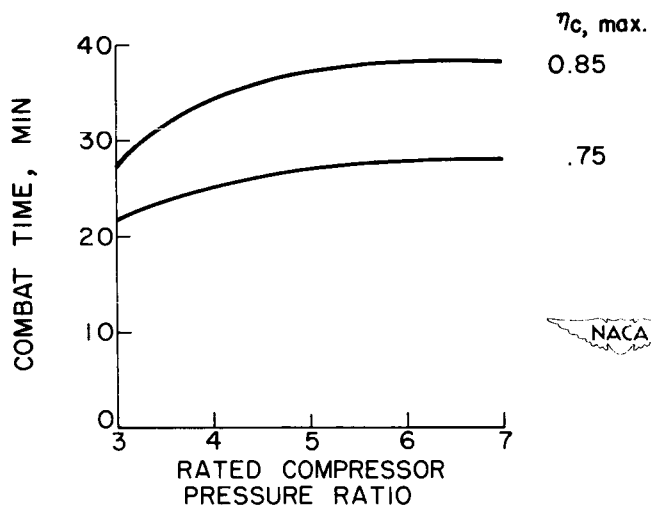


Figure 3

EFFECT OF COMPRESSOR EFFICIENCY AND PRESSURE RATIO ON AFTERBURNER INLET VELOCITY

DESIGN $M_0 = 1.35$

$W_a/A_c = 30 \text{ LB/ (SEC) (SQ FT)}$

$T_4 = 2000^\circ \text{ R}$

W_e/F (at $P_3/P_2 = 5$ and $\eta_c = .85$) = 0.3

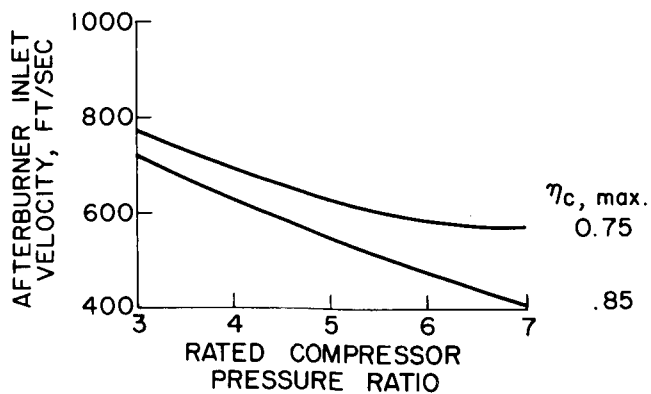


Figure 4

SECRET EFFECT OF AIR HANDLING CAPACITY ON COMBAT TIME

DESIGN $M_0 = 1.35$

$T_4 = 2000^\circ \text{R}$

$\eta_{c, \text{max.}} = .85$

W_e/F (at $P_3/P_2 = 5$ and $\eta_c = .85$) = 0.3

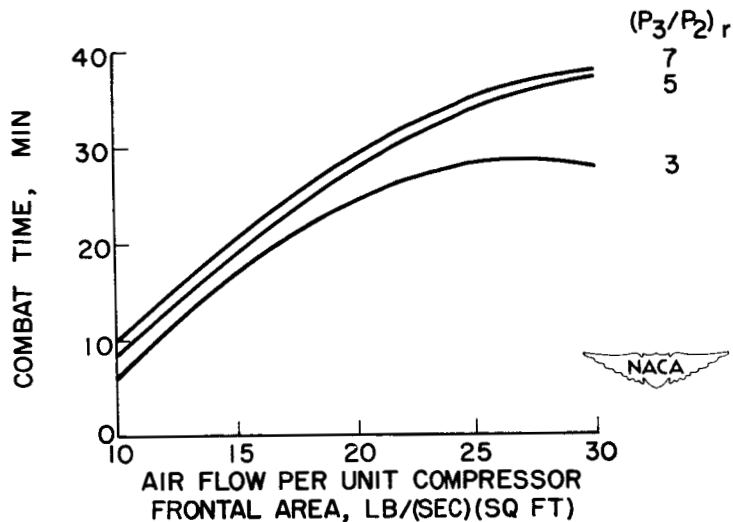


Figure 5

EFFECT OF AFTERBURNER OUTLET TEMPERATURE ON COMBAT TIME

DESIGN $M_0 = 1.8$

$W_a/A_c = 30 \text{ LB/(SEC)(SQ FT)}$

$T_4 = 2000^\circ \text{R}$

$\eta_{c, \text{max.}} = .85$

$(P_3/P_2)_r = 5$

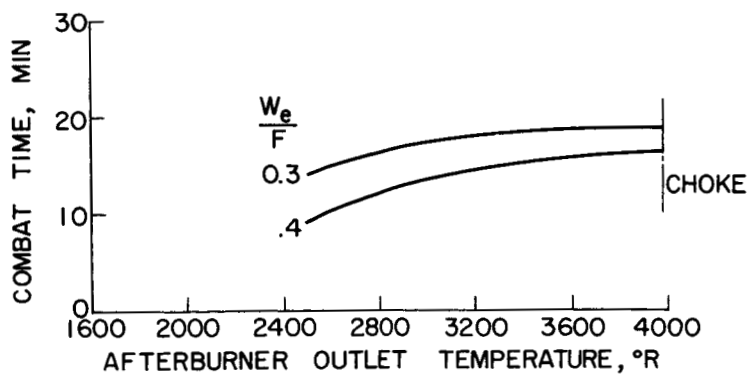


Figure 6

CONFIDENTIAL

EFFECT OF COMPRESSOR EFFICIENCY AND PRESSURE RATIO ON COMBAT TIME

DESIGN $M_0 = 1.8$ $W_0/A_c = 30 \text{ LB/ (SEC) (SQ FT)}$
 $T_4 = 2000^\circ \text{ R}$ W_e/F (at $P_3/P_2 = 5$ and $\eta_c = .85$) = 0.3

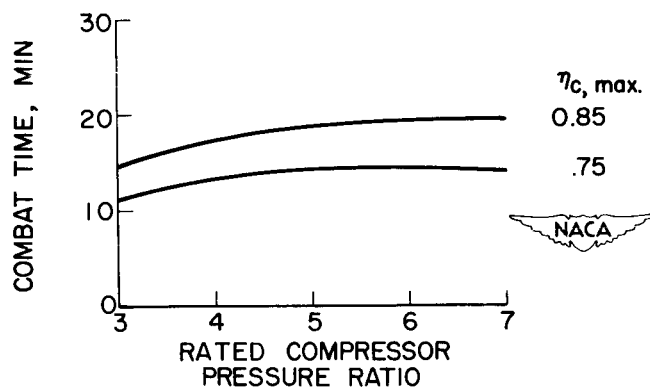


Figure 7

EFFECT OF COMPRESSOR EFFICIENCY AND PRESSURE RATIO ON AFTERBURNER INLET VELOCITY

DESIGN $M_0 = 1.8$ $W_0/A_c = 30 \text{ LB/ (SEC) (SQ FT)}$
 $T_4 = 2000^\circ \text{ R}$ W_e/F (at $P_3/P_2 = 5$ and $\eta_c = .85$) = 0.3

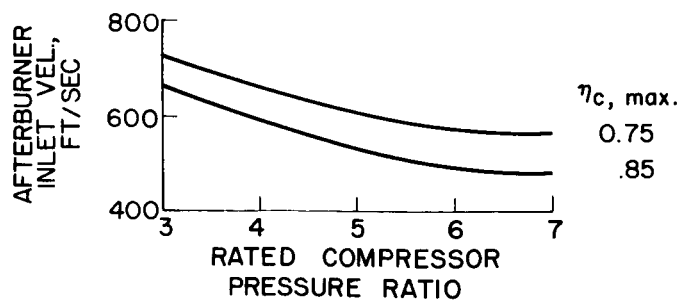


Figure 8

CONFIDENTIAL

2235-2

CONFIDENTIAL

[REDACTED]

DECLASSIFIED

EFFECT OF TURBINE COOLING ON COMBAT TIME

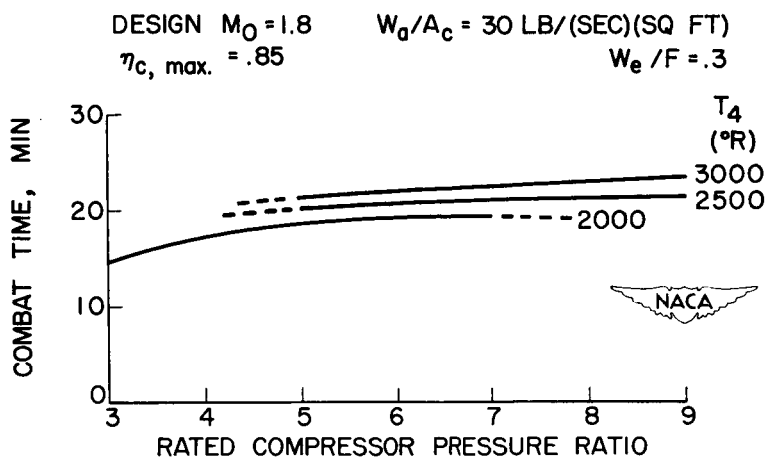


Figure 9

EFFECT OF TURBINE COOLING ON AFTERBURNER INLET VELOCITY

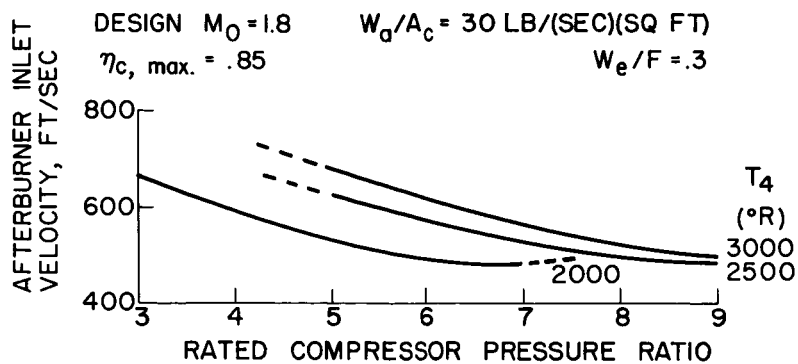


Figure 10

0371500000

EFFECT OF FULLY EXPANDED VARIABLE AREA NOZZLE

DESIGN $M_0 = 1.8$ $W_d/A_c = 30 \text{ LB}/(\text{SEC})(\text{SQ FT})$
 $T_4 = 2000^\circ \text{R}$ $(P_3/P_2) = 5$
 $\eta_{c, \text{max.}} = .85$ $W_e/F = .3$

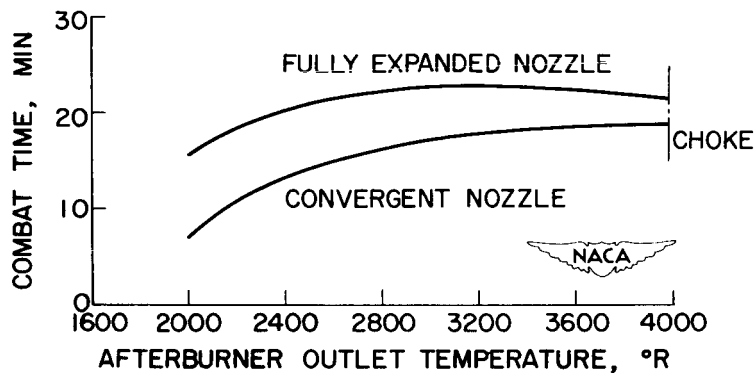


Figure 11

EFFECT OF SUBMERGED AND NACELLE INSTALLATION

DESIGN $M_0 = 1.8$ $W_d/A_c = 30 \text{ LB}/(\text{SEC})(\text{SQ FT})$
 $T_4 = 2000^\circ \text{R}$ $W_e/F \text{ (at } P_3/P_2 = 5 \text{ and } \eta_c = .85) = 0.3$
 $\eta_{c, \text{max.}} = .85$

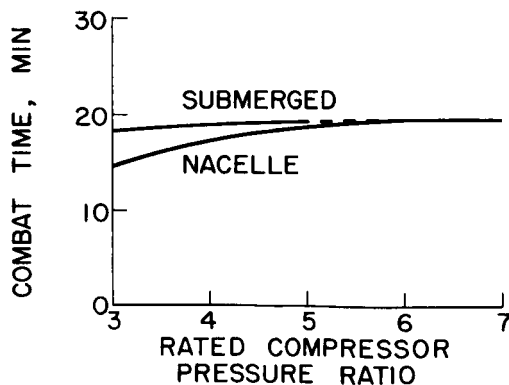


Figure 12

COMBAT TIME WITH SCHEDULED ENGINE WEIGHTS
AND EFFICIENCIES FOR CONVENTIONAL AXIAL-FLOW
COMPRESSOR TYPE ENGINE

$$W_a/A_c = 25.8 \text{ LB/(SEC)(SQ FT)}$$

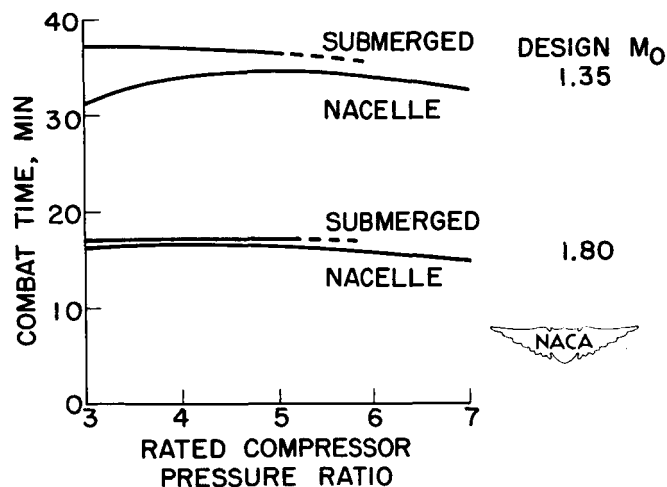


Figure 13

EFFECT OF AFTERBURNER TEMPERATURE ON
RANGE FOR SUPERSONIC BOMBER

$$T_4 = 2000^\circ \text{ R}$$

$$W_a/A_c = 30 \text{ LB/(SEC)(SQ FT)}$$

$$\eta_{c, \text{max}} = .85$$

$$(P_3/P_2)_r = 7$$

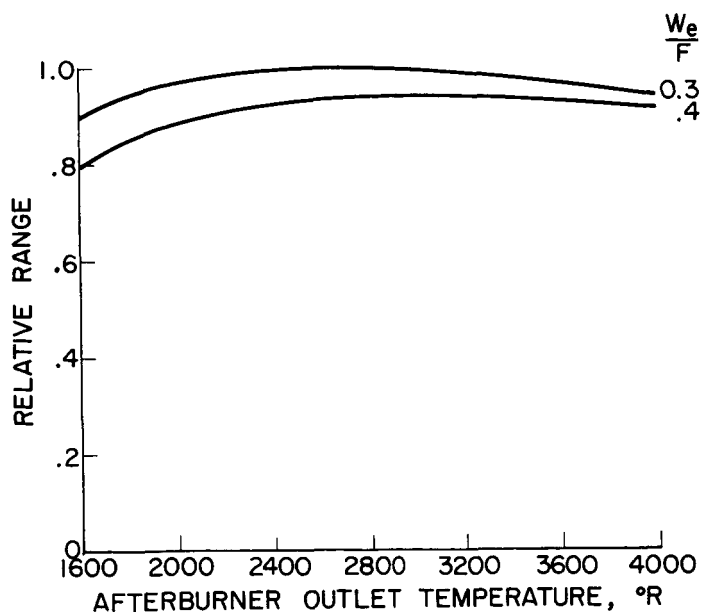


Figure 14

EFFECT OF PRESSURE RATIO ON SUPERSONIC BOMBER RANGE

$$W_a/A_c = 30 \text{ LB/(SEC)(SQ FT)}$$

$$T_4 = 2000^\circ \text{ R}$$

$$W_e/F = .4$$

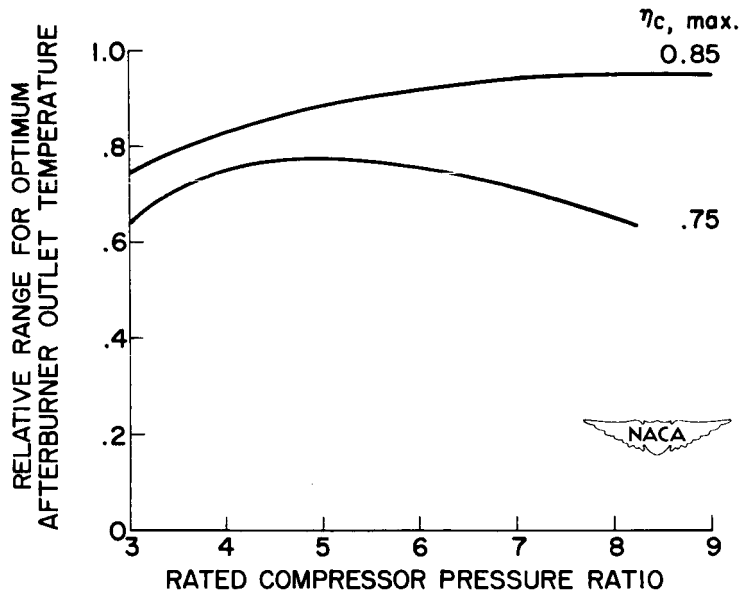


Figure 15

RELATIVE RANGE FOR CONVENTIONAL SUBSONIC AXIAL FLOW COMPRESSOR TYPE TURBOJET ENGINES WITH SCHEDULED WEIGHTS

$$W_a/A_c = 25.8 \text{ LB/(SEC)(SQ FT)}$$

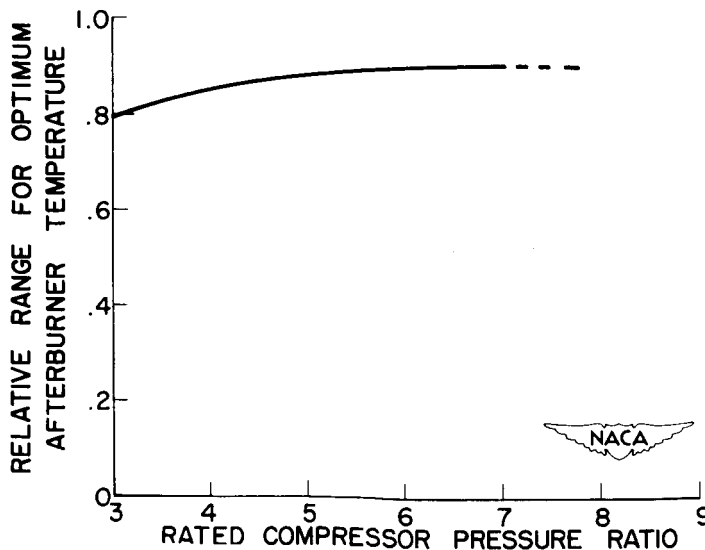


Figure 16

DECLASSIFIED

3. COMMENTS Ib

[REDACTED]

DECLASSIFIED

3. - COMMENTS Ib

By Bruce T. Lundin

2235

The principal results of the analysis of turbojet propulsive systems presented in the preceding paper may be conveniently summarized or highlighted with reference to the engine installations presented in figure 1. In the upper part of this figure is shown the nacelle engine installation for an interceptor airplane designed for a combat Mach number of 1.35, and in the lower part of the figure the nacelle installation for a flight Mach number of 1.80. For both design combat speeds the optimum, or most satisfactory, pressure ratio at sea-level rated conditions was shown to be in the region of 5, although the airplane performance was not sensitive to its exact value. While lower pressure ratios would be desirable with regard to engine weight, and would be satisfactory from the standpoint of engine cycle performance, the increase in afterburner inlet velocities, which would introduce not only combustion difficulties but also large thrust losses due to momentum pressure drop in the burner, offsets the weight advantage of the lower pressure ratios. Even with these values of pressure ratio, the afterburner inlet velocities are over 450 feet per second for both engines. It should be noted that these velocities are based on compressor air flows typical of current attainments. The principal difference in the two engines for the two flight conditions considered is the optimum afterburner outlet temperature, which was shown to be about 3100° R for the flight Mach number of 1.35 and about 3500° R for a Mach number of 1.80. These temperatures, it should be recalled, are the optimum values for best combat endurance for continuous operation. Higher temperatures are, of course, of interest for special combat maneuvers when a high rate of acceleration or short turning radius is required at the expense of total endurance.

The actual values of engine size required for the 40,000-pound gross weight interceptor are also included in this figure. For the airplane design for a flight Mach number of 1.35, each engine was found to require a rated air flow of about 180 pounds per second and a rated, nonaugmented take-off thrust of about 9500 pounds. For the higher flight speed, an engine about 15 percent larger was required, having a rated air flow of 213 pounds per second and producing a nonaugmented take-off thrust of nearly 11,000 pounds.

These engine characteristics are for a component efficiency of 85 percent and the value of this efficiency was shown in the previous paper to have an important influence on the airplane performance. If, for example, the component efficiency is reduced to 75 percent, such as may be obtained with some supersonic compressors, an engine approximately one-third larger than illustrated in figure 1 would be required, and the combat endurance would be correspondingly reduced. In addition to this

DECLASSIFIED

CONFIDENTIAL

decrease in airplane performance, a reduced component efficiency would also increase the afterburner inlet velocities considerably, which would introduce many difficulties of afterburner operation and, in some cases, severely limit the afterburner outlet temperature by thermal choking.

While pressure losses in the afterburner of a nacelle installation prevented reductions in compressor pressure ratios below 5, it was shown that if the afterburner could be increased in size in a submerged installation without greatly increasing the airplane drag, lower pressure ratios were advantageous because of the resulting lower engine weight. As shown in figure 2, where the nacelle and submerged installations are compared for a flight Mach number of 1.80, it is noted that the optimum pressure ratio of the submerged engine is about 3. In this installation, the afterburner area was considered to be 50 percent greater than the area of the compressor and turbine, while in the nacelle installation the afterburner was limited to an area of only 15 percent above that of the compressor because of aerodynamic drag penalties. The actual size of the single submerged engine is, of course, approximately twice that of the nacelle-installed engine. The rated air flow of this engine is over 400 pounds per second and the rated thrust is over 19,000 pounds; the need for large engines for this type of airplane is thus emphasized.

This analysis of turbojet propulsion systems, although subject to the usual restrictions and qualifications arising from the necessity of making many basic assumptions, provides some insight into the relative importance of various engine variables and an evaluation of the required operating conditions of the different components of the engine. While fairly satisfactory performance is obtainable with components such as those available in many current engines, there always exists, of course, the possibility of further improvement. The attainment of these improvements is the objective of many of the research investigations in progress at the NACA Lewis laboratory, some of which will be discussed in subsequent papers.

With regard to the afterburner component of the engine, the inlet velocities will, as has been shown, be fairly high even for a submerged engine installation where, although the size of the afterburner may be increased somewhat, high velocities will be required in order to realize the weight reductions afforded by a low pressure-ratio compressor. The range of pressures over which the afterburner must operate, which is of importance to both combustion efficiency and stability, will vary over a typical flight plan from roughly 1000 to 5000 pounds per square foot. In addition to the problem of obtaining efficient and stable combustion in the afterburner over this range of operating conditions, effective methods of maintaining the shell of the burner at safe temperatures must be provided, especially when very high gas temperatures may be required for special combat maneuvers.

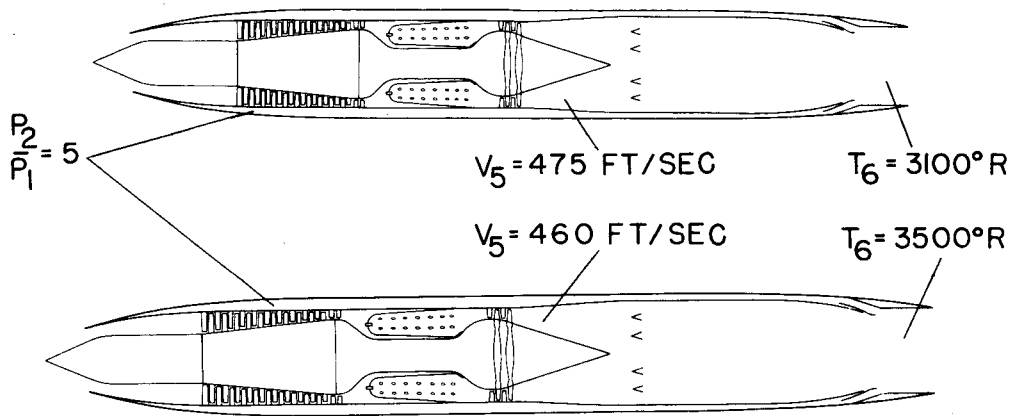
Some of the afterburner research investigations devoted to the attainment of these objectives will be discussed in the following paper.

CONFIDENTIAL

2235-3

[REDACTED]
INTERCEPTOR NACELLE INSTALLATION

DESIGN MACH NO=1.35
AIR FLOW = 180 LB/SEC
RATED THRUST = 9500 LBS

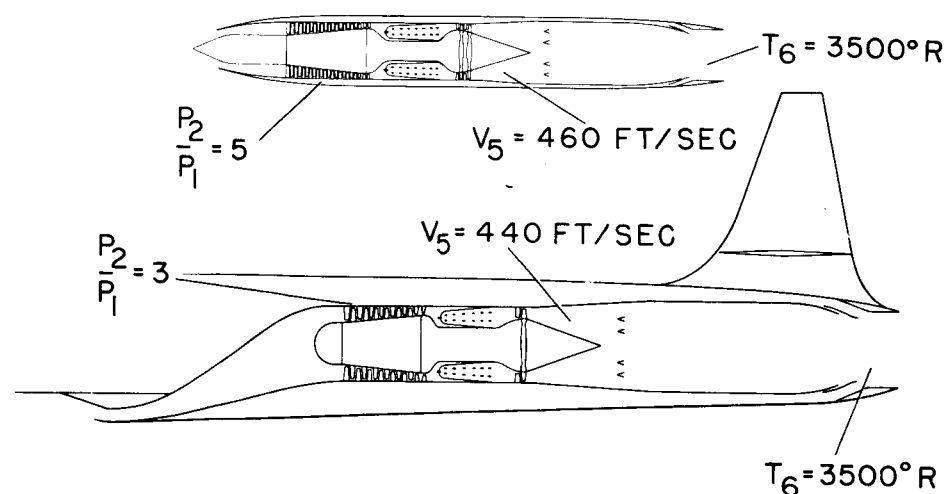


DESIGN MACH NO=1.80
AIR FLOW = 213 LB/SEC
RATED THRUST = 10,900 LBS

Figure 1

NACELLE INSTALLATION

AIR FLOW = 213 LB/SEC
RATED THRUST = 10,900 LBS



SUBMERGED INSTALLATION
AIR FLOW = 423 LB/SEC
RATED THRUST = 19.250 LBS

Figure 2



DECLASSIFIED

4. TURBOJET THRUST AUGMENTATION FOR SUPERSONIC PROPULSION

By William A. Fleming and E. William Conrad

~~CONFIDENTIAL~~

4. - TURBOJET THRUST AUGMENTATION FOR

SUPERSONIC PROPULSION

By William A. Fleming and E. William Conrad

INTRODUCTION

As illustrated in the first paper, thrust augmentation by means of tail-pipe burning with exhaust-gas temperatures between 3000° and 3500° R is a very definite requirement for the supersonic airplane. From the viewpoint of combat time in this or any other type of turbojet aircraft, it is, of course, important that the tail-pipe burner combustion efficiency be as high as possible.

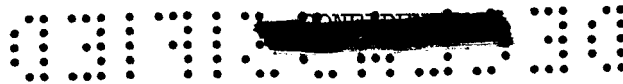
Because of the importance of high tail-pipe combustion efficiencies, the laboratory research program on thrust augmentation has been extended with emphasis on improved combustion efficiency. Considerable effort has also been directed toward more completely evaluating tail-pipe burner cooling requirements. Other factors including minimum size and weight, low internal pressure losses, and good control were, of course, considered in the designs investigated.

The discussion of tail-pipe burning will be centered on the performance obtained to date over a range of burner-inlet velocities. In addition, the tail-pipe burner cooling requirements will be discussed and combustion instability characteristics encountered will be reviewed.

BURNER PERFORMANCE CHARACTERISTICS

Some of the main tail-pipe burner design features indicated desirable by previous work (reference 1) are illustrated by a typical tail-pipe burner in figure 1. It was indicated that a V-gutter-type flameholder blocking about 30 percent of the burner cross-section area and having an included gutter angle of about 30° performed as well as or better than any other type of flameholder investigated at the NACA Lewis laboratory. A center pilot cone aided in stabilizing combustion. Uniform radial fuel-air mixtures and a mixing length of one to two feet between the fuel injectors and flameholder were shown to be important factors in maintaining high combustion efficiency. A burner length of about 4 feet was optimum; longer burners encountered serious shell overheating and shorter burners encountered reduced combustion efficiency particularly at high altitudes. Maintaining the burner-inlet velocity as low as possible was conducive to good combustion efficiency. An inner liner forming a 1/2-inch high passage inside the burner shell protected the shell from overheating at exhaust gas temperatures up to

~~CONFIDENTIAL~~



about 3400° R, with a small amount of air flowing over the outside of the burner. Highest exhaust-nozzle efficiencies with variable-area nozzles were obtained when the nozzle exit was planar, or nearly so, for all nozzle positions and when the movable and fixed portions of the nozzle were well sealed against gas leakage.

The combustion characteristics of a burner incorporating these design features and having an inlet velocity of 470 feet per second are shown in figure 2 for three burner-inlet total pressures. The tail-pipe fuel-air ratio indicated in this figure is defined as the ratio of tail-pipe fuel flow to unburned air flow entering the tail-pipe burner, when complete combustion in the primary combustors is assumed. For this burner the maximum temperature obtained at a burner-inlet pressure of 1739 pounds per square foot was about 3450° F with a combustion efficiency of 74 percent. At a burner-inlet pressure of 969 pounds per square foot, corresponding to operation at subsonic Mach numbers and an altitude of 50,000 feet, the maximum temperature obtained was about 3200° R with an efficiency of 65 percent. A maximum efficiency of 88 percent was obtained at a burner-inlet pressure of 2254 pounds per square foot.

This configuration was investigated some time ago. Two more recent configurations, including additional modifications indicated desirable by earlier work and designed for an inlet velocity of 360 feet per second, are shown in figure 3. The most important step in improved design technique for these configurations, designated A and B, as compared to the one shown in figure 1 was that the radial fuel distribution was carefully tailored to give a uniform temperature profile across the burner diameter. In addition, the inner liner was replaced by an external cooling shroud in anticipation of higher exhaust-gas temperatures. The two widely different diffuser and flameholder designs of these configurations resulted from two different attacks on combustion instability encountered, as will be discussed later. In spite of these differences, performance characteristics of these two configurations were nearly identical; consequently, only the performance of configuration A will be discussed herein.

Combustion efficiencies and exhaust-gas temperatures obtained with configuration A are compared in figure 4 with those obtained at a higher burner-inlet velocity. As indicated, the peak efficiencies were increased considerably, reaching values of 97 and 82 percent at burner-inlet pressures of 2450 and 925 pounds per square foot, respectively; the increases were about 10 percent over those obtained at the higher burner-inlet velocity with similar burner-inlet pressures. In addition, the regions of peak efficiency were shifted to higher fuel-air ratios, which is conducive to obtaining high exhaust-gas temperatures. As a result, the maximum obtainable temperature was 4000° R at the highest burner-inlet pressure and 3650° R at the lowest pressure. Points at



~~CONFIDENTIAL~~

the optimum exhaust-gas temperatures for the supersonic interceptors at Mach numbers of 1.35 and 1.80 and an altitude of 50,000 feet indicate that the combustion efficiencies at these conditions were approximately 83 and 94 percent, respectively.

Over-all performance characteristics of configuration A are shown in figure 5 for Mach numbers of 1.35 and 1.80 at an altitude of 50,000 feet, the design conditions selected in the supersonic interceptor analysis. In addition to interpolating the burner performance for configuration A, assumptions used in constructing these curves were that the engine was the one assumed for the interceptor analysis having a compressor-pressure ratio of 5.0 at sea-level standard conditions, and inlet pressure recoveries were the same as those used in the interceptor analysis. Both the augmented thrust ratio and specific fuel consumption increased with tail-pipe fuel-air ratio. At the operating points indicated by the interceptor analysis to give maximum combat time, the augmented thrust ratios were 1.85 and 2.30 and the specific fuel consumptions were 2.62 and 2.50 at Mach numbers of 1.35 and 1.80, respectively.

BURNER-INLET VELOCITY

The interceptor analysis indicated that combat time could be lengthened by increasing the air flow per unit area, which increases burner-inlet velocity. From the over-all airplane performance aspect it was indicated desirable that the burner-inlet velocity be approximately 500 feet per second so that the tail-pipe burner would have the same or only slightly larger frontal area than the engine. This discussion raises the question as to how the burner-inlet velocity affects the burner performance.

The effect of the burner-inlet variables, velocity, pressure, and temperature on combustion efficiency is shown in figure 6 where peak combustion efficiencies of several geometrically similar burners are plotted against PT/V . This correlation is similar to that used in reference 2 for correlating primary combustor performance and is useful in predicting the effect of the inlet variables on burner performance. The data shown correlate well and indicate that PT/V is a parameter which takes into account the primary effects on tail-pipe burner combustion efficiency. The dashed curve on figure 6 indicates the correlation of configuration A with the optimum operating conditions indicated for the interceptors at Mach numbers of 1.35 and 1.80 and an altitude of 50,000 feet. Data for other burners follow the trends shown in this figure: an increased velocity results in reduced combustion efficiency. Changing the burner geometry, of course, shifts the correlation curve, although it has been found typical of most burners that the knee of the curve occurs at a PT/V of about 4000.

~~CONFIDENTIAL~~



Improvements in combustion efficiency shown for configuration A at a given value of PT/V above those previously obtained are attributed to changes in burner design, particularly changes in fuel distribution. Because configuration A incorporated modifications previously indicated desirable, it is considered justifiable to refer to those data to indicate the effect of velocity on efficiency. Raising the burner-inlet velocity of this configuration from 360 to 500 feet per second would reduce the peak efficiency from 94 to 90 percent at a Mach number of 1.80 and from 87 to 81 percent at a Mach number of 1.35. Improvements in combustion efficiency at high burner-inlet velocities are possible by continued improvement in burner design.

A method of increasing average burner-inlet velocity, with possibly no loss in combustion efficiency, would be to provide a uniform velocity profile at the burner inlet. A velocity profile typical of those encountered with most burners is shown in figure 7. As illustrated in this figure, although the average velocity is 510 feet per second, the velocity approaching the outer gutter is about 700 feet per second; the velocity approaching the inner gutter is slightly over 500 feet per second; and, because of flow separation from the inner body, the velocity near the center of the burner is less than 200 feet per second. With a more nearly uniform velocity profile, the average velocity could be increased without raising the local velocity over the flameholder gutters.

A method of so changing the velocity profile is by the use of vortex generators, such as were recently brought to interest by the application in the United Aircraft Corporation wind tunnel (reference 3). An illustration of vortex generators installed on the inner body of configuration B is shown in figure 8. The principle of vortex generators, which are symmetrical airfoils attached to the diffuser inner body and set at angle of attack to the flow, is that the tip vortices peeling off the generators mix high-energy stream air with low-energy boundary-layer air, consequently providing more uniform velocity profiles through the diffuser, retarding flow separation from the diffuser wall, and improving the diffuser efficiency.

Data obtained at the NACA Langley laboratory on vortex generator installations (reference 4) in annular diffusers indicated that the optimum angle of attack was about 15° and the optimum span was equal to the distance from the wall to the point at which the local velocity equalled approximately 0.8 of the maximum stream velocity. Variations in chord from 1 to 3 inches had no apparent effect on diffuser performance.

By use of this design information, a set of counter-rotating vortex generators, alternate blades set at plus and minus 15° angle of



attack, having a 2-inch chord and 1/2-inch span, were installed on the inner body of configuration B at the diffuser inlet. The shift in velocity profile near the diffuser outlet produced by the vortex generators is shown in figure 9. Obtaining measurements at the burner inlet was undesirable on this installation because of the location of the fuel injectors in the diffuser. As shown in this figure, the peak velocity was lowered from 670 to 590 feet per second, and the velocity near the inner body was increased significantly. At the same time, the total pressure loss across the diffuser was halved. If the peak velocity could be maintained at the initial value and the velocity in the inner portion of the annulus increased as shown, it would be possible to increase the velocity at the measuring station from about 500 to 575 feet per second. This increase would correspond to an increase in burner-inlet velocity of configuration B from 360 to about 415 feet per second, possibly with no effect on combustion efficiency. This point has yet to be proven experimentally.

COMBUSTION INSTABILITY

Although previously encountered only at low altitudes, combustion instability was recently encountered at altitudes as high as 35,000 feet and low subsonic Mach numbers. Others working with tail-pipe burners have encountered combustion instability at one time or another. There are two types of combustion instability: one a high-frequency screaming combustion, and the other a relatively low-frequency buzzing combustion. Both types have a very destructive effect on the burner.

It is believed that the high-frequency instability is associated with flow separation along the diffuser inner body, and that the low-frequency instability is associated with the vortex frequency or some other flow pattern behind blunt bodies. In each case there is a combustible mixture present in the unstable or fluctuating flow region, which when ignited burns with explosive rapidity, thereby exerting a pressure pulse forward in the burner. This pressure pulse delays introduction of a fresh charge of mixture into the region until the initial charge is consumed. After the pulse is expended, a new combustible charge flows into the region and the cycle is repeated. The frequency of these pulses is related to the natural frequency of the respective system established; small volumes having a high frequency and large volumes, a low frequency.

Characteristics of unstable combustion have been observed by means of high-speed motion pictures of a small two-dimensional combustor with two V-gutter flame holders. In these experiments, with a stream velocity of 50 feet per second and atmospheric inlet pressure and temperature, the flame was observed to pulse intermittently upstream



between the flame holder gutters at a frequency of about 200 cycles per second. Observations made upstream of the flame holder indicated that each time the flame pulsed forward the progress of the column of air through the burner was essentially halted.

In order to avoid the high-frequency screaming combustion instability, it is considered important to provide good diffuser design so as to prevent flow separation. In addition, it is considered equally important to provide a flame seat at locations where flow separation or low velocities may exist. In order to avoid the relatively low-frequency buzzing instability, it is considered important to reduce the volume of combustible mixture susceptible to detonation by providing a flame seat in the unstable region.

With these principles, the combustion instability characteristics recently encountered at an altitude of 25,000 feet and a burner-inlet velocity of about 360 feet per second can be reviewed with the aid of figure 10, which shows several burner configurations. High-frequency screaming combustion was first encountered with configuration type 1 with the 2-ring V-gutter flameholder located downstream of the pilot cone. Observations through a periscope looking upstream into the combustor revealed unstable burning along the downstream portion of the inner body when screaming combustion occurred. It was felt that the prime reason for this instability was the low velocity or reverse flow which existed in the boundary layer along the downstream portion of the inner body. Two methods of attack to the problem were open. One was to eliminate the instability without appreciably altering the diffuser design, possibly by installing a flame seat in the region of unstable burning, and the second was to improve the aerodynamic design of the diffuser to eliminate flow separation. Both methods were investigated and the results of each are discussed.

It was reasoned that moving the gutter upstream as indicated in configuration type 1 would increase the velocity over the downstream portion of the inner body and also the presence of the flame front would provide a resistance reducing the adverse pressure gradient along the inner body retarding flow separation. Replacing the 2-ring V-gutter flameholder with a single ring flameholder at this location eliminated the screaming combustion.

In the process of improving combustion efficiency the pilot cone was enlarged as shown by the solid lines in configuration type 2 of figure 10. After this modification was made, with the flameholder and fuel system essentially unchanged, screaming combustion again occurred with unstable burning once more along the downstream portion of the inner body. It appeared that the close proximity of the flameholder and pilot cone with the low-velocity boundary layer between them



~~CONFIDENTIAL~~

4-7

promoted burning in this region. Providing a flame seat in the unstable region, by inserting a step on the inner body, once again eliminated the unstable combustion.

The other approach toward elimination of combustion instability, improved internal aerodynamics, resulted in the design of a long gradual diffuser as indicated by configuration type 3 of figure 10. In addition to the particular attention given to the lines of the inner body, vortex generators were installed at the diffuser inlet to delay separation and give a uniform velocity profile. This configuration was first operated with only the outer two rings of the V-gutter flame holder and with fuel injected at the downstream end of the inner body. A severe low-frequency buzzing combustion was encountered with an unstable flame in the center of the burner. Insertion of a third V-gutter ring in the center of the burner stabilized the flame front in this region and eliminated the buzzing combustion. Even with the fuel injectors moved upstream near the diffuser inlet, as indicated by the diagram, the combustion remained stable.

Such experiences with combustion instability verify the need for good internal aerodynamic design and the location of a flame seat in separated or low-velocity regions.

SHELL COOLING

A problem that has been receiving considerable study is cooling of the tail-pipe burner shell. There are three general types of cooling or controlling burner wall temperature that can be applied; the optimum type depends on the maximum temperature level at which the burner is designed to operate. These three types are: (1) for burners designed to operate up to about 3000° R, control of flameholder location and fuel distribution so that the burning takes place well away from the wall thereby providing a layer of unburned gas along the wall; (2) for burners designed to operate up to about 3400° R, a liner along the entire burner length through which about 6 percent of the tail-pipe gas flow is passed to provide cooling for the burner wall and prevent the liner, which has only thermal stresses, from overheating; and (3) for burners designed to operate at temperatures up to maximum obtainable temperatures, a shroud extending over the entire burner length through which ram air is pumped to cool the burner wall. Types 1 and 2 both require a slight amount of external cooling air also to prevent overheating of the airplane structure.

The effect of fuel distribution on the variations of average wall temperature at the downstream end of the liner and specific fuel consumption with exhaust-gas temperature are illustrated in figure 11. It should be noted that severe circumferential wall temperature

~~CONFIDENTIAL~~



gradients existed at the downstream end of the liner; local temperatures were in some cases as much as 300° F above the average values. Concentrating the area of fuel injection toward the inner wall of the diffuser, as indicated by the shaded regions in the sketch, lowered the wall temperature at the burner outlet by 50° F during operation with an exhaust-gas temperature of 3000° R. In both cases the wall temperature at the downstream end of the burner was well within allowable limits at an exhaust-gas temperature of 3000° R. A small amount of external cooling existed during these experiments, both convection to the low-velocity tunnel air stream and radiation to the tunnel wall. As indicated by the rise in specific fuel consumption, the reduction in wall temperature was accompanied by a slight decrease in combustion efficiency. This rise in specific fuel consumption is attributed to maintaining the flameholder geometry fixed while changing fuel distribution. The loss in specific fuel consumption may be recoverable by properly tailoring the flameholder to conform to the new fuel distribution.

Reductions in wall temperature at the burner outlet resulting from the installation of a liner are shown in figure 12. Installing a liner the full length of the burner section with no change in flameholder or fuel distribution lowered the wall temperature at the burner outlet from 1260° to 1050° F for operation at an exhaust-gas temperature of 3300° R. This reduction in wall temperature was achieved with no significant effect on combustion efficiency, as indicated by the specific fuel consumptions. Although the shell temperature was well within the operating limits, operation at exhaust-gas temperatures above 3300° to 3400° R is inadvisable because the temperature at the downstream end of the liner has reached 1700° to 1800° F. Because the liner is an essentially unstressed shield between the burner shell and burning region, these temperatures represent the allowable limits of operation.

Because difficulty is often encountered with liner warping, it may be desirable in some cases to replace the liner with shroud cooling in this range of exhaust-gas temperatures as well as at higher temperatures. In order to aid in evolving a correlation for shroud type cooling, a detailed cooling investigation was conducted in the altitude wind tunnel. An extensively instrumented burner was used which had a shroud fully insulated on the outside and which was designed to provide independent control of temperature, pressure, and air flow through the cooling passage. A cooling correlation was developed from these data to aid in predicting the cooling requirements at conditions other than those at which data were obtained. It is important to note that the correlation obtained was dependent upon the radial temperature profile across the burner. The burner used was typical of good design for operation at an exhaust-gas temperature of 3500° R; consequently, the data are generally applicable in this temperature range. For a burner



CONFIDENTIAL

designed to operate at an exhaust-gas temperature near 4000° R, consequently with a more uniform temperature profile, slightly more cooling air would probably be required than is indicated by the correlation.

Ram cooling air requirements based on the cooling correlation developed are shown in figure 13 for a shroud having a $1/2$ -inch passage height and extending the full length of the burner. As exhaust-gas temperature was increased or as cooling air flow was reduced, the wall temperatures at the burner outlet increased rapidly. For operation at exhaust-gas temperatures between 3600° and 4000° R at the limiting shell temperature of 1300° F, the cooling air required equalled 6 to 9 percent of the tail-pipe gas flow.

Some consideration has been given to techniques for reducing the cooling air flow requirements with a given burner geometry and wall temperature. One technique was that of finning the outer wall of the burner to increase the heat-transfer area in the cooling shroud. Calculations indicated that the increased pressure drop through a finned shroud outweighed the gains due to increased cooling surface. Another technique considered was that of insulating the inner wall of the burner shell with a ceramic coating to reduce the heat conduction from the gas stream to the burner shell. The insulating effect of a 0.015 inch thick coating was computed to reduce the shell temperature by about 60° F for a given cooling air flow.

The most promising method of more effective utilization of the cooling air is that of porous wall or transpiration type cooling. With this type of cooling, the burner shell would be constructed of finely woven wire cloth or other suitable porous material having a very low porosity and, of course, structurally supported. Air bled from the compressor outlet would pass between an external shroud and the porous burner wall, all of the air eventually passing through the wall to provide cooling. At present it appears that a suitable porous material will be available for future use.

The compressor bleed air required to maintain a burner-wall temperature of 1300° F with porous wall cooling was computed and is compared in figure 14 with the ram cooling air requirements for a shrouded burner having a $1/2$ -inch cooling passage height. In the case computed for porous wall cooling, it was found that the 340° F compressor bleed air passing through a shroud having a $1/2$ -inch passage height provided sufficient convective cooling for the first 2 feet of the 4-foot burner length assumed. The computations were therefore made for only the downstream half of the burner having a porous wall.

At an exhaust-gas temperature of 3500° R, only 1.9 percent of the compressor air flow would be required to cool the porous wall burner as compared to a ram cooling air flow equivalent to 5.1 percent of the

CONFIDENTIAL

CONFIDENTIAL

tail-pipe gas flow for shroud cooling. Even at a gas temperature of 4000°R , the porous wall burner would require only 2.4 percent compressor bleed air for cooling. At flight Mach numbers between 1.35 and 1.8, the amounts of compressor bleed air required with porous wall cooling would result in net thrust losses not exceeding 1 to 2 percent. Depending on the thrust losses associated with taking the external cooling air aboard and ducting it through the aircraft for shroud cooling, the porous wall method of cooling may prove most efficient for future use. This comparison is given further consideration in a subsequent paper by Mr. Wilsted.

CONCLUDING REMARKS

Data presented for recent tail-pipe burner investigations have shown that at flight Mach numbers between 1.35 and 1.80 at an altitude of 50,000 feet peak combustion efficiencies of 87 to 94 percent are available with a burner-inlet velocity of 360 feet per second. Correlation of the data indicated that an increase in burner-inlet velocity to 500 feet per second would reduce the peak combustion efficiencies for this range of conditions to 81 to 90 percent.

Encounters with combustion instability at altitudes as high as 35,000 feet have indicated the importance of good tail-pipe diffuser design to avoid flow separation and of the provision of flame seats at any location where separation or very low velocities may occur.

At exhaust-gas temperatures above 3500°R , shroud cooling of tail-pipe burners was shown to require ram cooling air exceeding 5 percent of the engine air flow. Computations indicate that porous wall cooling provides more efficient utilization of cooling air bled from the compressor; net thrust losses at these flight conditions would not exceed 1 to 2 percent.

REFERENCES

1. Fleming, W. A., Conrad, E. William, and Young, A. W.: Experimental Investigation of Tail-Pipe-Burner Design Variables. NACA RM E50K22, 1950.
2. Childs, J. Howard: Preliminary Correlation of Efficiency of Aircraft Gas-Turbine Combustors for Different Operating Conditions. NACA RM E50F15, 1950.
3. Taylor, H. D.: Design Criteria for and Applications of the Vortex Generator Mixing Principle. Rep. M-15038-1, Res. Dept., United Aircraft Corp., Feb. 15, 1948.
4. Wood, Charles C.: Preliminary Investigation of the Effects of Rectangular Vortex Generators on the Performance of a Short 1.9:1 Straight Wall Annular Diffuser. NACA RM (to be pub.)

[REDACTED]

TYPICAL TAIL-PIPE BURNER

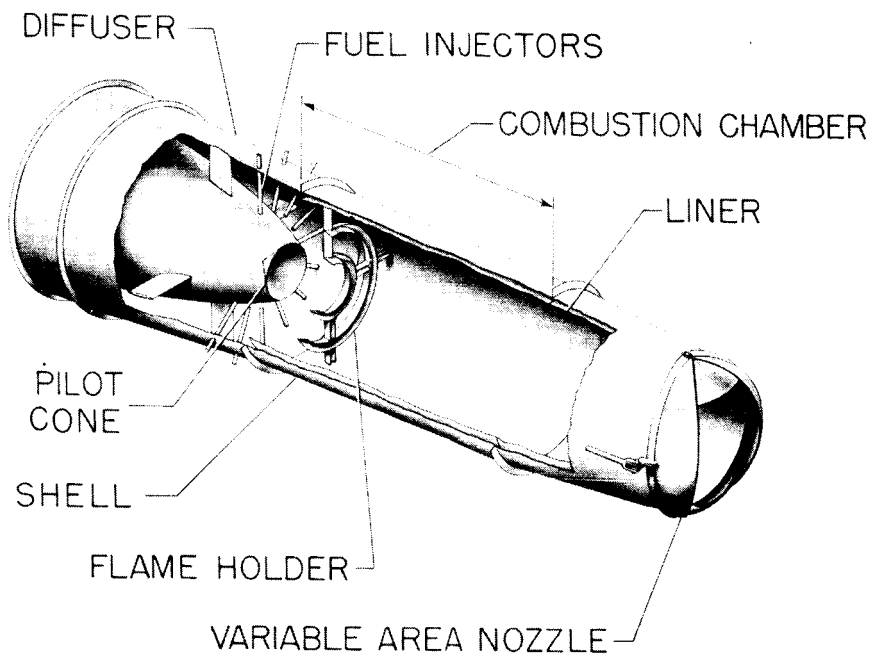


Figure 1

COMBUSTION CHARACTERISTICS OF TYPICAL TAIL-PIPE BURNER

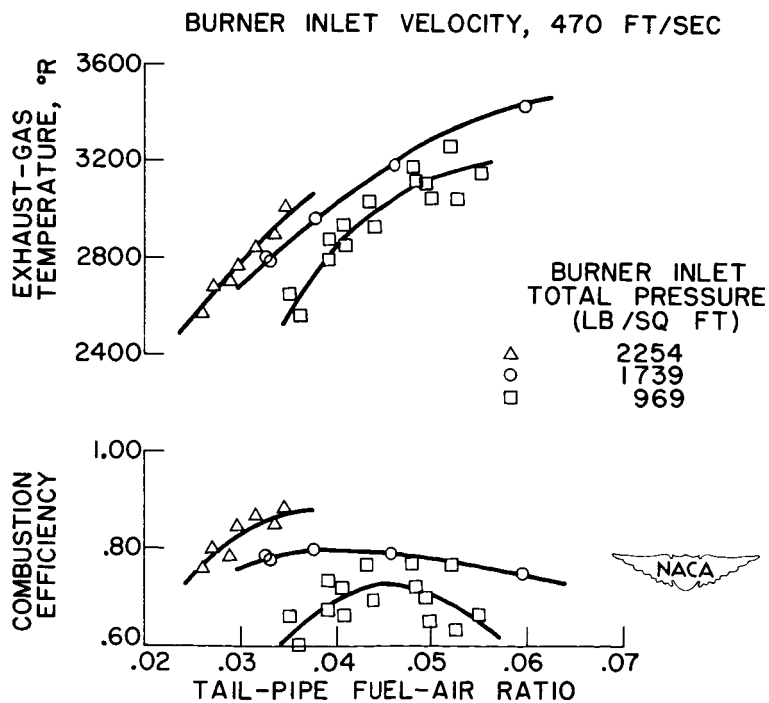
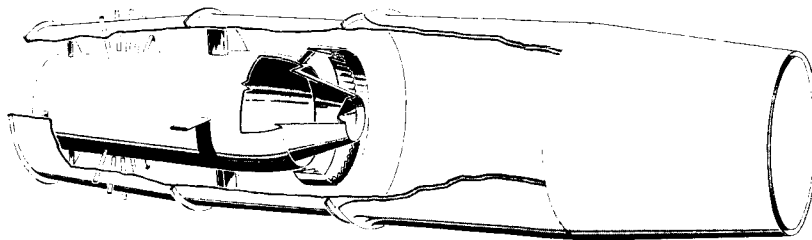


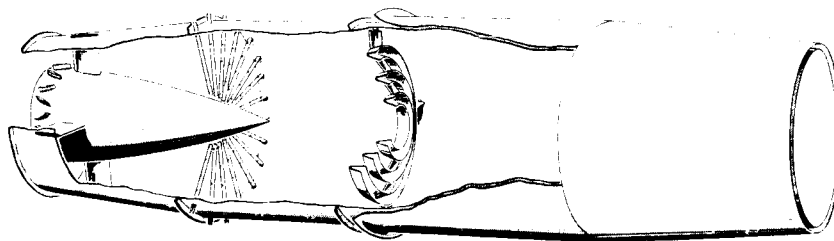
Figure 2

[REDACTED]

IMPROVED TAIL-PIPE BURNER DESIGNS



CONFIGURATION A



CONFIGURATION B

Figure 3

COMBUSTION CHARACTERISTICS OF CONFIGURATION A

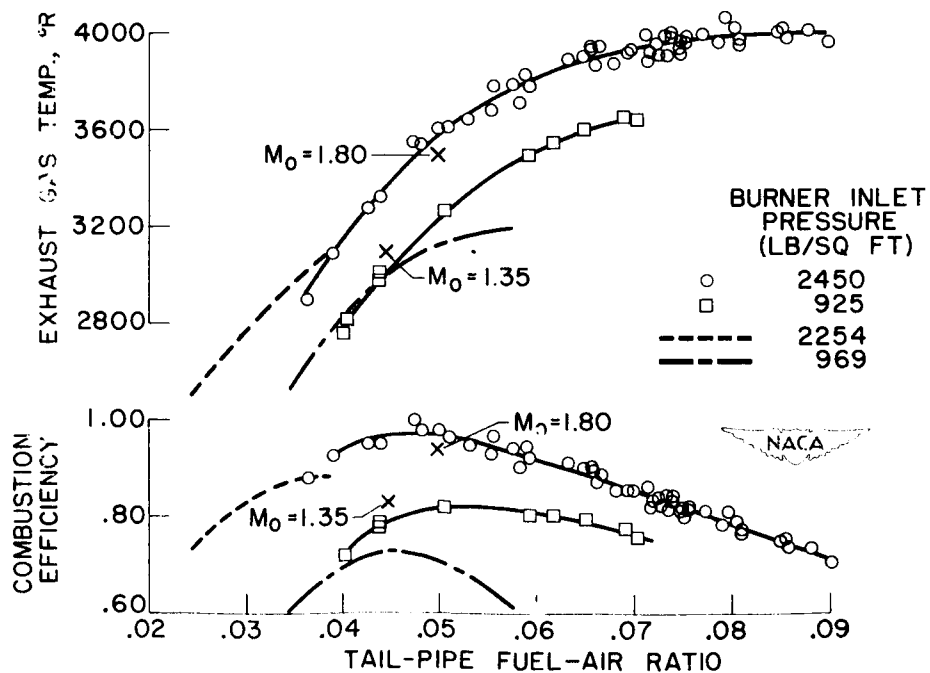


Figure 4

DECLASSIFIED

OVER-ALL PERFORMANCE CHARACTERISTICS OF CONFIGURATION A

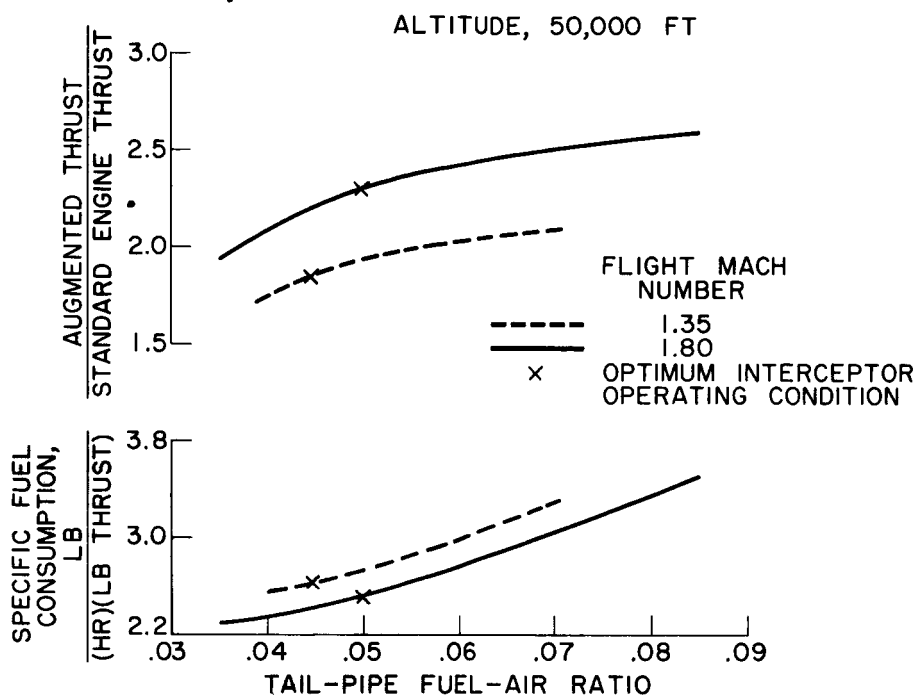


Figure 5

EFFECT OF BURNER INLET CONDITIONS ON COMBUSTION EFFICIENCY

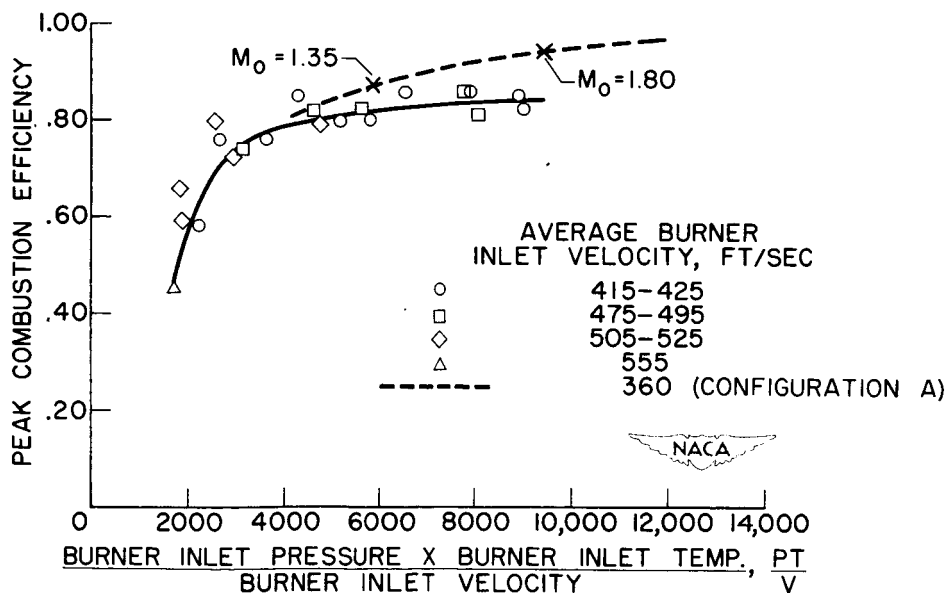


Figure 6

037102440

TYPICAL BURNER INLET VELOCITY PROFILE

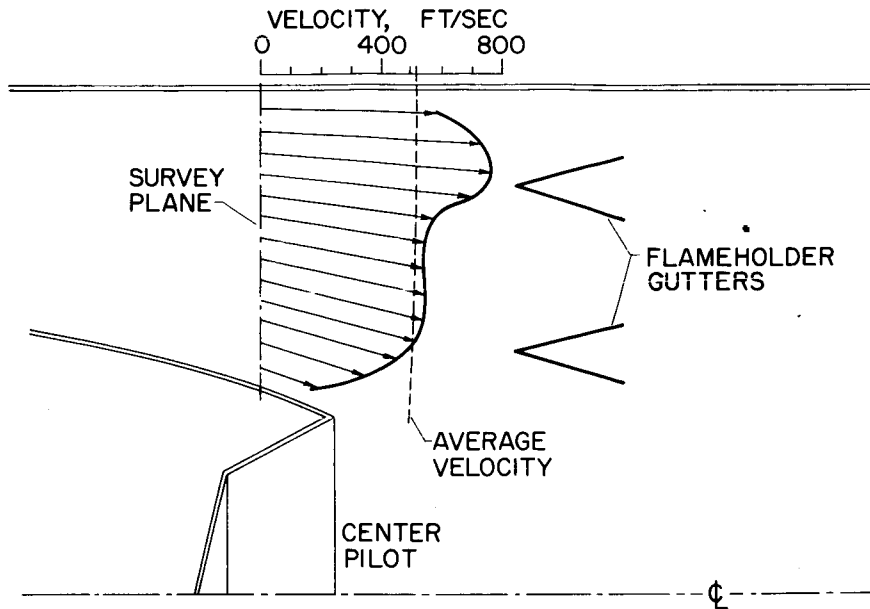


Figure 7

VORTEX GENERATOR INSTALLATION FOR CONFIGURATION B

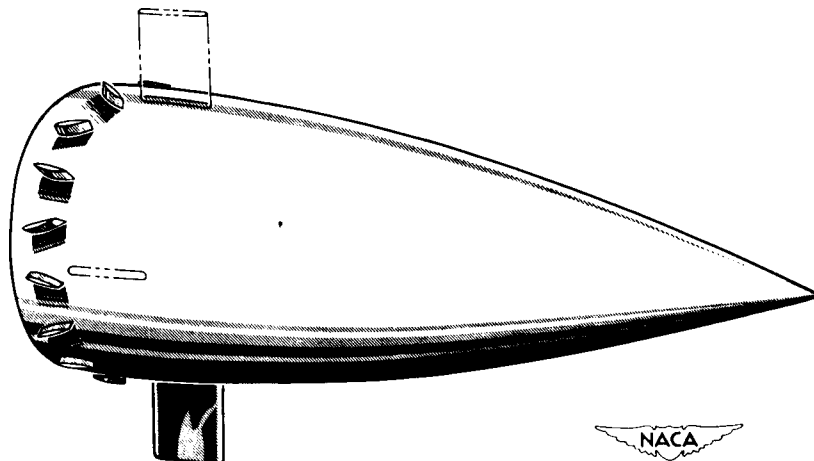


Figure 8

DECLASSIFIED

EFFECT OF VORTEX GENERATOR ON DIFFUSER OUTLET VELOCITY PROFILES

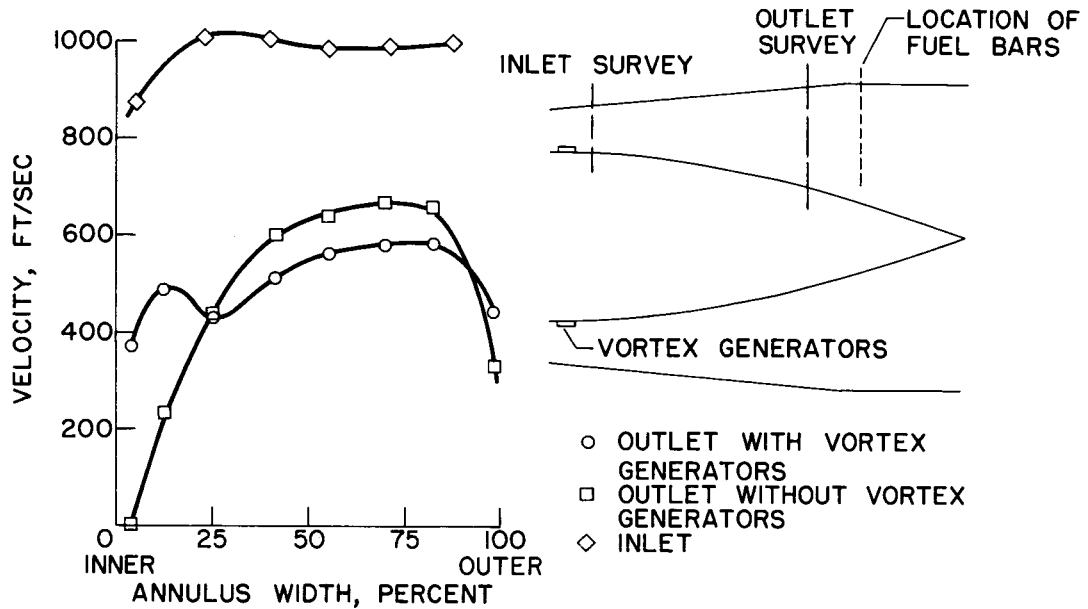


Figure 9

MODIFICATION FOR IMPROVING COMBUSTION STABILITY

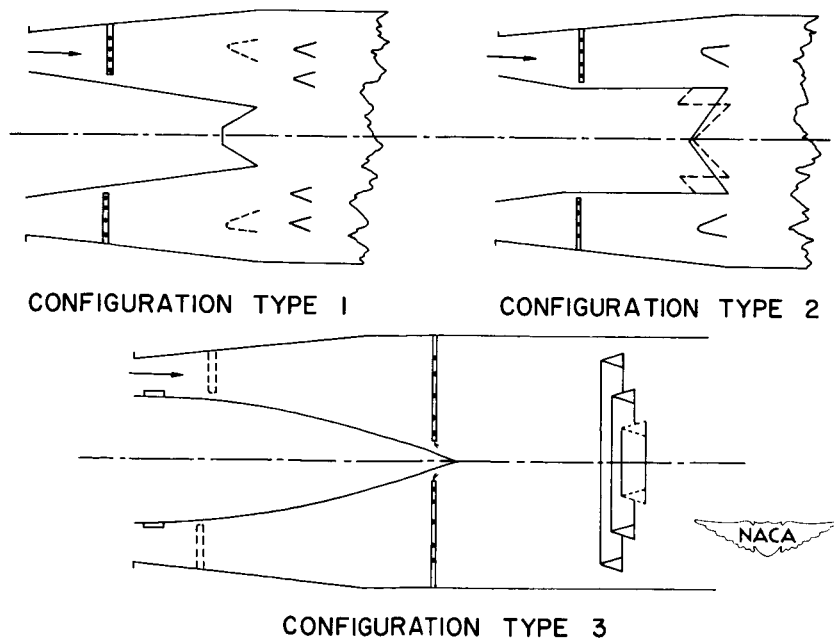


Figure 10

CONFIDENTIAL

EFFECT OF FUEL DISTRIBUTION ON BURNER WALL TEMPERATURE

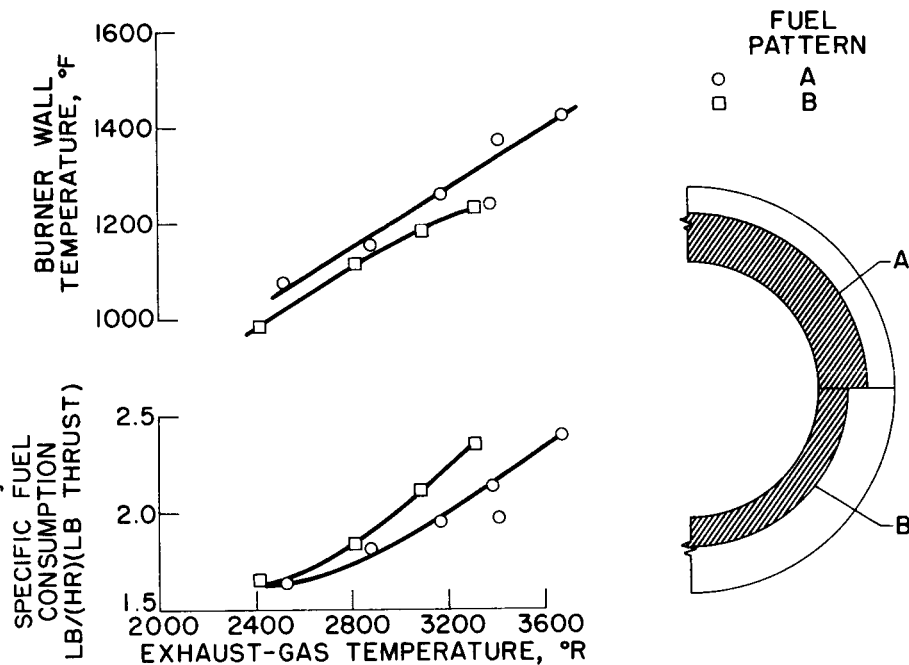


Figure 11

EFFECT OF LINER ON BURNER WALL TEMPERATURE

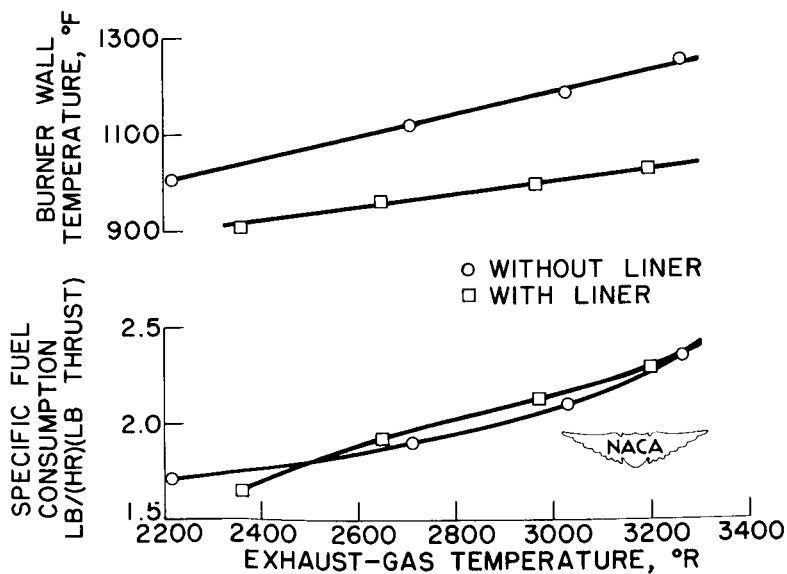


Figure 12

DECLASSIFIED

COOLING-AIR REQUIREMENTS WITH SHROUD

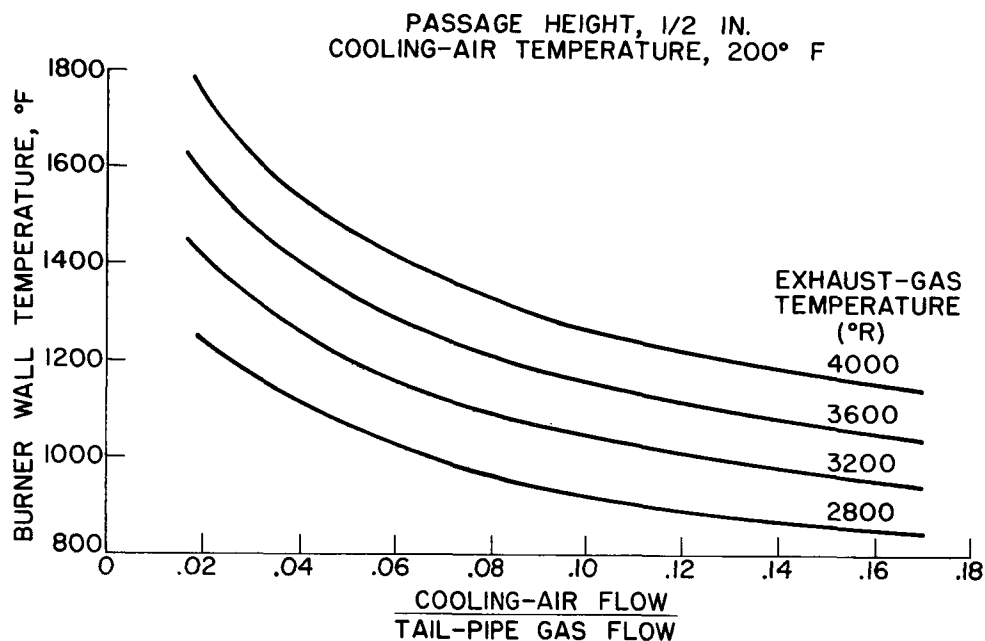


Figure 13

COMPARISON OF SHROUD AND POROUS WALL COOLING

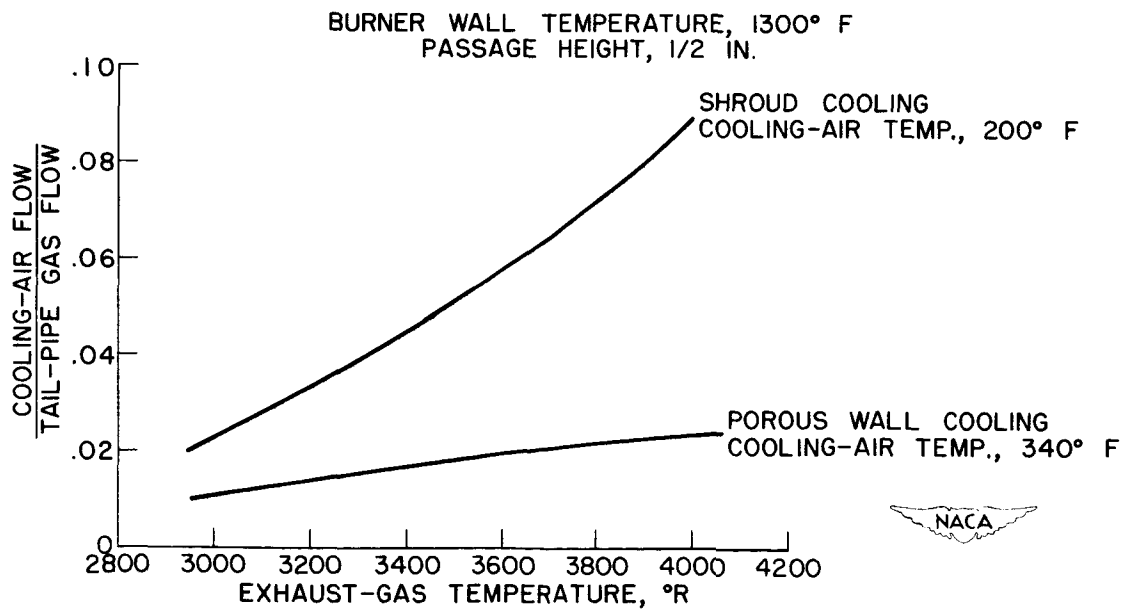


Figure 14

DECLASSIFIED

5. COMMENTS Ic

DECLASSIFIED

5. - COMMENTS Ic

By Bruce T. Lundin

Some of the desirable design features of an afterburner are illustrated schematically in the turbojet engine shown in figure 1. V-gutter-type flame holders and adequate mixing distance between the point of fuel injection and the flame holder still constitute the best afterburner configuration that has been investigated. It was also noted that flow separation from the diffuser inner cone has been encountered in the diffusers of many engines. Because fuel is usually injected into this annular passage to obtain the necessary mixing distances for good combustion efficiency, this flow separation may be the source of severe combustion instability or "screeching," particularly at high pressures. Thus, in order to obtain both stable combustion performance and the even velocity profiles that will be necessary for burners operating at high average velocities, good aerodynamic characteristics must be provided in the burner inlet diffuser. Diffuser inner cones that will provide a more gradual rate of change of flow area with axial distance than incorporated in many current engines are considered necessary, and vortex generators may prove helpful in preventing flow separation, particularly in engines having an unfavorable turbine-outlet velocity profile.

Although cooling of afterburners operating at gas temperatures of about 3400°R may be satisfactorily accomplished by an inner liner and an external air shroud, other cooling methods will probably be necessary for operation at higher gas temperatures. In this cooling at high gas temperatures, considerable promise is indicated by analytical investigations of porous-wall, or transpiration, cooling, such as are currently being studied for turbine-blade cooling.

With regard to the other components of the engine, specifically the compressor, the combustion chamber, and the turbine, improvements in their characteristics that will provide even better airplane performance than afforded by current types of components are, of course, possible and here the analysis summarized in the first paper provides an indication of the most important and promising avenues of approach. Both engine weight and component efficiency were shown to be variables of first-order importance; a high premium therefore exists on lightweight compressors that will handle a high mass flow rate and still retain a high efficiency over a reasonable operating range. When the rather large number of stages required in present axial-flow compressor designs are considered, together with the fact that from 35 to 40 percent of the total engine weight is concentrated in the compressor, methods of extending the Mach number limits of the first stage, thus permitting higher rotative speeds and increased effectiveness of all following stages, become particularly attractive methods of reducing engine weight.

DECLASSIFIED

CONFIDENTIAL

A second important engine design feature that has been previously discussed is the use of a convergent-divergent exhaust nozzle. While the development of such a nozzle presents many practical difficulties and may not be completely solved for some time to come, it is of interest to look a little further into some of the implications of the use of such a nozzle by referring to figure 2.

This figure, in which combat time is plotted against the afterburner outlet temperature for the two types of exhaust nozzle, is the same as previously presented in the first paper. As mentioned therein, the greater thrust per pound of air, and hence the smaller engine required when a convergent-divergent exhaust nozzle is used, decrease the emphasis on high thrust and increase the importance of specific fuel consumption, with the result that the optimum afterburner temperature is decreased. Even for this high Mach number flight condition, with its 2-g maneuverability requirement, the optimum temperature is in the region of 3000° R. If, now, a turbine-inlet temperature of the order of 3000° R becomes attainable by future developments in turbine-cooling methods, the optimum afterburner temperature is still further reduced and it is apparent that the desired temperature rise in the afterburner will be only a few hundred degrees. In this event, it may well be best, at least insofar as overall flight endurance is concerned, to use an engine without an afterburner and thus realize important weight savings at slight sacrifice in engine thrust. Although it has been previously pointed out that the use of a high turbine-inlet temperature does not greatly improve the airplane performance when an engine with a simple convergent nozzle is used, it can be seen here that the convergent-divergent exhaust nozzle, in addition to providing improved engine performance in its own right, places increased emphasis on the attainment of higher turbine-inlet temperatures through the application of turbine-cooling methods.

A brief review of some of the research investigation applicable to aerodynamic and structural problems involved in the development of compressors and in the attainment of higher turbine-inlet temperatures by effective methods of turbine cooling will be presented in the next paper.

DECLASSIFIED

TURBOJET ENGINE WITH SUGGESTED AFTERBURNER DESIGN FEATURES

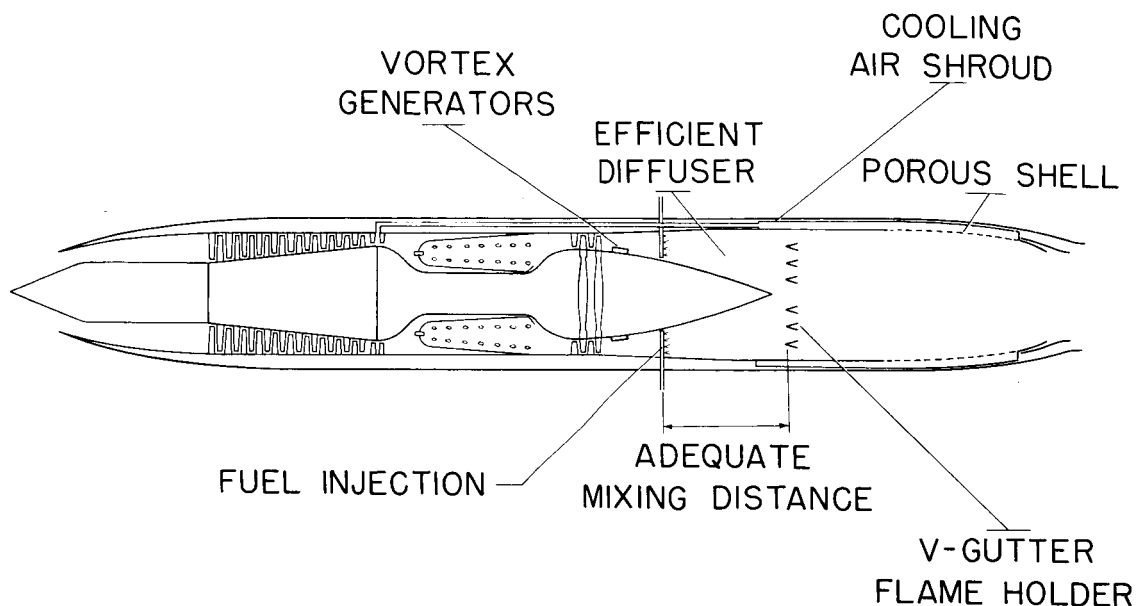


Figure 1

EFFECT OF FULLY EXPANDED VARIABLE AREA NOZZLE

DESIGN $M_0 = 1.8$

$W_a/A_c = 30 \text{ LB}/(\text{SEC})(\text{SQ FT})$

$T_4 = 2000^\circ \text{R}$

$(P_3/P_2) = 5$

$\eta_{c, \text{max}} = .85$

$W_e/F = .3$

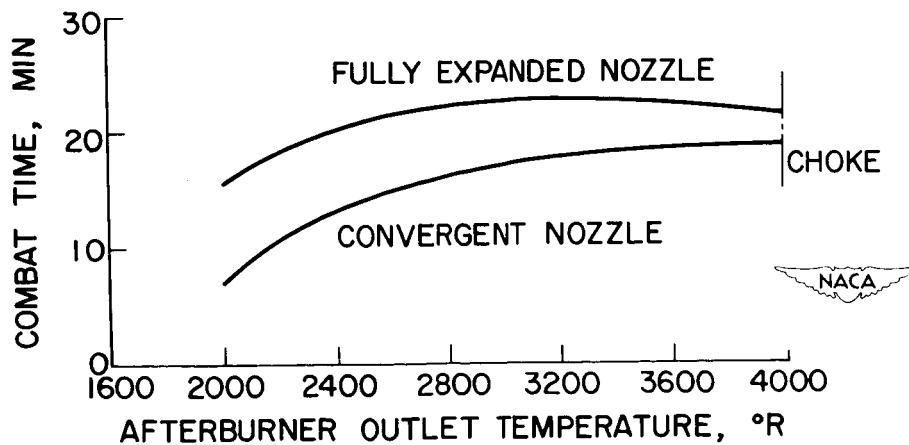


Figure 2

DECLASSIFIED

6. SOME NOTES ON ENGINE-COMPONENT RESEARCH

By Robert O. Bullock

[REDACTED]

SECRET

6. - SOME NOTES ON ENGINE-COMPONENT RESEARCH

By Robert O. Bullock

INTRODUCTION

As previously indicated, improved turbojet engines for supersonic flight will result from decreasing the size and the weight of the compressors and turbines and from increasing the turbine-inlet temperature, especially if it is high enough to eliminate afterburners. If the axial length, as well as the diameter, can be sufficiently reduced, decreases in size and weight can result from the use of higher rotative speeds so that the number of blades and the axial length of the rotating parts can be greatly reduced. These changes must be accomplished, however, without decreasing the flow capacity of the engine or sensibly reducing the efficiency. The principal obstacle to the development of compact and light compressors in this manner has been the lack of knowledge of how to cope with high Mach numbers on compressor blades. The principal turbine problem, on the other hand, has been the lack of knowledge of how to resist large centrifugal blade forces at high temperatures. This limitation not only prevents the use of higher rotative speeds, but also prevents the use of higher turbine-inlet temperatures. Combustion-chamber efficiency and life is another problem to be solved before higher turbine-inlet temperatures can be used. Overcoming these obstacles has been the continued objective of research programs at both the Lewis and Langley laboratories and a few of the results of these investigations will be presented in this paper. Since most of the work has been of the exploratory type, the results are presented not with the idea of suggesting immediate design changes in the components of turbojet engines for supersonic flight, but rather with the idea of indicating how the desired improvements may be obtained in the future by extending the degrees of design freedom.

COMPRESSOR BLADES FOR HIGH MACH NUMBERS

The necessity of limiting compressor-blade Mach numbers to the present values, which are of the order of 0.8, is particularly troublesome at the compressor inlet. High axial velocities are required to obtain the desired high flow rates; the rotative speed of the blades must therefore be limited. In the latter stages of the compressor, however, the air temperature is high, the volume flow rates are low, and the Mach numbers are greatly reduced. Higher rotative speeds can not only be tolerated, but are also desirable in the latter stages, because both the high temperatures and the comparatively low speeds combine to reduce the pressure ratios these stages can produce. In other words, these stages are penalized by the limitations in the final stages. If

CONFIDENTIAL

the speed could be raised, higher pressure ratios could be obtained in all stages, particularly in the latter stages, and the length and weight of the compressor would be reduced.

The cause of the Mach number limits on a compressor blade is the same as that on subsonic airfoils. Blade sections having flat pressure profiles at high subsonic Mach numbers, as well as blade sections deliberately designed for transonic and supersonic flow, may therefore be expected to alleviate the problem. The results obtained from this approach are indicated in figure 1 where efficiency of a blade row is plotted against the Mach number relative to the pitch section of the blade row. The data for the dashed curve were obtained from a rotor blade row composed of conventional blade sections. Eliminating the pressure peaks through a design developed and tested at Langley Field produced the solid curve. The third curve represents a typical trend of transonic and supersonic blade sections investigated at this laboratory. The blade designed to have a flat pressure distribution at high subsonic Mach numbers is obviously more efficient than the conventional blade section, and immediate benefits will result from its use. Although the curve for the supersonic blade section indicates a lower level of efficiencies, gains are still to be had because the slope of the efficiency curve is always low.

Suppose, for example, that a compressor with a pressure ratio of 5 consisted of a transonic inlet stage having a pressure ratio of 1.31 followed by conventional subsonic stages. The rotative speed of this compressor could be 20 percent higher than the speeds of a corresponding conventional compressor. Transonic Mach numbers would exist in the first stage only; fewer stages would be required. Even if the efficiency of the first stage was 10 percent lower than that of a conventional stage, the over-all efficiency of the compressor would be approximately only 1.5 percent lower than that of the conventional compressor. A preliminary version of such an inlet stage has recently been constructed at this laboratory. It is believed that this stage will not have a 10-percent penalty in efficiency, however, because higher efficiencies have been observed in supersonic compressor of greater pressure ratio than 1.3.

As previously noted, high subsonic Mach numbers may be realized in the latter stages as a consequence of higher rotative speeds. Some idea of the resulting pressure ratios attainable in these stages is presented in figures 2 and 3. The variation of total pressure ratio with peak rotor efficiency is shown in figure 2 as obtained from tests of the Langley blade presented in figure 1. Pressure ratios approaching 1.6 were obtained with rotor efficiencies of 90 percent. Slightly lower pressure ratios have been obtained from stages composed of conventional blade sections at relatively high subsonic Mach numbers. Results obtained from one of the single stages investigated at this laboratory

SECRET

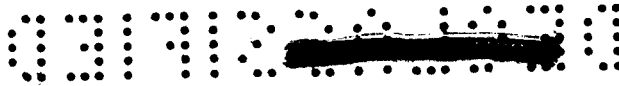
6-3

are shown in figure 3. Peak pressure ratios of 1.4 were obtained with a combined rotor and stator efficiency of 90 percent. Figure 3 is not to be directly compared with figure 2 since the cascade variables are not comparable. These data are presented only to show what might be done in the latter stages if the Mach numbers there are high enough.

The ultimate in high-pressure-ratio stages, of course, is to provide the pressure ratios desired in a compact single stage with few blades. Preliminary studies of one type supersonic compressor have indicated that the pressure ratios desired for supersonic flight (between 3 and 5) can be obtained in a single supersonic stage. An experimental rotor for this type of compressor is shown in figure 4. This rotor was designed to rotate at a speed of 1600 feet per second with no static pressure rise in the rotor itself; that is, it was designed as an impulse rotor. All the diffusion and shocks were to take place in stators downstream of the rotor, so that perforated diffusers and other devices could be used to reduce the losses. Experience with the first rotor and stator tested, however, showed that simple, fairly efficient diffuser blades could be designed as long as the Mach number ahead of the blades did not greatly exceed 1.5. The investigation also showed that the best over-all performance was obtained when there was a shock within the rotor and near the trailing edge, as well as in the diffuser blades. This rotor is now an impulse rotor in name only. The combined performance of such a rotor and stator is shown in figure 5. At the rotor speed of 1000 feet per second, where the flows in both the rotor and stator were transonic, an over-all pressure ratio of 1.8 was obtained with an efficiency of 85 percent. At 1200 feet per second, the pressure ratio was 2.3 with an efficiency of 77 percent. At higher speeds the efficiency was rapidly reduced. A second experimental rotor for this type of compressor has been constructed, but so far only the rotor, without stators, has been investigated. The data obtained are presented in figure 6. A total pressure ratio of 5 was obtained at design speed with a rotor efficiency of 84 percent. The investigation of the previous rotor and stator combination showed that stators having a 15-percent loss in total pressure can be designed to handle the flows leaving the rotor at the high-pressure-ratio condition. Accordingly, a complete stage containing this rotor is expected to produce a total pressure ratio of 4.2 with an efficiency of 76 percent. Stator blades are now being constructed to determine whether or not this expectation can be realized; even higher efficiencies may reasonably be expected to result from future developments.

TURBINE BLADES OF HIGH TAPER

Before high-speed compressors can be utilized, the problem of coping with centrifugal forces on turbine blades must be solved. The problem is usually most severe at the trailing edge of the rotor, where the density is lowest and the required height of the blade is greatest. The



stresses resulting from the centrifugal forces can be reduced by tapering the blade chord in the manner illustrated in figure 7. The profile shown here is the projection of a rotor blade on a plane through the axis of rotation and represents a configuration which could be designed to drive a high-speed supersonic compressor. In this particular turbine the maximum permissible taper in blade thickness was used, and the chord at the inner surface was approximately twice that at the outer surface. The performance of this turbine is shown in figure 8, where efficiency is plotted against blade-to-jet speed ratio. Efficiencies above 87 percent were observed in the vicinity of the indicated design point. Exploration of the possibilities of this type of design is being continued. Regarding the efficiency of high-speed turbines, it may be noted that higher speeds offer higher blade-to-jet speed ratios for the development of a given amount of power. Improvements in efficiency usually result from raising this ratio.

TURBINE COOLING

Higher turbine speeds can also be realized when turbine cooling is used. If the cooling of the blades is strong enough, the high temperature alloys can be replaced by alloy steels which have greater strength and lower strategic-material content. The larger allowable stresses permit the higher speeds to be utilized. A large background in turbine cooling has been accumulated at the Lewis laboratory as the result of research to ease the critical materials problem. Many of the results of this research have been presented in previous conferences at the NACA Lewis laboratory and only the results of a recent investigation will be highlighted at this time.

Several air cooled blades formed from aircraft-quality steels have been inserted in the turbine of a turbojet engine and subjected to endurance runs. All these blades were essentially hollow blades in which numbers of tubes were inserted to provide the necessary internal heat-transfer surfaces. The endurance runs consisted of repeating the following cycles of operation until some evidence of failure was observed: 5 minutes at the idling speed of 4000 rpm, 15 second acceleration to military power at 11,500 rpm, 15 minutes at military power, then 15 seconds deceleration to idling speed. The following table summarizes some of the test conditions and results of these runs.

Blade	Endurance at military rating			Total endurance time (hr)	Remarks
	Time (hr)	Turbine inlet temperature (°R)	Coolant-flow ratio		
9-tube cast SAE 4130 steel	22	2130	0.05	30.7	80 cycles. Test terminated by excessive creep
12-tube formed SAE 4130 steel	39	2130	0.05	52.3	154 cycles. Test terminated by excessive tip oxidation
12-tube formed Timken alloy 17-22A[S]	50.5	2130	0.05	67.7	200 cycles. No evidence of failure

The best endurance was obtained from the blade formed from a Timken alloy, 17-22A[S], which contained the following strategic-materials content: 1.25 percent chromium, 0.5 percent molybdenum, and 0.25 percent vanadium. Over 50 hours of operation at military power, together with 200 accelerations and decelerations with the attending heat shocks and suddenly applied loads, were successfully completed without any mechanical evidence of blade failure. The cooling airflow required for these runs was 5 percent of the compressor mass flow. Better cooling techniques have since been devised, and revised blades will be similarly investigated in the near future. It is anticipated that equal endurance will be obtained with 2 percent of the compressor mass flow instead of 5 percent.

Turbine cooling also permits the use of higher turbine-inlet temperatures to realize the improvements in performance outlined in the comments preceding. Available data indicate that nonstrategic turbine blades may operate with turbine-inlet temperatures as high as 2500 °R by using of the order of 5 percent of the compressor mass flow for cooling. By increasing the strategic content of the blades, the cooling airflow may be reduced or the turbine-inlet temperature may be even further increased.

COMBUSTION CHAMBER FOR HIGHER TEMPERATURE

Another problem in the development of higher turbine-inlet temperatures is the problem of combustion-chamber design. Two questions arise: How can the higher than normal fuel-air ratios be efficiently utilized, and how do the higher temperature levels affect the life of the

037130 [REDACTED]

combustion chamber? Preliminary investigations have given a partial answer to the first question, but the work is not sufficiently advanced to shed any light on the answer to the second. In figure 9 are presented the results of a preliminary investigation to determine how the efficiency of a conventional combustion chamber is affected when the fuel-air ratio is increased beyond the normal limits. Combustion temperature rise is plotted against fuel-air ratio, and lines of constant combustion efficiency are drawn. Point A shows the fuel-air ratio and temperature rise required for the engine of the previously discussed interceptor at 1.8 Mach number, with a compressor pressure ratio of 5 and a turbine-inlet temperature of 2000° R. Point B represents the corresponding requirements for 2500° R. A small change in efficiency was observed, but the efficient attainment of higher temperatures does not seem to present a difficult problem. The problem of life must await future investigations, however, but it appears that the structural members behind the burner will present greater difficulties than the liner itself.

SUMMARY

Developments in compressor and turbine-blade designs and turbine-blade cooling indicate that moderate increases in rotative speeds can be made at the present time for reducing the size and weight of engines. Moderate increases in turbine-inlet temperature can also be made. A consideration of the rate of progress in the supersonic-compressors and turbine-cooling fields indicates that designs for light and compact research engines with higher turbine-inlet temperatures may be made in the near future; applying these ideas to production engines, however, will take more time and effort.

[REDACTED]

CONFIDENTIAL

EFFECT OF RELATIVE INLET MACH NUMBER ON ADIABATIC EFFICIENCY

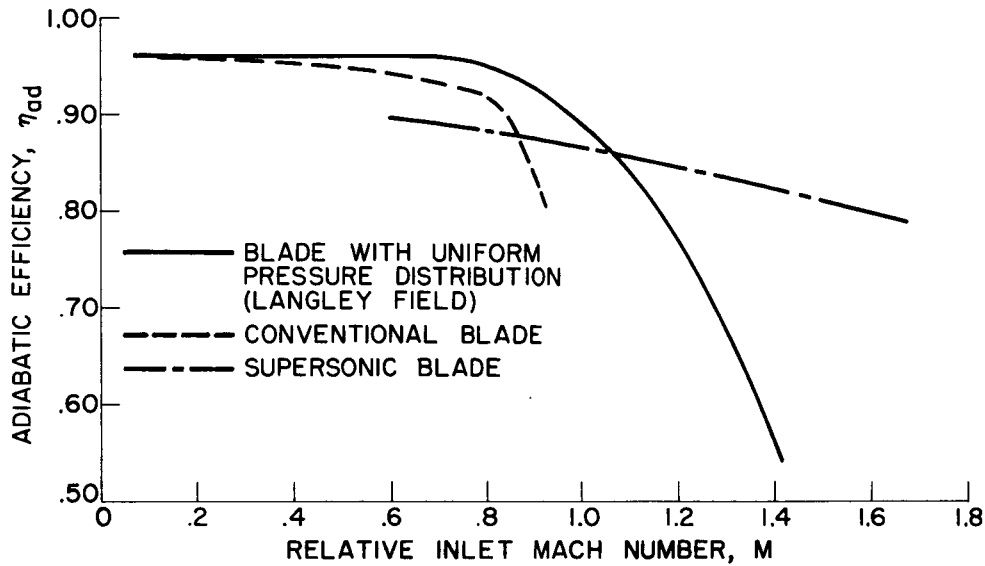


Figure 1

BLADE WITH UNIFORM PRESSURE DISTRIBUTION

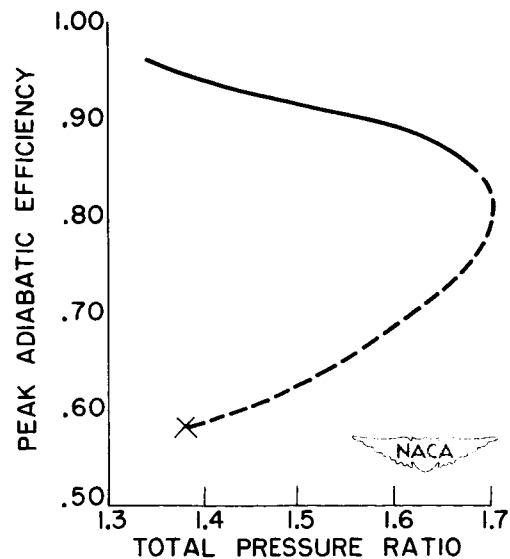


Figure 2

CONFIDENTIAL

CONVENTIONAL STAGE

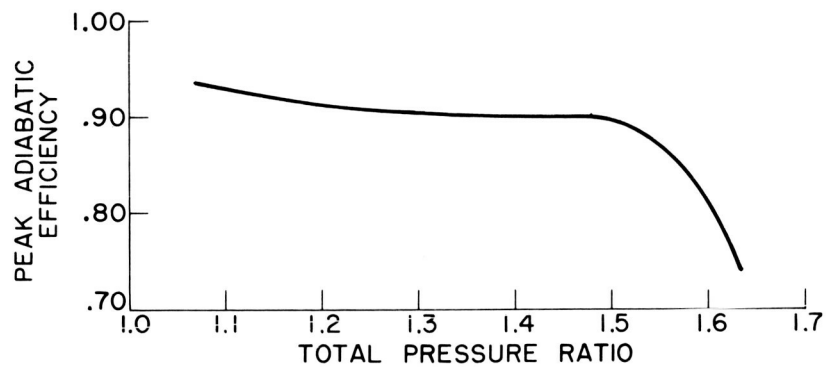


Figure 3

16" SUPERSONIC IMPULSE ROTOR

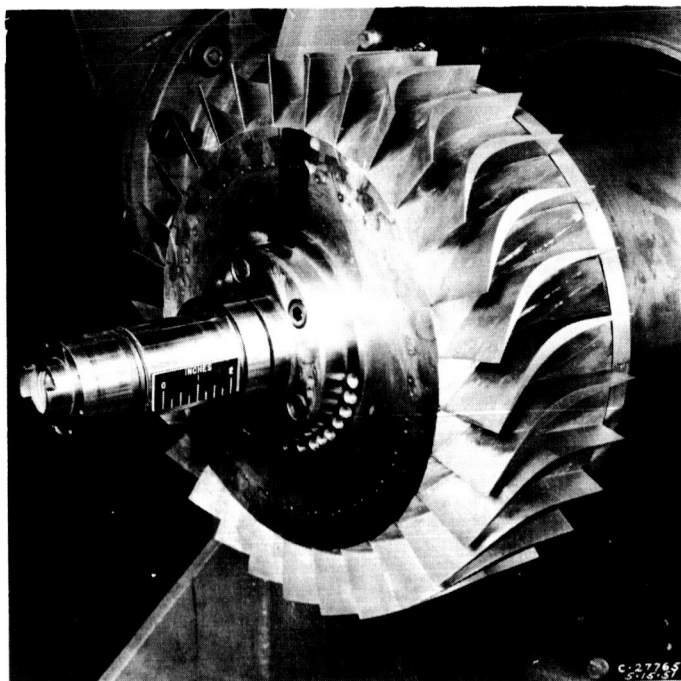


Figure 4



CONFIDENTIAL

DECLASSIFIED

2235-6

STAGE CHARACTERISTICS OF IMPULSE-TYPE SUPERSONIC COMPRESSOR

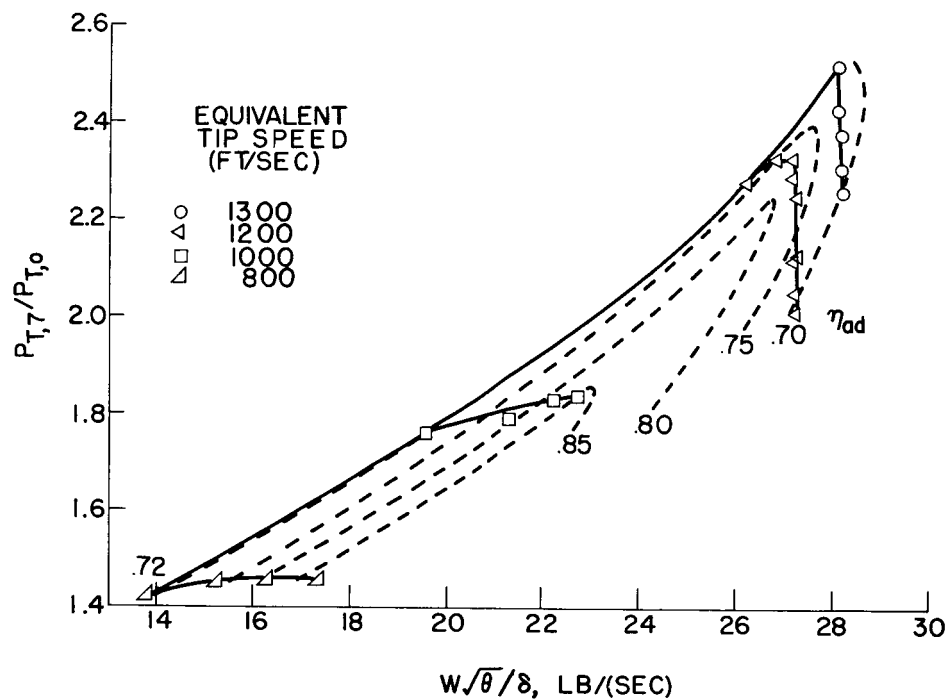


Figure 5

ROTOR PERFORMANCE OF IMPULSE-TYPE SUPERSONIC COMPRESSOR

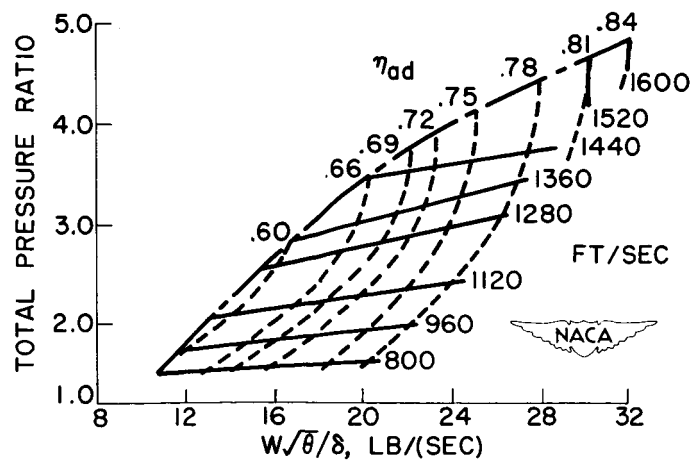


Figure 6

0371024430

BLADE CONTOUR OF TURBINE WITH LARGE HUB TAPER

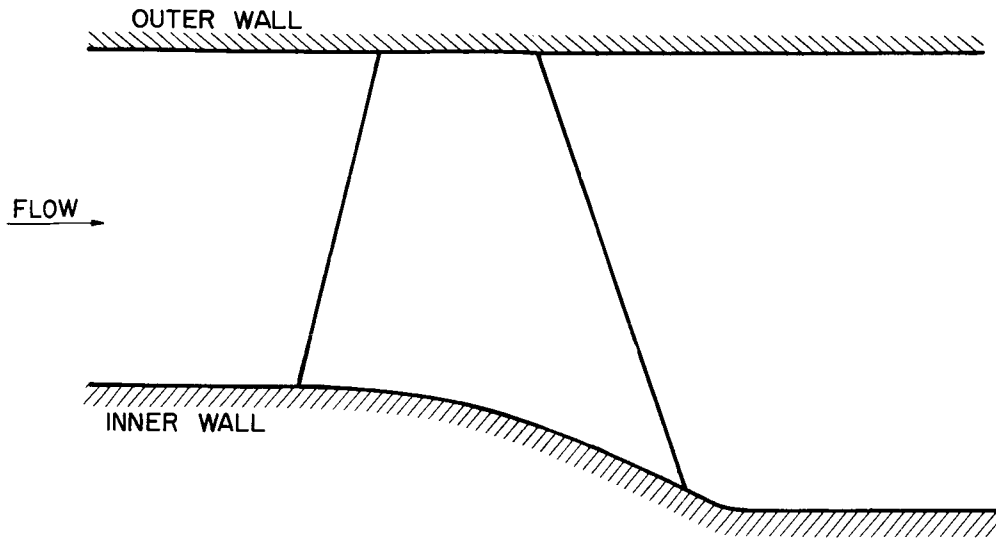


Figure 7

EFFICIENCY OF TURBINE WITH LARGE HUB TAPER

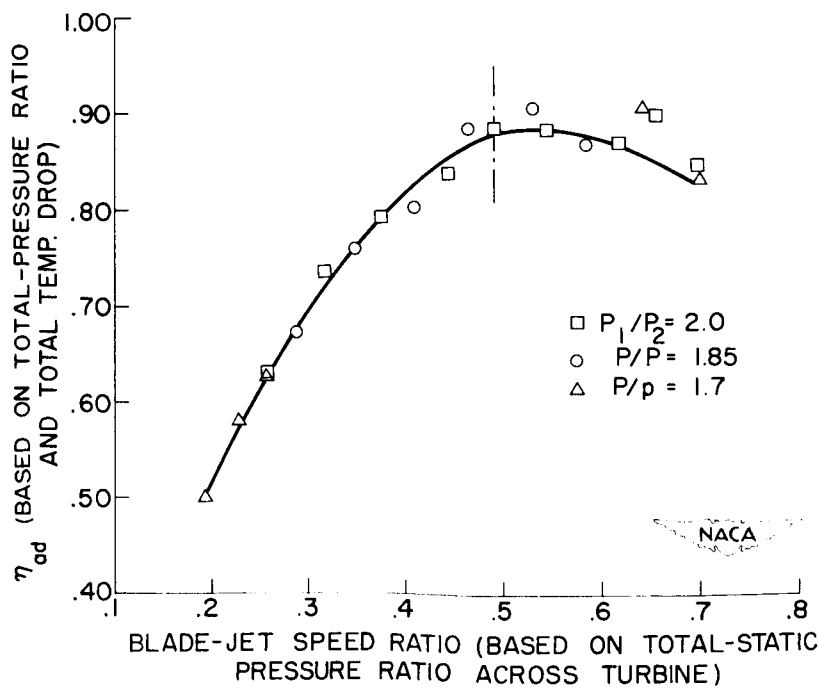


Figure 8

DECLASSIFIED

2275-6

VARIATION OF MEAN TEMPERATURE RISE WITH FUEL-AIR RATIO

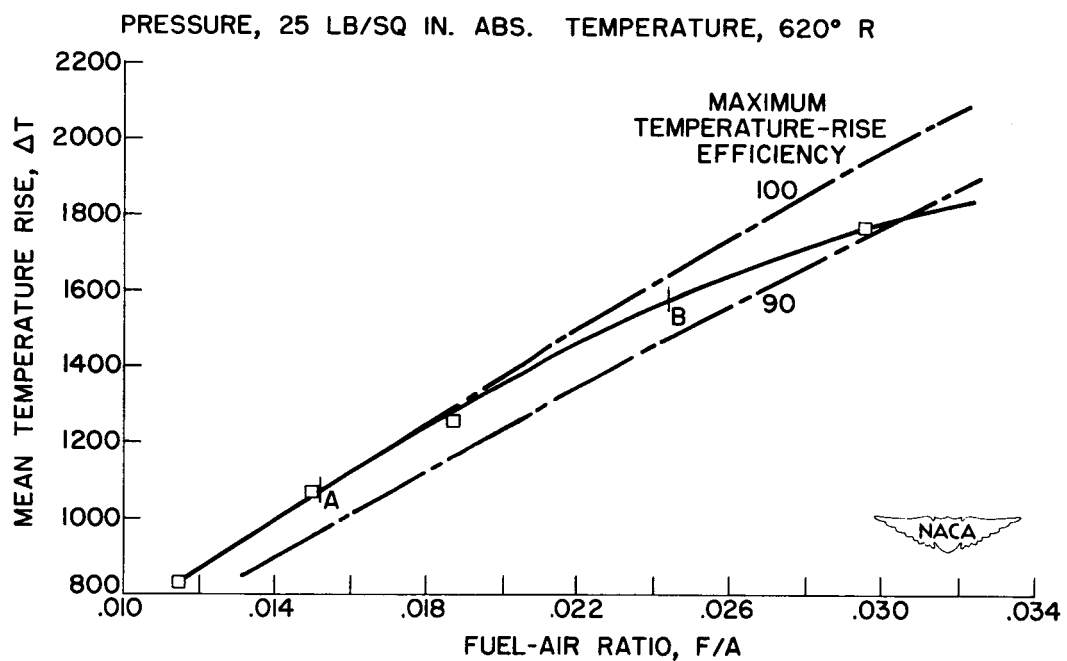


Figure 9

~~DECLASSIFIED~~

7. COMMENTS Id

[REDACTED]

SECRET

7. - COMMENTS Id

By Bruce T. Lundin

2235

In some of the cascade and supersonic compressor research cited in the preceeding paper, it was observed that operation at transonic rather than purely supersonic conditions was possible with fairly high efficiencies. Design studies of compressors specifically designed for this type of operation further indicate that appreciable increases in air flow capacity may be possible with this type of compressor and the very desirable characteristic of high efficiency may be retained. Such a compressor, which may be termed a transonic compressor, is illustrated in the engine shown in figure 1. For a pressure ratio of 5, a possible arrangement would be to use a transonic first stage followed by four or five more conventional subsonic stages. This use of an inlet stage that has high mass flow characteristics and that may be rotated at high speed will increase the effectiveness, or pressure ratio per stage, of all of the following subsonic stages with a resulting reduction in the total number of stages required, and hence a potential saving in engine weight. Although the efficiency of the inlet stage is somewhat lower than would be desired, its combination with the more efficient subsonic stages should provide a compressor with an over-all efficiency that is not appreciably lower than that of many present axial-flow designs.

Both turbine cooling and combustion research were also reviewed that indicated that operation at a turbine-inlet temperature of about 2500°R is possible with air-cooled turbine blades and conventional combustion chambers. Continued increases in these operating temperatures are, of course, to be expected by future research and developments.

In addition to the principal internal components of the engine that were discussed in the previous papers, a satisfactory control system for the engine must be provided. The control of a turbojet engine with an afterburner becomes considerably more complicated than that of a simple turbojet engine because of the extra degree of freedom possessed by the engine. Not only must the primary fuel flow be regulated to maintain the correct engine speed, but the exhaust-nozzle area must be manipulated in accordance with the afterburner fuel flow in order to maintain the proper value of turbine gas temperature. Moreover, the thrust output of the engine, and hence the integrated or scheduled values of these three operating variables, must be also regulated by the movements of a single control lever or throttle. One of the principal problems encountered in the development of control systems for this purpose is to provide a system that will enable the thrust of the engine to be changed quickly from one level of operation to another and that will still operate stably over wide ranges of flight and operating conditions.

SECRET

03170 [REDACTED] 00

In addition to these control system requirements of providing a rapid thrust response without oscillatory operation, the problem of flight speed stability at supersonic speeds has been frequently discussed. This problem may be illustrated with reference to figure 2, where the thrust and drag are plotted against the flight Mach number. The thrust curve in this figure is representative of the output of an afterburning turbojet engine operating at constant speed and temperature conditions, and the drag curve is typical of supersonic airplanes. In the subsonic speed region, the drag increases rapidly with an increase in flight speed, while the engine thrust curve is fairly flat; therefore, as the thrust is reduced to establish a given flight speed, the thrust curve will intersect the drag curve with a large angle, and stable speed conditions will be provided. In the supersonic speed region, however, the thrust curve is approximately parallel to the drag curve, and its intersection with the drag curve may occur at a very small angle or even be superimposed on the drag curve for fairly wide speed ranges, thus resulting in an unstable flight speed condition. Control systems for stable speed conditions must therefore provide a variation in thrust with flight speed that will intersect the drag curve at large angles and yet permit the attainment of maximum thrust output when required for acceleration.

Some possible solutions to these control problems of flight speed stability, rapid thrust response, and stable engine operation will be discussed in the next paper.

[REDACTED]

SECRET

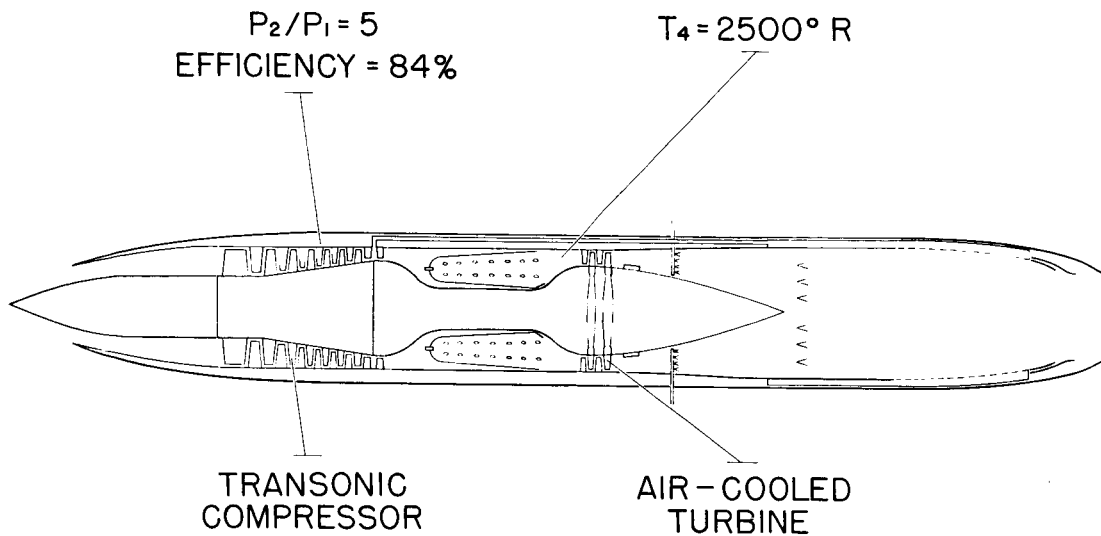
TURBOJET ENGINE WITH TRANSONIC
COMPRESSOR AND AFTERBURNER

Figure 1

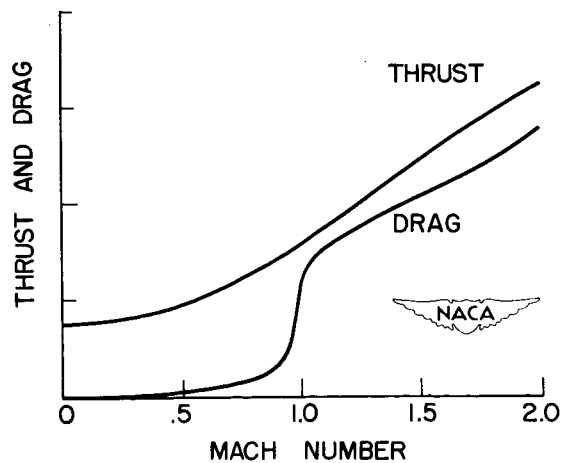
TYPICAL VARIATION OF THRUST
AND DRAG WITH FLIGHT SPEED

Figure 2

DECLASSIFIED

8. TURBOJET-ENGINE CONTROL SYSTEMS IN SUPERSONIC
FLIGHT

By John C. Sanders

[REDACTED]

CONFIDENTIAL

8. - TURBOJET-ENGINE CONTROL SYSTEMS

IN SUPERSONIC FLIGHT

By John C. Sanders

INTRODUCTION

Surveys of the principal problems in control at supersonic flight have shown that flight speed instability and the necessity for adjusting the inlet diffuser to the engine constitute two problems which are of particular interest in supersonic flight. The object of this paper is to survey the problems involved in providing a control system that will afford safe regulation of the engine, permit the obtaining of maximum power and lowest fuel consumption, and provide stable flight speed. A commonly proposed control system is described herein that will provide safe operation and maximum power. A discussion of the difficulties involved in this type of control, means of improving the safe operation, and means for avoiding oscillation in thrust will be included. An investigation of methods of incorporating a system for stabilizing flight speed will then be made, and finally consideration will be given to the control system for regulating the diffuser.

CONTROL TO PROVIDE SAFE OPERATION

A control system for the turbojet engine with afterburner is required to operate the engine safely, to permit the engine to develop its maximum thrust, to operate the engine most economically at any thrust output, and to achieve rapid changes in thrust. Danger of injury to the engine results from overspeeding the engine rotor or from excessive turbine temperature. On the other hand, when the afterburner is in operation, the maximum thrust and minimum specific fuel consumption will be realized at maximum engine speed and turbine temperature. Consequently, the engine control will be required to maintain these two conditions.

One commonly proposed control system that will maintain maximum engine speed and temperature is shown in figure 1 for an engine with an afterburner. The engine speed is regulated by a speed controller that measures the speed of the engine and compares that speed with the desired speed, which is set by a schedule connected to the pilot's throttle. The difference between the measured speed and the desired speed excites a calculator which in turn adjusts the engine fuel flow to achieve the desired engine speed. The temperature control is of similar nature. The temperature at the turbine outlet is measured and compared with the

CONFIDENTIAL




desired turbine-outlet temperature as set by the pilot's throttle through a schedule. The difference between the desired temperature and the observed temperature excites a calculator which changes the exhaust nozzle to the engine in such a way as to establish the desired temperature. When the afterburner is in use, thrust is adjusted by scheduling the corrected afterburner fuel flow with throttle position.

An idea of how well this control system meets its requirements may be formed by inspection of experimental data obtained with an engine and control tested in the altitude wind tunnel. A transient record of the time history of thrust, engine, and turbine-inlet temperature following a change in afterburner fuel flow is shown in figure 2. This record shows that the thrust rose to its full value in less than two seconds. The engine speed was regulated within close limits since the increase in fuel flow to the afterburner caused the engine speed to drop only about 2 percent and the speed returned to its set value in about 2 seconds. The turbine-outlet temperature was not quite so accurately regulated, since a temperature overshoot of 300° resulted. However, the control returned the temperature to approximately its original value in less than 2 seconds. Thus, in this particular case, the control provided quick change in thrust and held the engine speed and temperature within reasonably narrow limits. The control, however, did exhibit one objectionable feature in that a severe thrust oscillation occurred. Thrust oscillation was equal in magnitude to the total thrust augmentation of the afterburner. This thrust oscillation was sufficiently severe to reduce the impulse of the afterburner 40 percent.

The cause of this oscillation can be seen if the cycle of events is traced in figure 1. The change in fuel flow caused a rise in the pressure at the discharge to the engine turbine, which in turn caused the engine speed to decrease. The speed control increased the engine fuel flow thereby raising the turbine-outlet temperature. The high turbine-outlet temperature excited the temperature control to open the nozzle. Opening of the nozzle reduced the turbine-outlet pressure, which in turn caused the engine speed to rise. The speed control then reduced the fuel flow thereby reducing the temperature. Thus, a long operating cycle occurs when a change is made in afterburner fuel flow and a considerable time lag exists between the change in fuel flow and the change in nozzle area. This long time lag between disturbance and correction makes oscillation likely.

The designer has a choice in the design of the calculators in the speed and temperature controllers. The calculators must have sufficiently high gain to hold the speed and temperature within the limits specified, but the higher these gains are made the more prone the system is to oscillate. Calculations have been made for a particular engine to show the effect of the gain of these calculators upon the accuracy with which the speed and temperature are regulated and the likelihood of oscillation. The dynamic constants used in this computation (fig. 3) are as follows:



Engine constants from equilibrium data

Speed change/engine fuel flow change, percent.	85.0
Turbine-outlet temperature change/engine fuel flow change, percent.	54.9
Speed change/nozzle area change, percent	54.3
Turbine-outlet temperature change/nozzle area change, percent.	24.4
Speed change/afterburner fuel flow change, percent	31.3
Turbine-outlet temperature change/afterburner fuel flow change, percent.	15.6

Engine constants from transient data

Turbine-outlet temperature change/engine speed change, percent.	-15.5
Response time constant of engine speed, seconds	1.0

Control system constants

Engine fuel valve lag time constant, seconds	1.0
Engine fuel hydraulic lag time constant, seconds	0.29
Thermocouple lag time constant, seconds.	0.1
Afterburner fuel valve lag time constant, seconds.	1.0
Exhaust nozzle (second order) first lag time constant, seconds.	1.0
Exhaust nozzle (second order) second lag time constant, seconds.	0.29

The results of this calculation are shown in a stability chart presented in figure 3. This figure shows that if only small deviations in engine speed N and turbine-outlet temperature T are specified, high values of gains in the speed and temperature controls must be used. However, high values of speed and temperature control gain create conditions of oscillation. Thus, it may be seen that there is a limit to the accuracy with which the speed and temperature may be regulated with this system. If a very close tolerance is set upon the speed and temperature deviation, some modification of this control system is necessary.

The condition under which the worst deviation in speed and temperature occur is when a large change in afterburner fuel flow is made. Consequently, if some system could be devised whereby the shock upon the speed and temperature control circuits resulting from this change in afterburner fuel flow could be reduced, then the requirements upon the speed and fuel-flow controls could be considerably relaxed and would permit the use of a stable control. The principles of control design for minimization of shock loads of this type are discussed in a general



manner by Boksenbom and Hood in reference 1. An application of these principles to the afterburner control problem is illustrated in the control system presented in figure 4. In figure 4, the control system is essentially the same as shown before, except that an additional loop has been added as shown by the broken lines. This loop connects the throttle with the nozzle. Changing thrust by moving the throttle in this case causes the following chain of action: (a) the throttle moves the fuel valve to the afterburner thereby increasing the fuel flow to the afterburner, (b) it simultaneously moves the nozzle area to approximately the value it should have when the system settles out, (c) then the remaining actions of the speed and temperature controller are to set the nozzle at exactly its proper position. Thus, this neutralizing control merely guesses the change in nozzle area which will be required and therefore greatly reduces the shock load upon the speed and temperature circuits. It is theoretically possible to design this neutralizer control circuit so that it completely eliminates the shock load resulting from change in fuel flow. In this case, a change in throttle position will cause a change in thrust with no deviation in speed and temperature.

Figure 5 shows the results of an analog computation of the time history of response of engine temperature and engine speed to a change in afterburner fuel flow with the original afterburner control and with the afterburner control including the neutralizing link. This figure shows close correspondence with experimentally observed response of figure 2. It is seen that a large deviation in temperature and speed occurs in the original control system. With the neutralizer link, the deviations in temperature and engine speed are almost eliminated. With the neutralizer link, the demand for high gains in the speed and temperature controls is therefore eliminated, and the design of a stable afterburner control system is simplified.

STABILIZATION OF FLIGHT SPEED

Several schemes for stabilizing flight speed are available. However, these schemes should be restricted to those that permit the engine to develop its full thrust without causing engine damage. If the engine is to get full thrust, the control must know the compressor-inlet pressure or density. If the control is to provide flight stabilization, it must know either the atmospheric pressure or the flight Mach number. Therefore, for flight speed stabilization, an additional quantity must be measured. The suggestion is made here that the flight Mach number be sensed and used to regulate the afterburner fuel flow as shown in figure 6. The control in figure 6 is the same as the previously discussed control including the neutralizer link in the afterburner nozzle circuit. However, in this case, the throttle does not adjust the afterburner fuel flow, but rather sets a desired flight speed. This flight



SECRET

speed is compared with the measured flight speed and the difference between the measured and the desired flight speed excites a calculator in such a manner that it adjusts the afterburner fuel flow to make the flight speed equal to the desired speed.

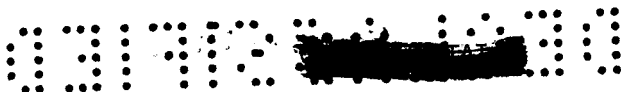
This control scheme introduces an additional control loop. The elements of this complete control loop can be seen in figure 7. In this figure the engine with its afterburner control system produces thrust upon the airplane. The airplane responds to a change in thrust by changing its flight Mach number. The change in flight Mach number is compared with the desired flight Mach number and the difference is fed to the flight speed calculator which adjusts the fuel flow to the afterburner, thus completing the control loop. There is an opposing control loop in this system, however, in that a change in flight Mach number would change the diffuser operation in such a manner as to change the airplane drag, change the engine thrust, and change the afterburner fuel flow which also changes the engine thrust. Now these two control loops have opposing action, because increase in flight Mach number operates through the diffuser to the engine to increase the thrust, whereas the increase in flight Mach number is compared with the set Mach number through the controller to reduce the thrust.

The control designer can make a choice of the gain of the flight speed calculator. The higher gain of the calculator will provide an increasing stability of the aircraft. In order to examine the effect of calculator gain upon stability, the index of stability for the complete control system is now reviewed.

The index for the stability is the time required for the airplane to reach the set Mach number. If the airplane takes an infinitely long time to reach its final speed, the system is completely unstable, as is the case with the previous control systems described. The more stable controls will reach the final or set Mach number more quickly. The number used to indicate this stability is the time constant of response of the entire engine airplane control system to a change in the set speed. (This criterion of stability is applicable if the response time of the engine is small compared to the response time of the airplane.) The response time is the time required for the flight speed to change 63 percent of the required change in flight speed. When this time constant is infinity, the system is unstable. The reciprocal of the time constant is therefore used as the index of stability in order to avoid the occurrence of infinity in the calculation.

Figure 8 shows the effect of the flight speed calculator gain upon the stability parameter, which is the reciprocal of the flight speed time constant. It also shows the fluctuation in afterburner fuel flow

SECRET



as a function of the gain of the flight speed calculator. This chart is applicable only to the particular combination of airplane and engine chosen for the illustration. It shows that a certain minimum gain is required of the flight speed calculator to produce a stable system. Above this gain the airplane responds more and more quickly and shows greater and greater stability. However, increasing the gain of the flight speed controller results in greater fluctuations in afterburner fuel flow and the gain can be set so high that the fluctuations in afterburner fuel flow could cause afterburner blow-out.


Another problem, the possibility of oscillation, is involved in the use of high gains. In general, if the response time of one element is much longer than any other element in a closed loop, little likelihood of oscillation exists. The time constant of response of the airplane to the change in thrust is about 30 seconds, whereas the time constant of the response of the engine to a change in afterburner fuel flow should not be greater than two seconds. The ratio here is one to fifteen, indicating little likelihood of oscillation. However, if the gain of the control is selected to be very high, oscillation will nevertheless occur. A condition of oscillation with moderate gain in the flight speed calculator may occur in the transonic flight speed range, for in the transonic flight speed range the time constant of the airplane falls to as low as 2 seconds. The problem of oscillation at transonic speed requires further study.

DIFFUSER CONTROL

The need for adjusting the diffuser for flight Mach number is presented in a subsequent paper by Luidens and Esenwein. Adjustment to the diffuser with flight Mach number is necessary to achieve maximum thrust possible from the engine and to achieve the lowest specific fuel consumption. The plan considered herein for adjusting the diffuser is to schedule the position of the diffuser with flight Mach number, as shown in figure 9.

In this application, a variable geometry diffuser is applied to the airplane having scoops on the side of the fuselage. A portion of the fuselage ahead of the diffuser entrance is hinged and can be adjusted to vary the angle between the side of the fuselage and the surface of the ramp. The adjustment of this ramp angle also changes the area of the inlet diffuser to the engine. A device senses the flight Mach number of the airplane and positions this ramp in schedule corresponding to the flight Mach number.

This control appears to be reasonably independent of the engine. However, a change in the position of the diffuser changes the diffuser efficiency, which changes the pressure at the inlet to the engine; this



DECLASSIFIED

8-7

2235-8
pressure will change the thrust of the engine. A change in the engine thrust will change the flight Mach number which will be sensed by the diffuser control; the control loop is thereby closed and oscillation is possible. The elements of the complete control loop are shown in figure 10.

The time constant of the airplane is shown to be about 30 seconds, whereas the response time of the engine is 2 seconds, and the diffuser control should certainly be able to move the diffuser position in 2 seconds. Therefore, since the time constant of the airplane is long compared to the time constants of the engine or diffuser, oscillation is unlikely. However, a condition exists where oscillation is possible. In the transonic speed range, the time constant of the airplane becomes very low, of the order of 2 seconds, and in this case oscillation could occur. However, the schedule of ramp angle for the diffuser flight Mach number shows that the diffuser ramp angle can be constant from Mach number of 1.2 down to lower speeds; if such a schedule were set, the control would be inoperative in that flight speed range and oscillation would not occur.

CONCLUDING REMARKS

A preliminary study of the problem of control of the turbojet engine at supersonic flight speed has indicated that it is possible to design a control for service at supersonic flight speed that will assure safe engine operation with quick thrust response, flight speed stability, and proper adjustment of the inlet diffuser.

In the course of this presentation several dynamic constants have been used, particularly in connection with the stability chart of figure 3. These constants were chosen to represent a particular engine at a selected flight condition. It has been found that these dynamic constants vary with flight operating conditions and from one engine design to another. Furthermore, the behavior of the control system is quite sensitive to some of these constants. The only reliable method known at present for obtaining these constants is by direct measurement on the engine during transient operation. Of particular importance is the determination of these constants at the extreme conditions under which the control must operate, such as high altitude.

If a control designer did not have accurate knowledge of the significant dynamic constants, he might choose a control system that either would give poor protection and show poor response or would produce severe thrust oscillation.

[REDACTED]

CONFIDENTIAL

REFERENCE

1. Boksenbom, Aaron, and Hood, Richard S.: General Algebraic Method Applied to Control Analysis of Complex Engine Types. NACA Rep. 980, 1950.

CONFIDENTIAL

DECLASSIFIED

CONTROL FOR TURBOJET WITH AFTERBURNER

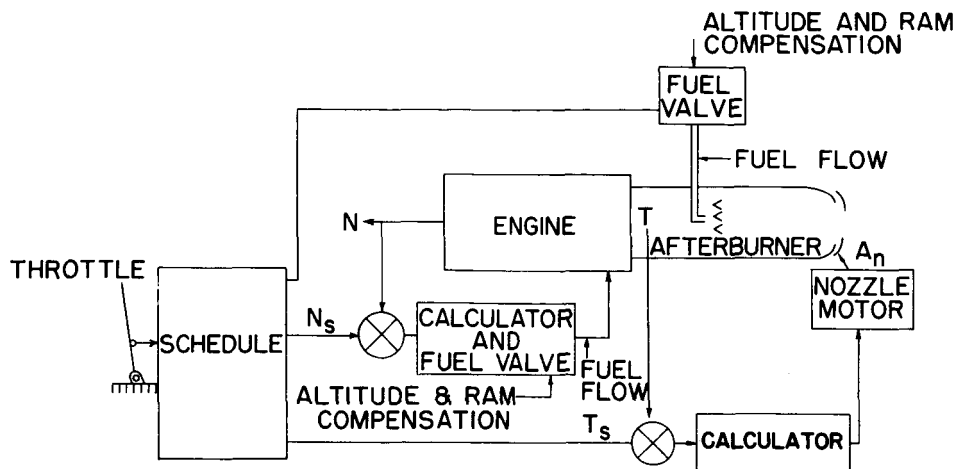


Figure 1

BEHAVIOR OF AFTERBURNER CONTROL

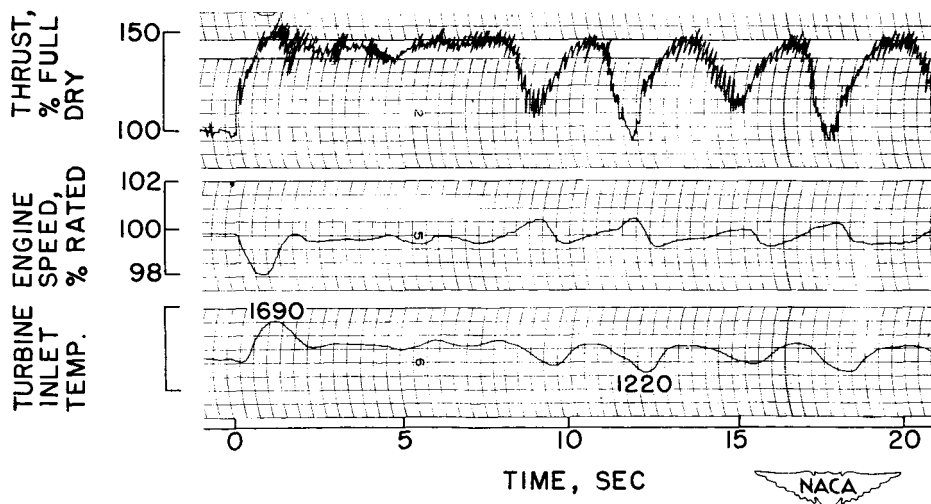


Figure 2

03712 [REDACTED]

STABILITY OF AFTERBURNER CONTROL

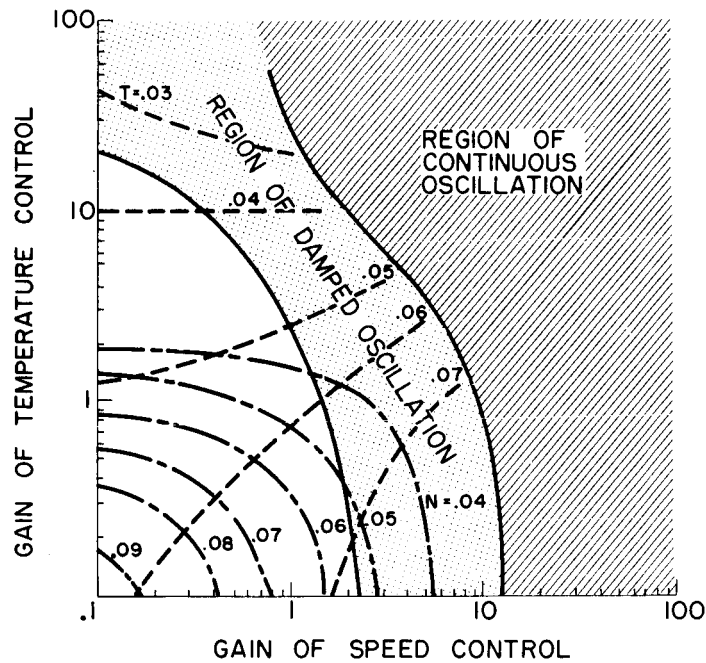


Figure 3

NEUTRALIZING LINK FOR AFTERBURNER CONTROL

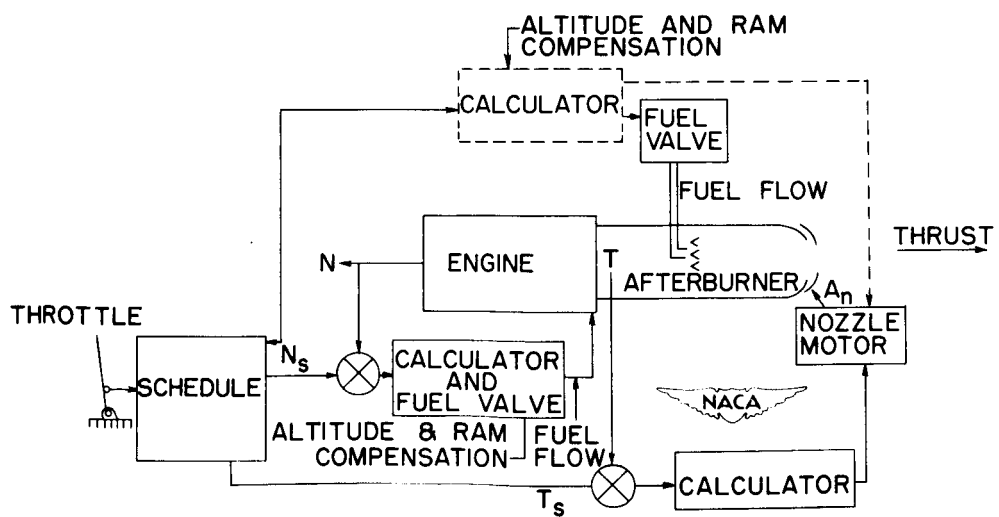


Figure 4

[REDACTED]

FLIGHT SPEED STABILIZER

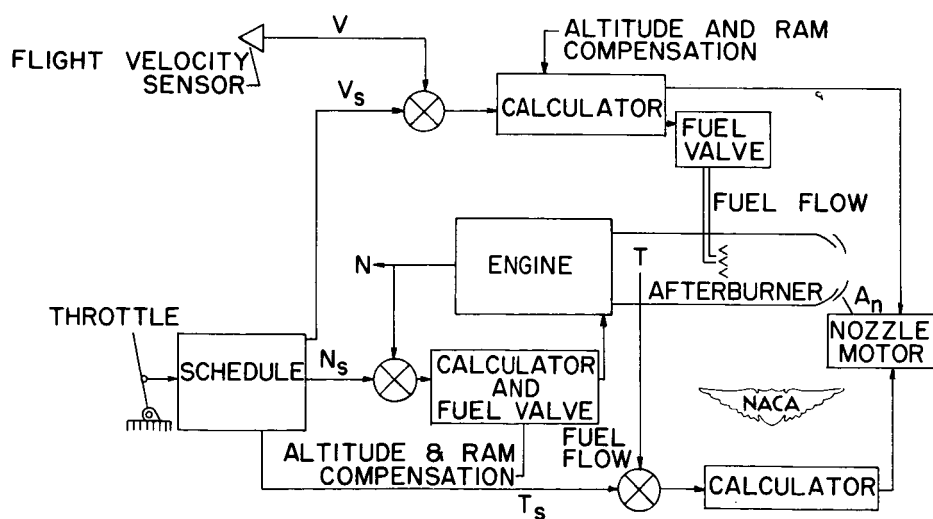


Figure 6

CONFIDENTIAL

FLIGHT SPEED CONTROL LOOP

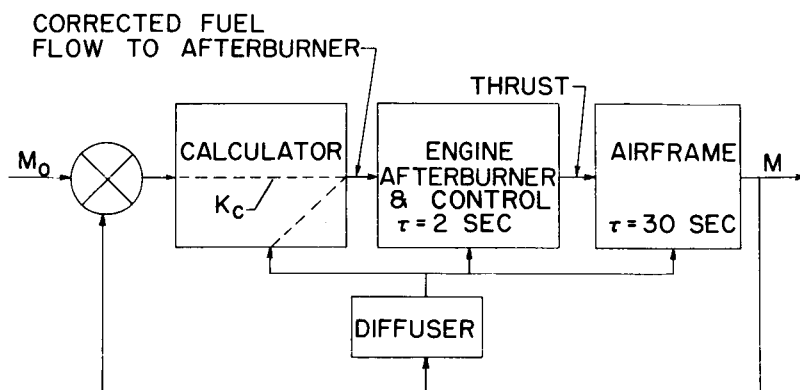


Figure 7

CONTROL GAIN EFFECT ON FLIGHT SPEED STABILITY AND AFTERBURNER FUEL FLOW FLUCTUATION

.1 CHANGE IN FLIGHT MACH NO.

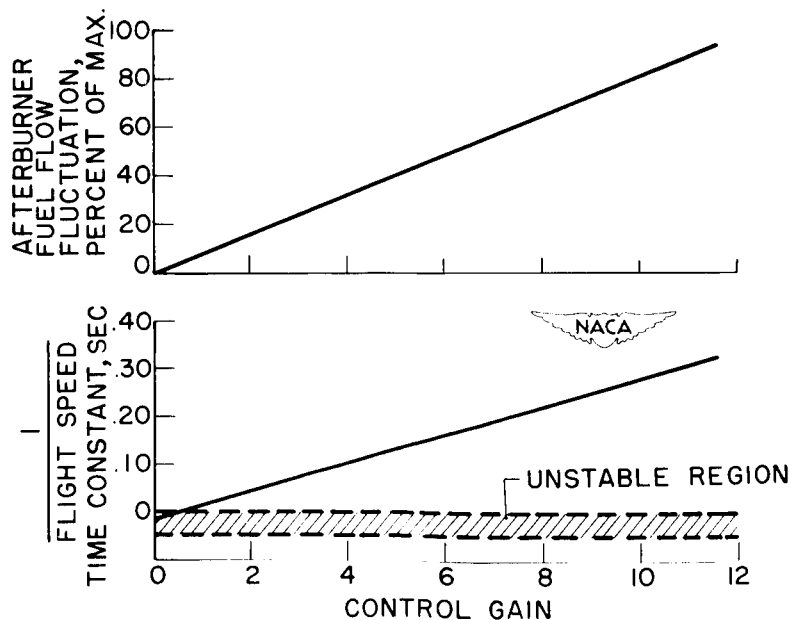


Figure 8

CONFIDENTIAL

DECLASSIFIED

CONTROLLED INLET DIFFUSER

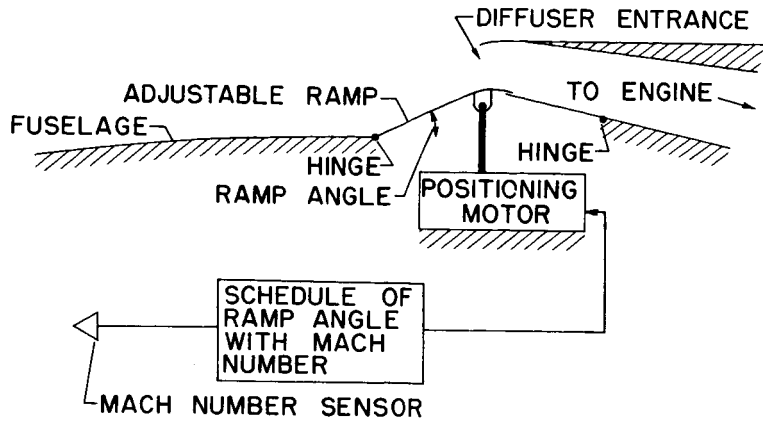


Figure 9

CONTROL SYSTEM FOR DIFFUSER AND ENGINE

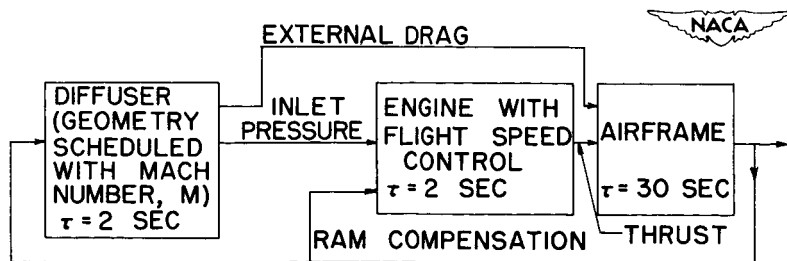


Figure 10

DECLASSIFIED

9. INTRODUCTION AND COMMENTS IIa

By Demarquis D. Wyatt

SECRET

9. - INTRODUCTION AND COMMENTS IIa

By Demarquis D. Wyatt

In the next section some of the problems associated with the installation of turbojet engines in supersonic aircraft will be discussed. One of the major problems is that of getting the charge air to the engine in the most efficient manner; that is, the inlet problem. There are many ramifications to this problem, but the essential ingredient in any inlet design is the attainment of high pressure recovery.

The importance of pressure recovery to the performance of turbojet engines can be illustrated in the manner indicated on figure 1. In this figure the percent change in engine thrust per percent change in inlet total pressure recovery is plotted as a function of flight Mach number for a typical engine. Sea-level and high-altitude flight are illustrated for engine operation with and without afterburning. Sea-level flight in the lower speed range results in an engine thrust loss of the order of 1.5 times the inlet total pressure loss. At high altitudes and supersonic speeds the thrust loss is reduced somewhat, but remains on the order of 1.2 times the inlet pressure loss. The loss in thrust arises from two factors. There is a one-to-one reduction of engine airflow with pressure loss and a consequent one-to-one reduction in thrust. In addition losses in inlet total pressure are reflected in reductions in cycle efficiency and account for the remaining thrust losses. The mass-flow reduction is the same for afterburning or nonafterburning configurations; however, the reduction in cyclic efficiency is comparatively lessened for the afterburning engine because of the higher jet thrust, and consequently the net effect is a lesser penalty for inlet pressure losses with the afterburning engine as compared with the nonafterburning engine.

Although the engine thrust is more sensitive to inlet pressure losses in the subsonic flight region, high pressure recoveries are easier to attain in this region than at supersonic speeds where diffusion problems are complicated by the well-known tendency of supersonic airstreams to decelerate through nonisentropic shock patterns. Consequently, although percentage thrust losses are lowered in the supersonic range, the total thrust loss potentialities with imperfectly designed inlets are in general greatly increased.

Although the threshold of an era of turbojet powered supersonic airplanes is now being approached, certain aspects of the supersonic diffuser problem have been well explored. The principles for efficient supersonic diffusion enunciated by Kantrowitz and Donaldson, Oswatitsch, Ferri, and Evvard (references 1 to 4) have been widely

CONFIDENTIAL

applied in nose inlet diffusers suitable for nacelle installations. The general level of maximum pressure recoveries that appear possible with well designed nose inlet installations is indicated on figure 2 as a function of flight Mach number. The pressure recovery for theoretical normal shock is included for reference.

At flight Mach numbers up to 2 or slightly above, adequate nose inlet configurations are possible. Pressure recoveries from approximately 90 percent up appear reasonable up to Mach number 2.0. In the higher speed range it is hoped that further research will result in pressure recoveries higher than those currently achieved, although a general leveling of the recovery curve is not to be expected.

From many nonaerodynamic considerations, principally radar, the nose inlet is not currently considered as suitable generally as the side inlet for supersonic airplanes, particularly of the interceptor type. Until recently, however, experimental pressure recoveries achieved with side-inlet configurations have been considerably lower than those indicated on figure 2 as possible with nose inlets.

The side inlet operates under several inherent difficulties as compared with the nose inlet. Schematically represented two-dimensional nose and side inlets satisfying the same design parameters of area ratio and length are presented in figure 3. The principal difference in the inlets lies in the nature of the boundary layer which may be encountered in the diffusion process. The nose inlet may generally be considered to be free of initial boundary layer so that only the boundary layer accruing on the inner cowl and inner body is present to complicate the diffusion process. At Mach numbers up to 2.0 this boundary layer does not significantly affect the diffuser performance. Subsonic diffuser pressure recoveries from 95 to 97 percent are not uncommon at Mach number 2.0.

The side inlet is not free of initial boundary layer, on the other hand, and will in fact encounter the whole boundary layer accumulated on the fuselage ahead of the inlet unless this boundary layer is removed. If any part of the fuselage boundary layer is allowed to enter a side inlet of the general type illustrated, poor diffusion may result because of the internal geometry.

Whereas the nose inlet generally discharges on the same axis as the inlet, the side inlet will generally require a translation of the flow to discharge on a centerline inboard of the inlet centerline. For the configuration illustrated, maximum local curvatures and consequently maximum local pressure gradients will occur on the inboard duct surface. This is the surface washed by any initial boundary layer allowed to enter the inlet and separation possibilities are enhanced.

CONFIDENTIAL

It is therefore not surprising that side-inlet pressure recoveries have been generally lower than nose-inlet recoveries.

The initial boundary layer that must be removed to give possibilities for good side-inlet pressure recoveries is, of course, a function of the body geometry ahead of the inlet. The complicated problem which confronts the designer of an adequate boundary-layer-removal system is illustrated by the data in figure 4. These data were obtained from pitot surveys in the vicinity of a parabolic body of revolution in the 8- by 6-foot tunnel at a Mach number of 2.0. Contours corresponding to a measured pressure to free-stream total pressure ratio of 0.6 are presented at the bottom of the figure for the maximum thickness and base planes of the body.

At 0° angle of attack, the uniform boundary layer thickens as the rear of the body is approached, as would be expected. At an angle of attack, the boundary layer tends to flow to the top or lee side of the body and to form into symmetrical lobes which develop as the rear of the body is approached. This phenomenon of cross-flow separation has been treated by Allen (reference 5).

It is obvious from an examination of figure 4 that the boundary-layer-removal problem ahead of a side inlet can be very complex. If the inlets are located on the upper quadrants of a circular fuselage of the type shown, the inlet may be practically immersed in boundary layer at high angles of attack. Locating inlets on the side of the body would reduce the magnitude of the boundary layer but would still yield nonuniform boundary-layer distribution at angle of attack. Locating an inlet on the bottom would of course be optimum for the body illustrated.

Not only is the boundary layer on a body dependent on the axial and circumferential location of the inlet and on the angle of attack of the body, but it will vary with body shape, Mach number, and Reynolds number. A generalization of the boundary layer problem and its influence on side inlet performance is therefore difficult; however, some recent research conducted by the NACA has clarified the problem. This work will be discussed in the next paper.

03171230 1434
[REDACTED]

REFERENCES

1. Kantrowitz, Arthur, and Donaldson, Coleman duP.: Preliminary Investigation of Supersonic Diffusers. NACA ACR L5D20, 1945.
2. Oswatitsch, Kl.: Pressure Recovery for Missiles with Reaction Propulsion at High Supersonic Speeds (The Efficiency of Shock Diffusers). NACA TM 1140, 1947.
3. Ferri, Antonio, and Nucci, Louis M.: Preliminary Investigation of a New Type of Supersonic Inlet. NACA RM L6J31, 1946.
4. Evvard, John C., and Blakey, John W.: The Use of Perforated Inlets for Efficient Supersonic Diffusion. NACA RM E7C26, 1947.
5. Allen, H. Julian, and Perkins, Edward W.: Characteristics of Flow over Inclined Bodies of Revolution. NACA RM A50L07, 1951.

2235

[REDACTED]

REF ID: A60150

EFFECT OF PRESSURE RECOVERY ON THRUST

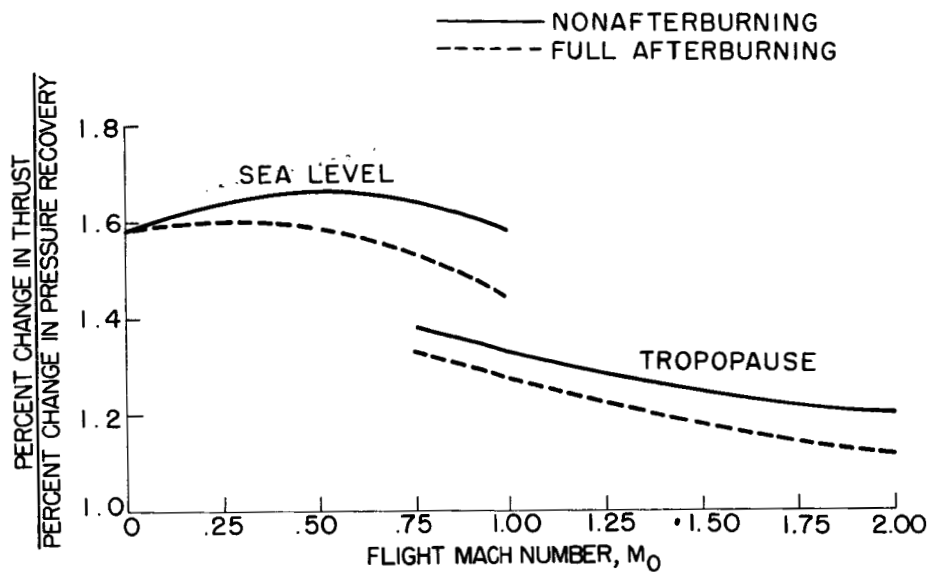


Figure 1

NOSE INLET PRESSURE RECOVERY

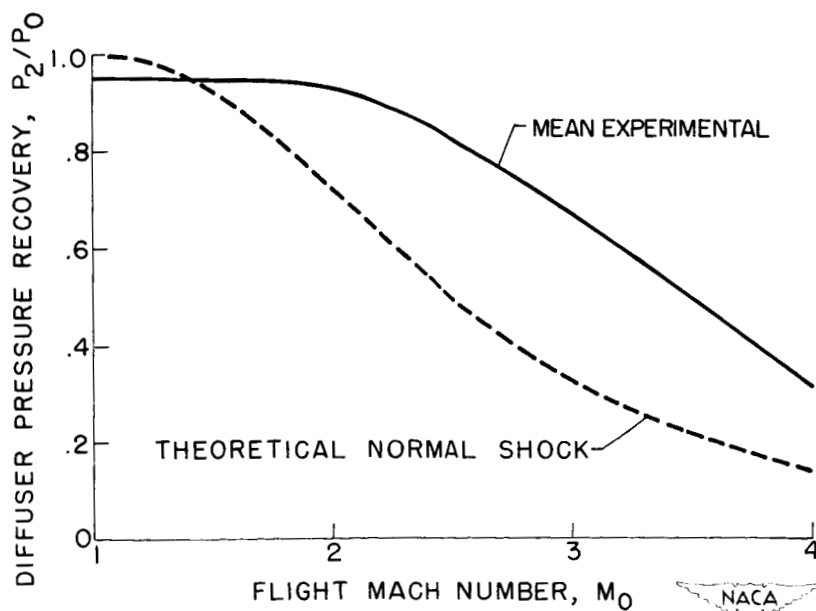
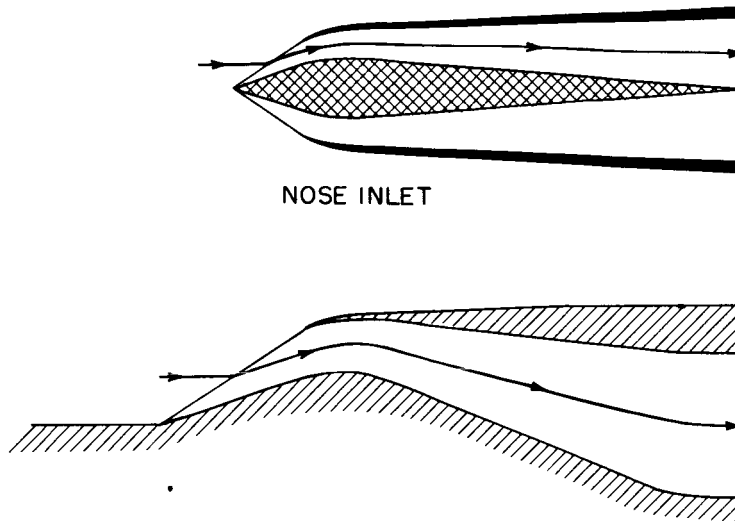


Figure 2

0317103444

COMPARISON OF INLETS

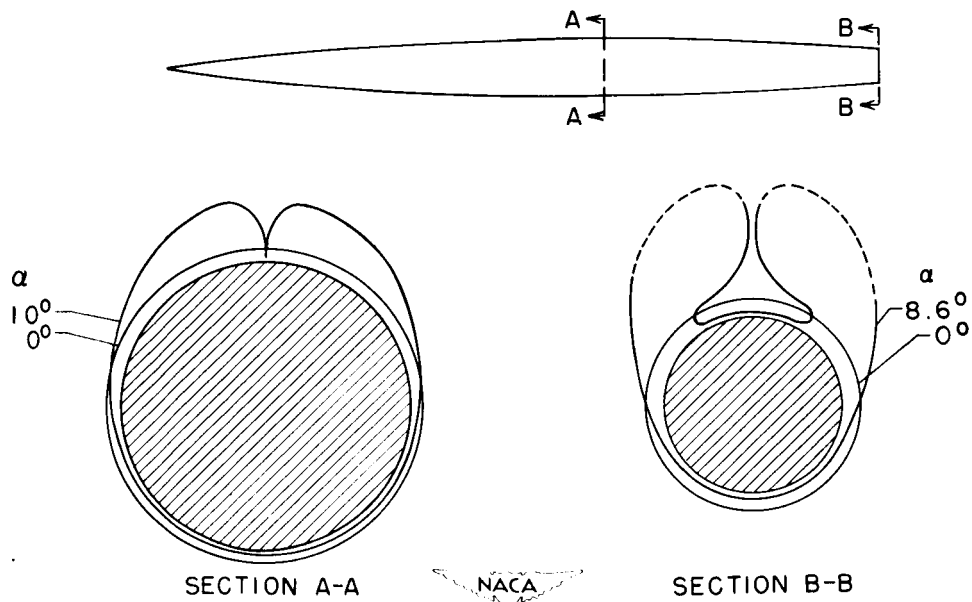


NOSE INLET

SIDE INLET

Figure 3

BOUNDARY LAYER ON CIRCULAR BODY $M_0, 2.0$



SECTION A-A

NACA

SECTION B-B

Figure 4

~~CONFIDENTIAL~~

10. EFFECT OF BOUNDARY-LAYER CONTROL ON PERFORMANCE OF
SIDE INLETS AT SUPERSONIC SPEEDS

By Edgar M. Cortright

~~CONFIDENTIAL~~

~~SECRET~~

10. - EFFECT OF BOUNDARY-LAYER CONTROL ON PERFORMANCE OF

SIDE INLETS AT SUPERSONIC SPEEDS

By Edgar M. Cortright, Jr.

In the introduction to this paper some inherent problems in the use of side or scoop type inlets were discussed. Among the foremost of these problems is the fact that the boundary layer that has developed on the body ahead of the inlet may flow into the inlet and thereby reduce its efficiency. The effect of an initial boundary layer on the performance of several types of side inlets utilizing various means and degrees of boundary layer control is presented, in some detail in this paper.

The side inlet configurations investigated utilized three types of supersonic diffusers, which are shown in figure 1. The most systematic and thorough research has been conducted on the spike diffuser. This diffuser consisted of half of a 50° conical-spike or Ferri-type nose inlet with all external compression. The second supersonic diffuser considered was a modified ramp type wherein the external compression was obtained by means of a 14° two-dimensional ramp. The face of the inlet was approximately semicircular in shape. The third diffuser obtained external compression by means of a 28° included angle wedge mounted normal to the body surface. The cross-section of the inlet was generally semicircular with the inlet lip swept so as to lie in the plane of the shock wave generated by the wedge. Each inlet faired into a subsonic diffuser which developed into a circular discharge duct.

The majority of the data presented on the spike-type inlet were obtained with the model shown in figure 2 and are reported in reference 1. The diffuser is mounted on a flat plate in the 18- by 18-inch supersonic wind tunnel at the NACA Lewis laboratory. The inlet was at zero angle of attack and zero yaw with respect to the local stream of Mach number of 1.88. The length of the flat plate ahead of the inlet was varied in order to vary the thickness of the initial boundary layer. In order to insure a fully developed turbulent boundary layer, the leading edge of the plate was roughened. Removal of various amounts of the initial boundary layer was accomplished by means of the ram-type boundary-layer scoop shown at the tip of the conical compression surface. The height of this scoop was varied by moving the inlet relative to the flat plate. It is interesting to note that the boundary-layer removal system was "self energized" in that discharge to free stream static pressure constituted sufficient pumping for supercritical operation of the scoop.

The internal geometry of the main duct and the boundary layer duct as well as some significant dimensions are indicated in figure 3. The

~~SECRET~~

CONFIDENTIAL

flow area of the main duct developed from an annular to a circular cross section as indicated. Pressure surveys of both ducts were made at stations 2. It was found that the flow in the main duct tended to separate from the inboard surface and that transverse Mach number gradients at the duct discharge were correspondingly large.

In this paper inlet performance will be discussed in terms of peak total-pressure recovery of the inlet P_2/P_1 , where P_1 is the total pressure of the free stream ahead of the inlet and P_2 is the average total pressure at the subsonic-diffuser discharge. In figure 4 peak pressure recovery is plotted as a function of boundary-layer scoop-height parameter h/δ where h is defined as the height of the scoop and δ is defined as the thickness of the initial boundary layer to the point where the velocity is equal to 0.99 times the local stream velocity. In figure 1 the parameter h/δ indicates the amount of the initial boundary layer removed since the boundary-layer scoop was operating supercritically, that is, capturing its full projected frontal area of boundary-layer air. The ratio of the boundary-layer thickness to the inlet radius δ/R was approximately 0.093. When all of the initial boundary layer was permitted to flow into the inlet ($h/\delta = 0$) a very low pressure recovery of 0.68 was recorded. When the boundary-layer scoop height was increased, the inlet-pressure recovery increased in an approximately linear manner. At a value of scoop-height parameter of 0.9, a peak pressure recovery of 0.89 was recorded which compares favorably with the pressure recovery obtainable with the nose-inlet counterpart.

If theoretical shock losses alone are considered, a pressure recovery of approximately 0.94 would be expected. When the average decrement in total pressure ahead of the inlet due to the presence of the initial boundary layer is subtracted from this value of pressure recovery, a pressure recovery of 0.91 is predicted with all of the boundary layer flowing into the inlet ($h/\delta = 0$). The large additional decrement in pressure recovery obtained experimentally was determined to occur for the most part in the subsonic diffuser. The fact that these internal losses decreased greatly as the initial boundary layer was removed is indicative of the role of the boundary layer in destroying the subsonic diffuser efficiency.

Experiments at the NACA Langley laboratory with essentially the same supersonic-diffuser configuration (reference 2) have indicated the large improvements in pressure recovery with removal of the initial boundary layer to be obtainable throughout the Mach number range from 1.3 to 1.9 as indicated in figure 5. The complete inlet consisted of half of an axially symmetric nose inlet and hence the subsonic diffuser imposed less severe turning requirements on the internal flow. An apparent result was that the inlet was less adversely affected by the initial boundary layer than the spike inlet previously described; for

CONFIDENTIAL

example, a pressure recovery of 0.75 at Mach number 1.9 was obtained with no boundary-layer removal as compared with a pressure recovery of 0.68 with the first inlet at the same conditions.

In actual practice the boundary layer ahead of the inlet may not be of uniform depth. The fuselage cross-section shown in figure 6 is not as conducive to cross-flow separation as the circular fuselage described in the introduction because it is streamlined in the cross-flow direction. The initial boundary layer as experimentally determined, however, is nonuniform. In order to investigate the effect of a non-uniform initial boundary layer, the leading edge of the flat plate used to generate the boundary layer was swept resulting in the condition indicated in figure 6 with the maximum thickness δ only slightly greater than the original δ of the uniform boundary layer. For a given setting of the scoop-height parameter h/δ therefore, less low-energy boundary layer is permitted to pass into the inlet than with the uniform boundary layer. This replacement of some low-energy air with free-stream air did not improve the inlet performance, however, as indicated on the plot of peak pressure-recovery variation with scoop-height parameter for both boundary-layer conditions. The maximum thickness of the entering boundary layer is therefore indicated to be significant in the determination of the extent of the internal losses.

Up to this point only the cases of the boundary-layer scoop operating at maximum mass flow with no spillage (supercritical) have been considered. It is of interest to know how subcritical operation of the boundary-layer scoop affected the inlet performance. This is shown in figure 7 where peak pressure recovery for the spike-type inlet is plotted as a function of scoop-height parameter for various mass-flow ratios m/m_{\max} of the boundary-layer scoop. The term m is defined as the actual mass flow handled by the boundary-layer scoop and m_{\max} is the maximum mass flow that could be captured with the particular boundary layer present. For relatively small values of scoop-height parameter, a reduction of boundary-layer scoop mass flow spilled low-energy air into the inlet (fig. 8(a)) and reduced the inlet performance in much the same manner as if the scoop height had been reduced. In the case of large scoop heights any reduction of the scoop mass-flow ratio below approximately 0.75 resulted in unstable scoop and inlet flow with large associated reductions in inlet-pressure recovery.

The sensitivity of the inlet to boundary-layer scoop spillage is undesirable. Accordingly, three alternative boundary-layer control systems were investigated (fig. 8(b) to 8(d)). The first of these consisted of the original ram scoop with the sides removed to permit spilled air to pass to the sides. The second alternative scoop (fig. 8(c)) was designed to accomplish the same thing; in addition, the leading edge of the scoop lip was swept back at the conical shock angle. This is the type scoop utilized in reference 2. In the present

CONFIDENTIAL

investigation the boundary-layer ducts were completely blocked and hence represented only the limiting case of no flow. They may also be considered to represent the case where it is desired not to take any air aboard but merely to deflect it around the inlet. In such an application, however, the blunt type of deflection represents an extreme case. The last method of boundary-layer control investigated consisted of cutting out the lip of the cowl at the junction of the cowl and boundary-layer surface in lieu of any removal of boundary layer ahead of the inlet. (fig. 8(d)). The large pressure differential between the interior and the exterior of the inlet thus tends to cause the boundary-layer air, which was found to accumulate in the corners of the annulus, to flow to the outside. This type of control could also be combined with a duct if desired.

The results obtained with these systems are shown in figure 9 where peak pressure recovery is plotted as a function of scoop-height parameter. The two limiting cases of maximum and zero mass flow through the original ram scoop are also included for reference. The ram scoop with sides removed was not completely effective in deflecting the boundary layer; a maximum pressure recovery of 0.81 was obtained. One cause of this was the strong disturbance, arising from the blunt type duct blockage, that was in evidence ahead of the splitter plate. Use of a low angle-deflection wedge would presumably improve the performance. The scoop with a swept leading edge was more effective than the previous scoop and yielded a maximum pressure recovery of 0.85. In the case of the slotted cowl, h is defined as the slot height. At a slot-height parameter h/δ of 1.5, a pressure recovery of 0.86 was obtained.

Considerable evidence has been presented to demonstrate the desirability of preventing the initial boundary layer from flowing into a spike-type side inlet. The ramp-type inlet, which was introduced at the beginning of this paper represents another type that has been investigated. This inlet was designed for use on a supersonic research aircraft and submitted to the NACA Lewis laboratory for study in the 8-by 6-foot supersonic tunnel. Photographs of the inlet mounted on the aircraft fuselage are shown in figure 10. Provision was made for boundary-layer removal ahead of the compression ramp by means of a ram scoop.

The performance of this inlet is shown in figure 11 where peak pressure recovery is plotted as a function of scoop-height parameter for a range of Mach numbers of 1.2 to 1.8. The Mach numbers indicated do not represent the free-stream Mach numbers but rather those that occurred ahead of the inlets which were approximately 0.2 less than free stream at a body cruising angle of attack of 3° . At this altitude the inlet was approximately aligned with the local stream. Peak pressure recovery was referenced to the total pressure of the local free stream ahead of the inlet, which corresponded closely to free-stream total

CONFIDENTIAL

DECLASSIFIED

10-5

pressure. With the original boundary-layer scoop the inlet-pressure recovery was 0.77 at Mach number of 1.8. This low recovery was due to two factors: The boundary-layer scoop height was only about half the boundary-layer thickness and the boundary-layer scoop mass-flow ratio was considerably less than 1, due to mass-flow limitations of the boundary-layer ducting. By removing the sides of the ram scoop the effective scoop mass-flow ratio was increased to approximately 1 with the expected improvement in inlet-pressure recovery. When the scoop height was increased to remove all of the initial boundary layer, the inlet-pressure recovery was increased to 0.87. With elimination of the boundary-layer scoop the inlet-pressure recovery at a scoop-height parameter of 0 was obtained. The resulting variation of peak pressure recovery with scoop-height parameter was found to be much the same as for the spike-type inlet. At lower Mach numbers the improvement in inlet performance due to boundary-layer removal was again present.

In an effort to decrease the sensitivity of side inlets to the entering initial boundary layer, the normal wedge-type inlet was designed at the NACA Lewis laboratory. This inlet, which was described earlier, is shown in figure 12 mounted on the same aircraft fuselage for test in the 8- by 6-foot tunnel. Investigations were conducted with the original ram scoop with a scoop-height parameter of 0.55 and a scoop-mass-flow ratio of 0.65 for purposes of comparison, the scoop was eliminated to allow all of the initial boundary layer to enter the inlet.

Peak pressure-recovery performance of the normal wedge inlet is shown in figure 13 as a function of boundary-layer scoop-height parameter. The same general trend of improved performance with removal of the initial boundary layer was observed. The inlet was less adversely affected by the initial boundary layer however, as exemplified by comparison of the performance with that of the ramp inlet. This result is apparently due to the reduced curvature of the internal surface onto which the initial boundary layer flows as illustrated in the sketches of figure 13.

The foregoing data were obtained with the inlet aligned with the local stream. With the body at angle of attack, changes in both the initial boundary layer and the local flow angularities occurred. In figure 14 the peak pressure recovery of the ramp-type inlet is shown as a function of body angle of attack at a free-stream Mach number of 2.0. The lower curve was obtained with the boundary-layer scoop in its original condition. (The dip in this curve at $\alpha = 3^\circ$ is as yet unexplained and probably slightly exaggerates the difference between the ramp and wedge inlet in figure 13.) The upper curve was obtained with the scoop modified to remove all of the initial boundary layer at cruise altitude. With the larger scoop height, the inlet-pressure recovery was less adversely affected by the increase of fuselage angle of attack from 0° to 12° . In addition it was observed that at 12° angle

0371500000

of attack, the boundary layer had thickened ahead of the inlet so that the scoop-height parameter h/δ for the larger scoop had decreased from 1 to a value of approximately 0.65. The decrement in pressure recovery due to angle of attack was therefore only slightly greater than would be expected from boundary layer considerations alone.

Any decision to use boundary-layer control must, of course, consider the penalties in drag, mechanical complication, and weight of the various boundary-layer removal systems. If the boundary-layer air is to be taken aboard for cooling purposes the system must also be matched to the cooling requirements. A detailed consideration of these factors is beyond the scope of this paper; however, a general insight into the drag penalties of boundary-layer removal as compared with the improvement in engine thrust may be obtained from figure 15. In this figure the effect of boundary-layer control ahead of a spike-type inlet on the maximum thrust performance of a typical turbojet engine with afterburner operating at 35,300 feet and Mach number of 1.88 is presented. The ratio of engine thrust minus boundary-layer removal drag to engine thrust without boundary-layer control is plotted as a function of boundary-layer scoop-height parameter. The boundary-layer thickness varies from 0.093 to 0.11 times the inlet radius. With larger initial boundary-layer thicknesses, the drag due to boundary-layer removal would increase correspondingly.

In the case where the boundary-layer removal is considered to result in no drag increase, the net thrust (thrust minus drag due to boundary-layer removal) increases 33 percent when most of the boundary layer is removed. If all of the total momentum of the boundary layer removed is considered lost, which represents an extreme case, the net thrust still increases approximately 27 percent. If the boundary layer is taken aboard by means of a ram scoop and discharged in the downstream direction through a choked nozzle, the maximum net-thrust increase using experimentally determined pressure recoveries in the boundary-layer duct, was calculated to be only slightly reduced. When the boundary-layer air is deflected around the inlet, the cost in drag is again indicated to be relatively small. In one phase of the investigation of the ramp inlet in the 8- by 6-foot tunnel, a 68° deflecting wedge was placed under the splitter plate of the ram scoop. Pressure measurements on the wedge as well as force measurements on the aircraft forebody were obtained which yielded a drag coefficient for the deflecting wedge. When this coefficient is utilized with the spike-inlet data, a maximum increase in net thrust of approximately 30 percent with optimum boundary-layer removal is indicated.

In summary, it was demonstrated that complete removal of the initial boundary layer ahead of side- or scoop-type inlets generally resulted in large improvements in the inlet performance. The cost in drag due to boundary-layer removal was generally small in comparison with the thrust increases available with the improved inlet performance.

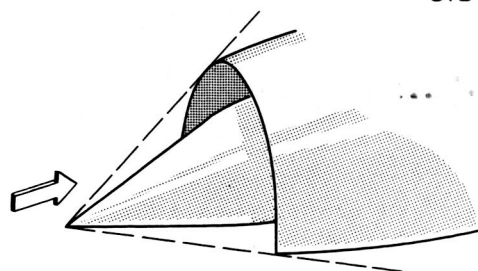
2235

DECLASSIFIED

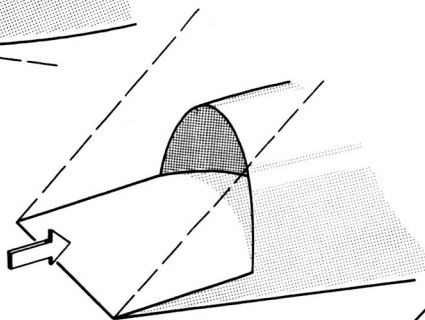
10-7

1. Goelzer, H. Fred, and Cortright, Edgar M., Jr.: Investigation at Mach Number 1.88 of Half of a Conical-Spike Diffuser Mounted as a Side Inlet with Boundary-Layer Control. NACA RM (to be pub.)
2. Wittliff, Charles C., and Byrne, Robert W.: Preliminary Investigation of a Half-Ferri-Type Supersonic Scoop Inlet. NACA RM (to be pub.)

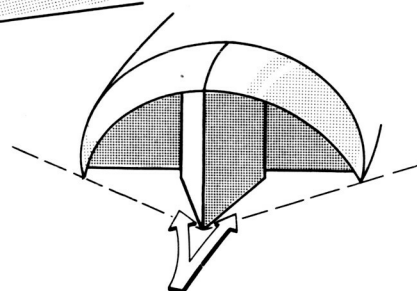
REF ID: A60157
SIDE INLET TYPE



SPIKE DIFFUSER
50° CONICAL SPIKE



RAMP DIFFUSER
14° RAMP



NORMAL WEDGE DIFFUSER
28° WEDGE



Figure 1

SPIKE INLET MOUNTED IN 18- BY 18-INCH TUNNEL

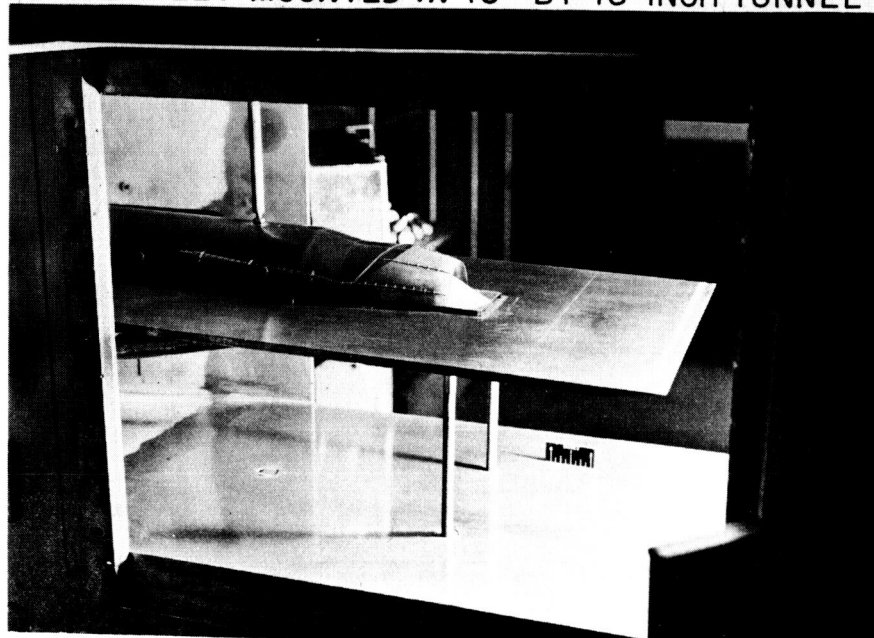


Figure 2

037120 [REDACTED]

2235-10

DIMENSIONS AND INTERNAL CONTOURS OF SPIKE INLET

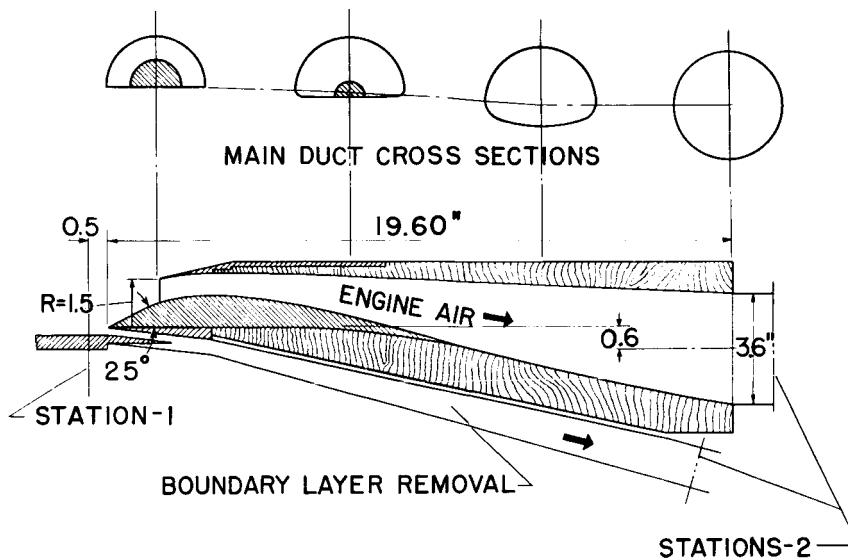


Figure 3

EFFECT OF BOUNDARY LAYER ON SPIKE INLET PERFORMANCE

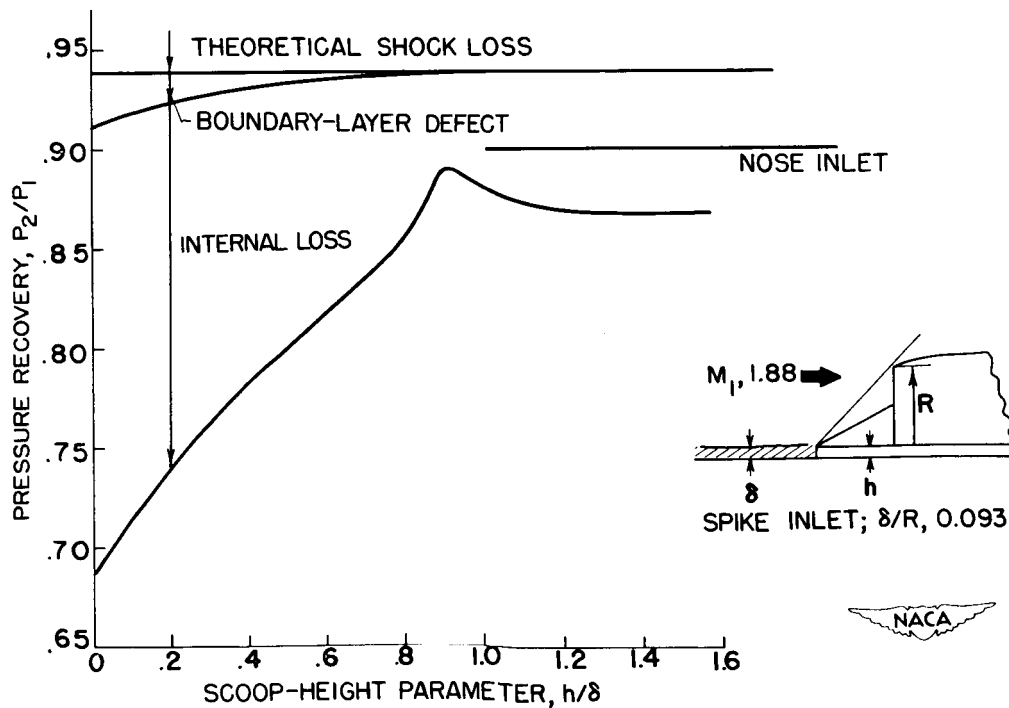


Figure 4

[REDACTED]

EFFECT OF BOUNDARY LAYER AT VARIOUS MACH NUMBERS

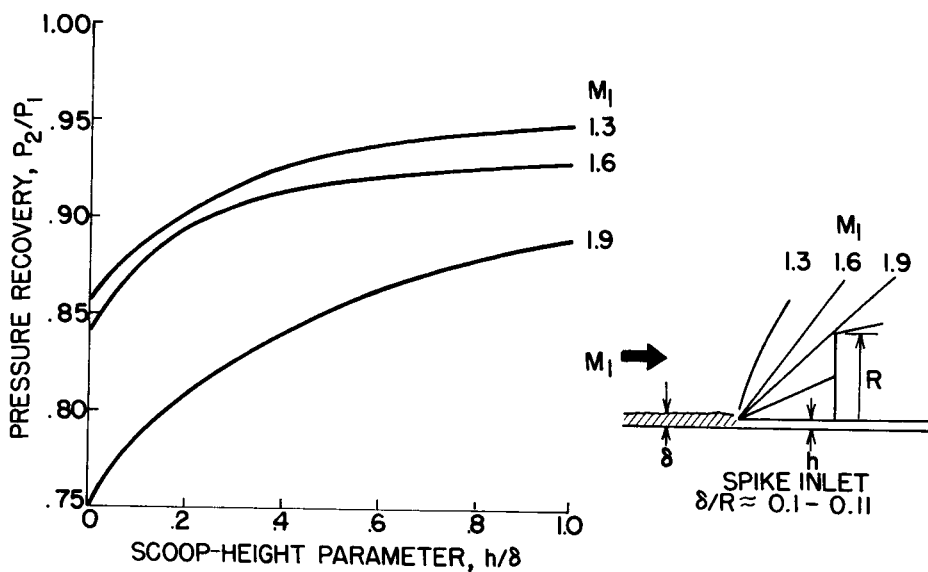


Figure 5

SPIKE INLET PERFORMANCE WITH NONUNIFORM INITIAL BOUNDARY LAYER

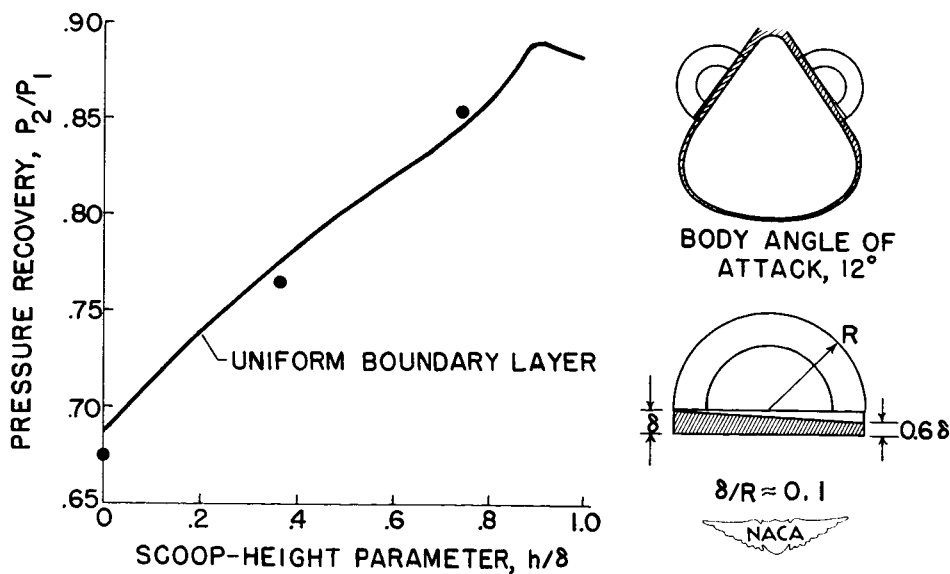


Figure 6

0371230 1030

EFFECT OF SUBCRITICAL OPERATION OF BOUNDARY-LAYER SCOOP

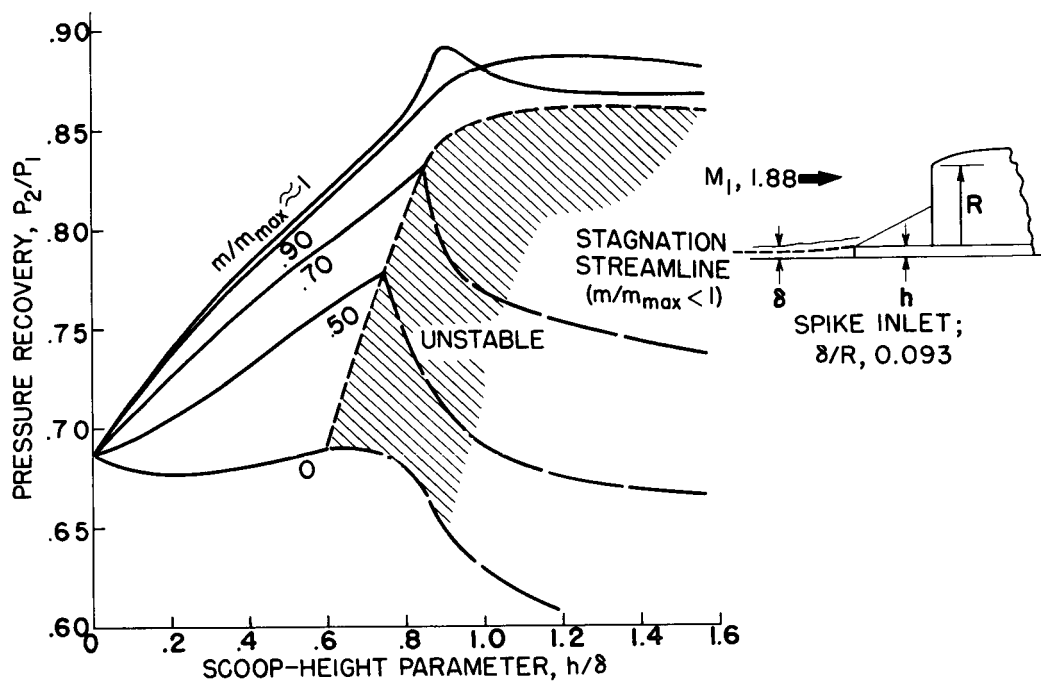
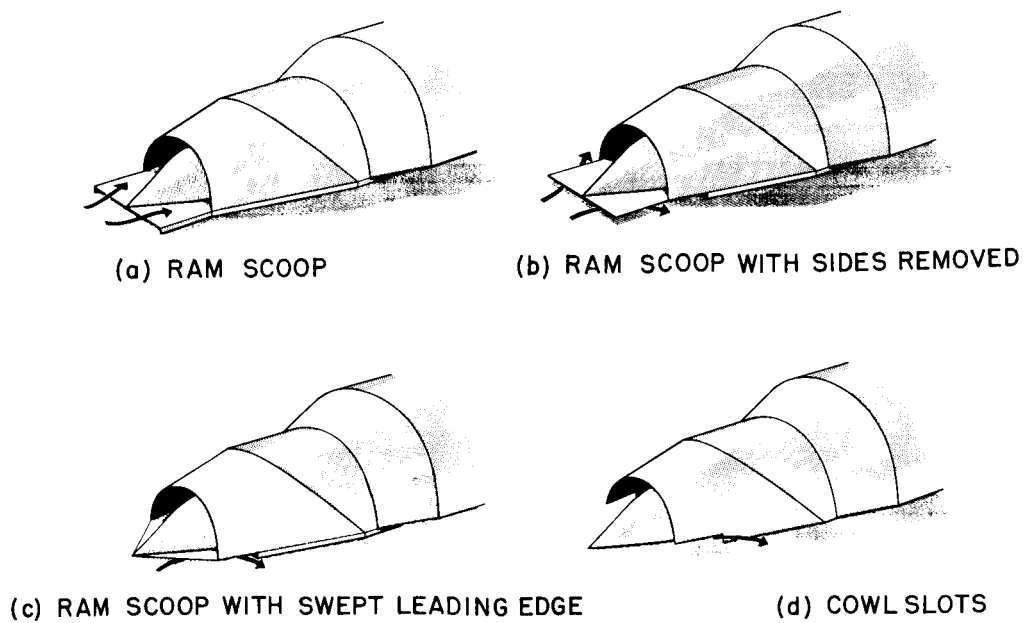


Figure 7

BOUNDARY LAYER CONTROL SYSTEMS



NACA

Figure 8

SPIKE INLET PERFORMANCE WITH VARIOUS BOUNDARY-LAYER-CONTROL SYSTEMS

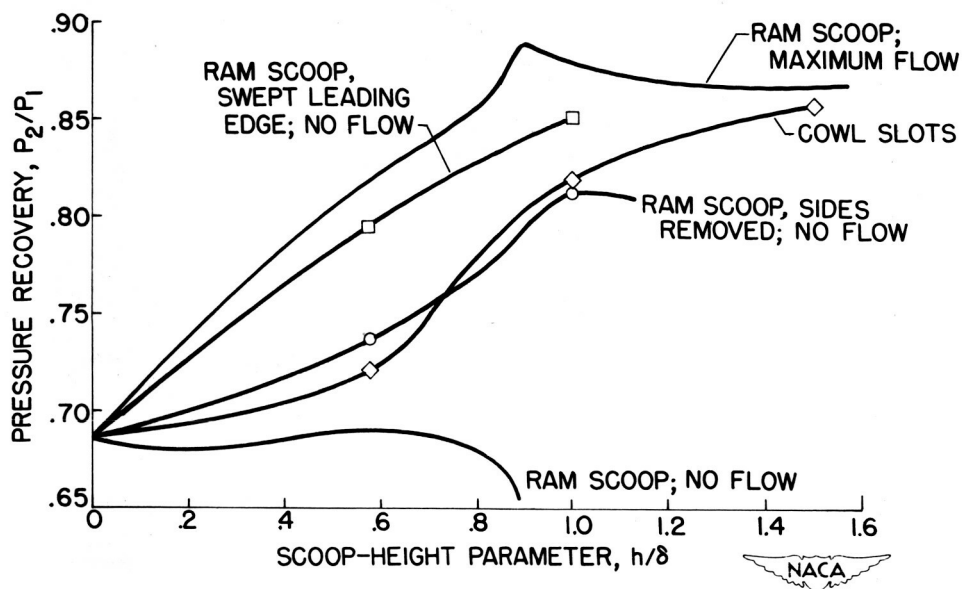


Figure 9

RAMP INLET ON SUPERSONIC AIRCRAFT FUSELAGE

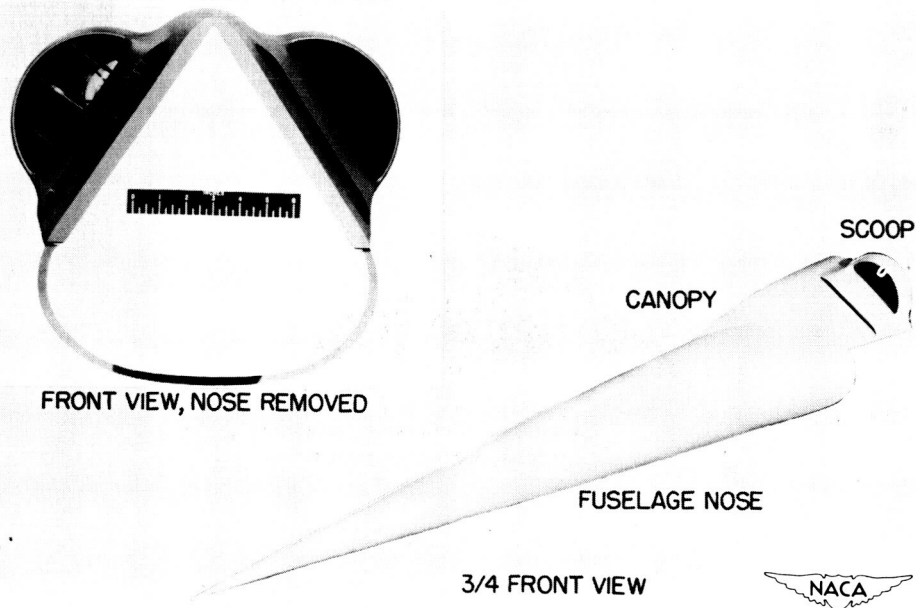


Figure 10

CONFIDENTIAL

EFFECT OF BOUNDARY LAYER ON RAMP INLET PERFORMANCE

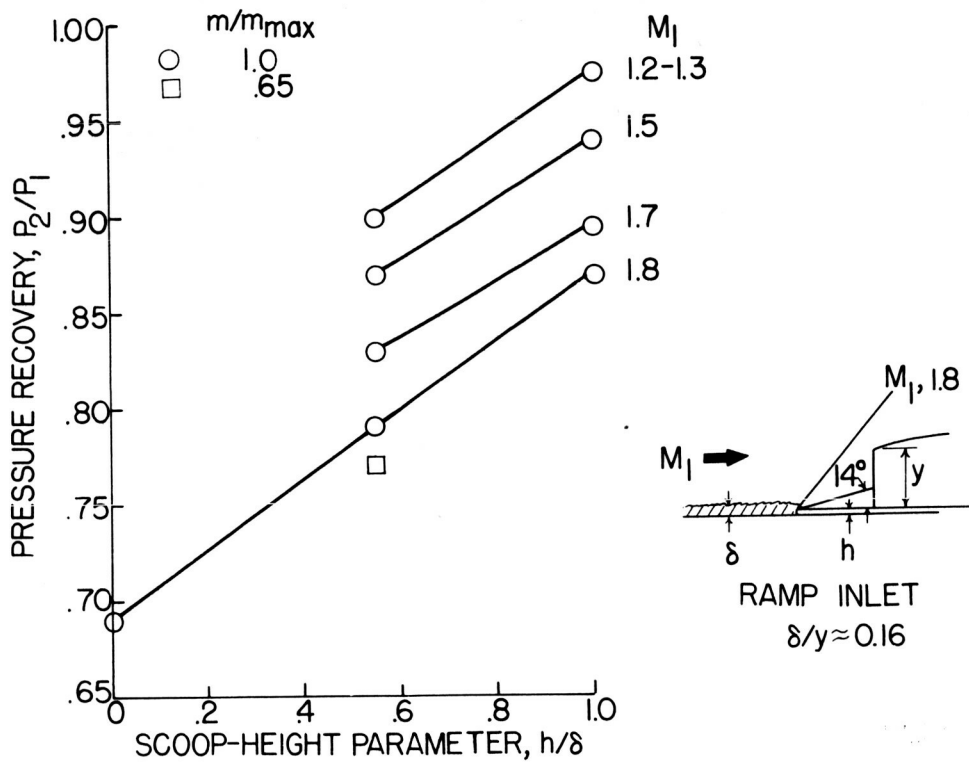


Figure 11

NORMAL WEDGE INLET ON AIRCRAFT FUSELAGE

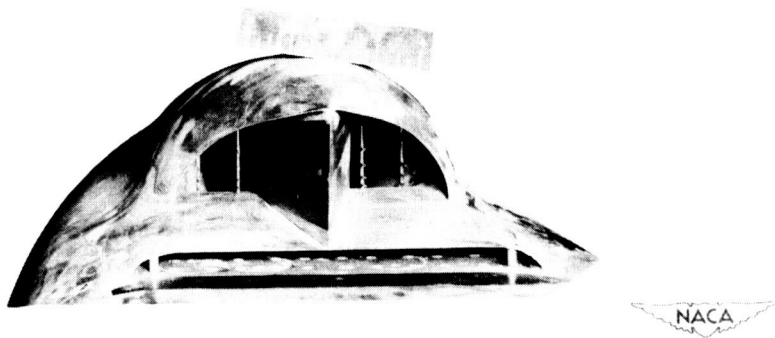


Figure 12

CONFIDENTIAL

2235-10

CONFIDENTIAL

DECLASSIFIED

EFFECT OF BOUNDARY LAYER ON NORMAL WEDGE INLET PERFORMANCE

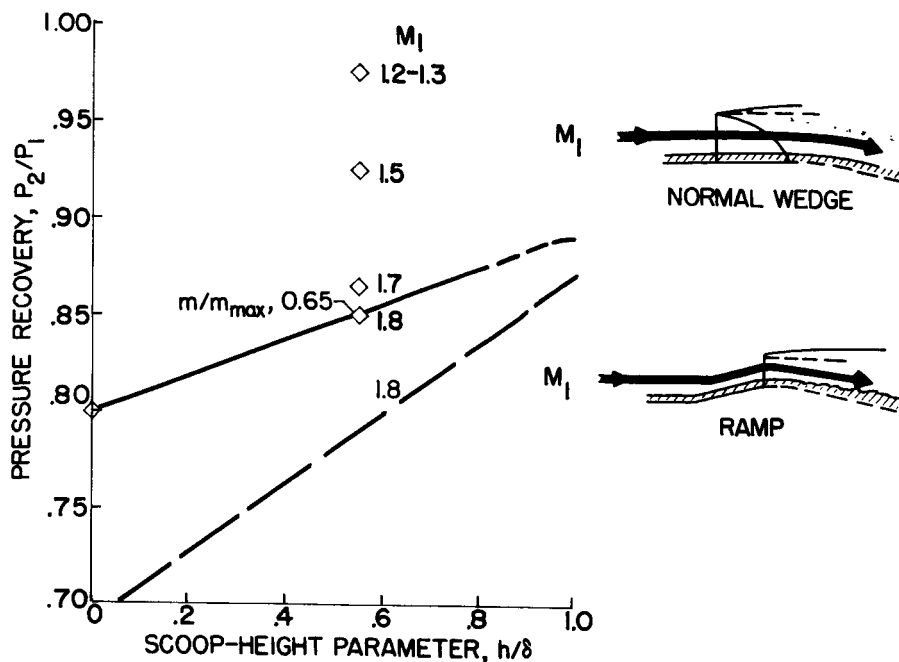


Figure 13

EFFECT OF ANGLE OF ATTACK ON RAMP INLET PERFORMANCE

$M_0, 2.0$

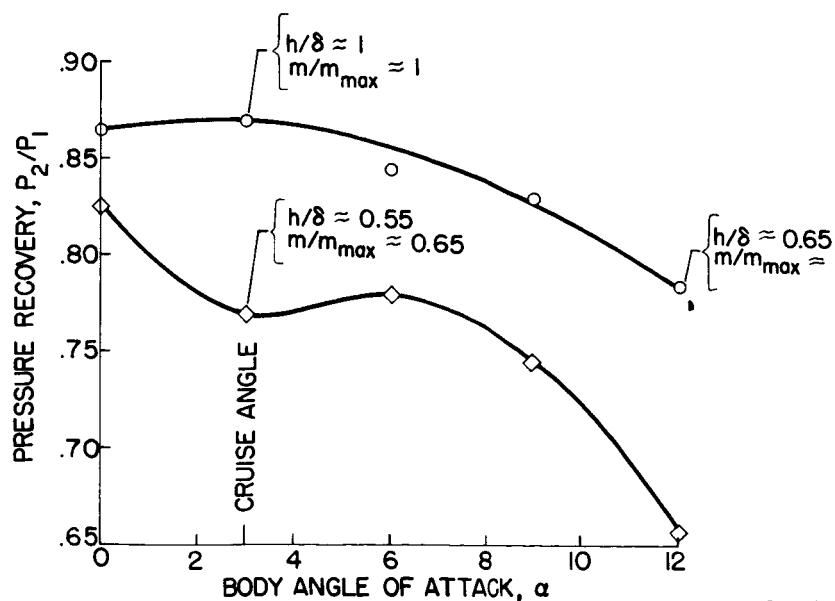


Figure 14



CONFIDENTIAL

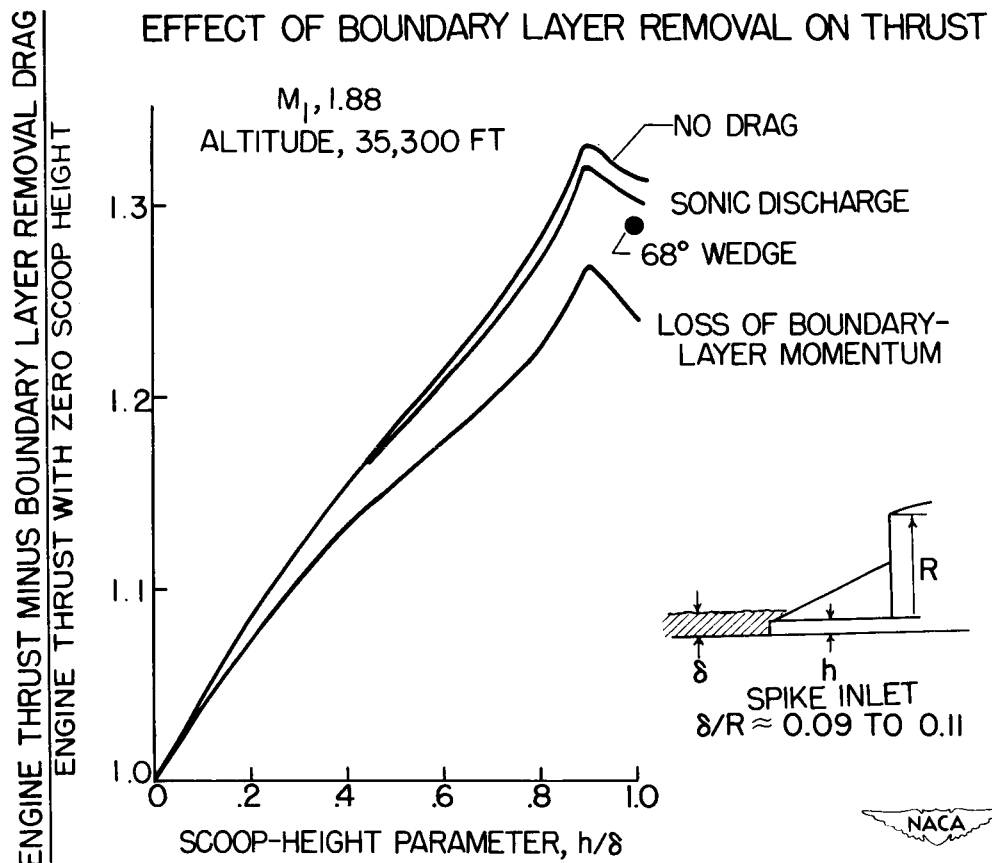


Figure 15

UNCLASSIFIED

11. COMMENTS IIb

[REDACTED]

SECRET

11. - COMMENTS IIb

By Demarquis D. Wyatt

2235 After air inlet problems are sufficiently under control to permit the attainment of high pressure recoveries at a given flight Mach number or over a range of Mach numbers, there yet remains the problem of matching the air handling characteristics of the inlet to the air requirement characteristics of the turbojet engine. A consideration of this topic will be discussed in the next paper.

The matching problem is fortunately simplified by a fundamental characteristic of the turbojet engine that is illustrated in figure 1. When the corrected air flow handled by the engine is plotted as a function of corrected engine speed, the data fall on a single line (neglecting Reynolds number effects). In figure 1 the air flow and engine speed are plotted as percentages of the respective rated sea-level values.

For a flight path on which the true engine speed is constant, the corrected air flow is affected only by the inlet stagnation temperature. The inlet stagnation temperature is a unique result of the flight speed and ambient-air temperature and is quite independent of the inlet attached to the engine.

The corrected air flow can be directly and uniquely related to a compressor-inlet Mach number. Hence it is possible to replace the generalized air-flow map of figure 1 by a map of the compressor-inlet Mach number as a function of flight Mach number and flight altitude as in figure 2. The curves hold as shown only for a constant true engine speed. The compressor-inlet Mach number decreases as flight speed is increased at a given altitude because the inlet stagnation temperature is increased. Correspondingly, the inlet Mach number increases with an increase in altitude for a fixed flight Mach number because the stagnation temperature decreases.

For constant engine speed, the compressor-inlet Mach number indicated on figure 2 for a specified flight condition represents the unique operating point of the engine, independent of the inlet. For a given flight Mach number and altitude, the engine will operate at the value of compressor-inlet Mach number shown by figure 2 regardless of whether the inlet has 100-percent or 10-percent pressure recovery. The compressor-inlet Mach number may be considered as the required inlet discharge Mach number for the specified flight condition.

SECRET

CONFIDENTIAL

If the engine is neglected and the inlet is considered as an isolated component, a fixed geometry inlet is found to operate over a wide range of discharge Mach numbers. This is shown on figure 3 for a hypothetical inlet where diffuser pressure recovery is plotted as a function of diffuser discharge Mach number for a range of flight Mach numbers. At each flight Mach number, the diffuser-pressure-recovery characteristic is represented by two curves. The right-hand region of decreasing pressure recovery represents supercritical or constant air flow operation. The decrease in pressure recovery is the result of shock recession into the diffuser as the discharge Mach number is increased. The left-hand constant-pressure-recovery line represents subcritical flow or operation with constantly decreasing mass flow as the discharge Mach number is decreased. (In practice, the subcritical pressure recovery is seldom constant but is so represented on fig. 3 for simplicity.) The intersection of the sub- and supercritical regions, labeled critical, represents maximum pressure recovery with maximum mass flow and minimum drag for the inlet represented.

Although a wide range of discharge Mach numbers can be obtained from an isolated diffuser at each flight Mach number, there is only one discharge Mach number that is of any significance when the inlet is connected to a specified turbojet engine at a given altitude and engine speed. The designer can arbitrarily set the matching Mach number for one flight condition, but the intersection of the engine and diffuser characteristics at any other flight condition is wholly dependent on the compressor-inlet Mach number schedule.

The consequences of this inflexibility are illustrated in figure 4. On the left of figure 4, the diffuser curves from figure 3 are reproduced. The operating schedule for a typical turbojet engine at constant altitude is superimposed. In this example it has been assumed that the designer sized the inlet so that the engine operating point coincided with the critical diffuser condition at a Mach number of 2.0. This choice would be sensible, since maximum engine thrust and minimum inlet drag would be attained. For the example chosen, however, the engine characteristic would fall into the subcritical diffuser region for all lower flight Mach numbers. Thus, the inlet would be too large at lower flight speeds, and large amounts of air would have to be spilled around the inlet in order to satisfy the engine requirements. Undesirably large additive drags might therefore penalize the installation at Mach numbers below 2.0. As a secondary consideration, many inlets in practice operate with pulsing inlet flow in the subcritical region, which might be harmful to the engine.

If the designer seeks to avoid spillage the results are indicated on the right of figure 2. The diffuser has now been assumed to be

8
DECLASSIFIED

11-3

sized to give critical inlet flow for the engine operating condition at a Mach number of 1.0. The engine characteristic is now seen to intersect the diffuser characteristic in the supercritical region for all higher Mach numbers with large reductions in pressure recovery. At a Mach number of 2.0, for example, the matching point occurs at an inlet pressure recovery of only 0.72.

2235 The matching problem which confronts the airplane designer has been illustrated by figure 4. In general, a fixed inlet design at supersonic speeds will result either in thrust losses due to low pressure recovery or in drag losses due to air spillage. (The example chosen assumed a constant maximum air-flow capacity of the inlet independent of flight Mach number. Practical external compression inlets have a variable mass-flow capacity which tends to crowd the diffuser characteristics together. For such inlets the general trend shown is reversed; that is, the inlet sized for Mach number 1.0 will spill air at Mach number 2.0 and vice versa. The general difficulty in matching is still present.)

There are, of course, other matching problems than the constant-altitude supersonic Mach number case shown in figure 4. The design of an inlet must accommodate altitude variations and subsonic flight speed operation, either of which may present critical performance problems. The example chosen has, however, illustrated the probable inadequacy of a fixed-geometry inlet to yield maximum performance. The next paper will therefore discuss recent analytical and experimental evaluations of variable geometry inlet designs that may improve the installation performance.

[REDACTED]

DECLASSIFIED

ENGINE AIR FLOW CHARACTERISTIC

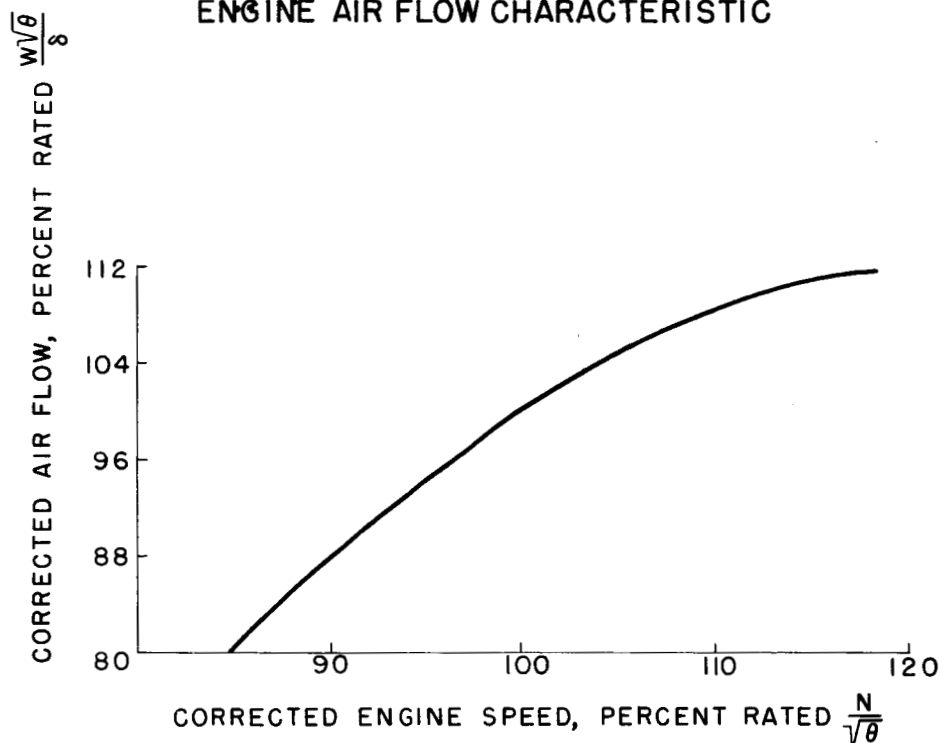


Figure 1

TYPICAL TURBOJET CHARACTERISTIC (CONSTANT RPM)

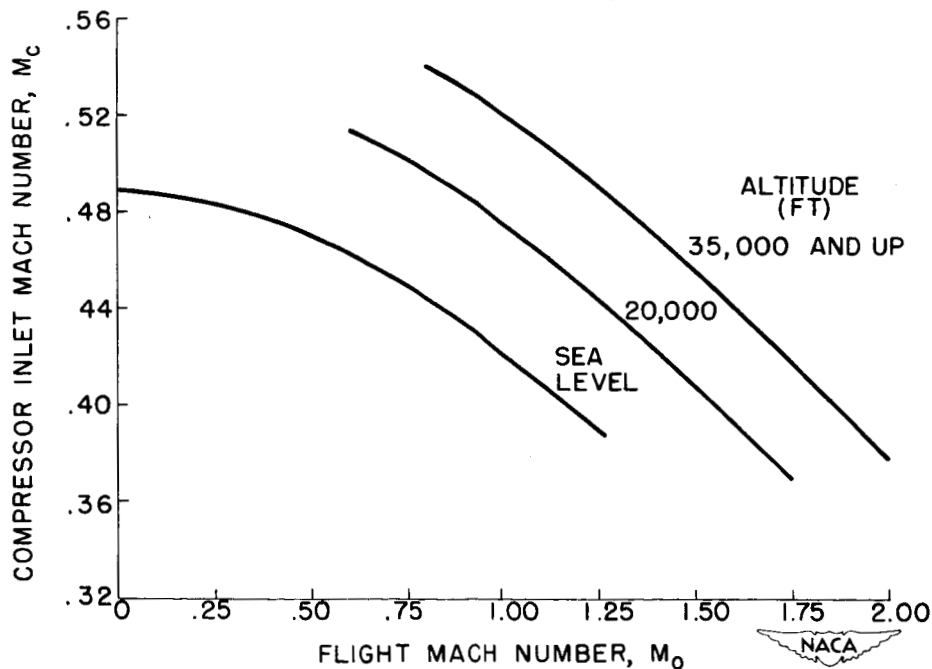


Figure 2

031710 001970

2235-11

TYPICAL DIFFUSER CHARACTERISTIC

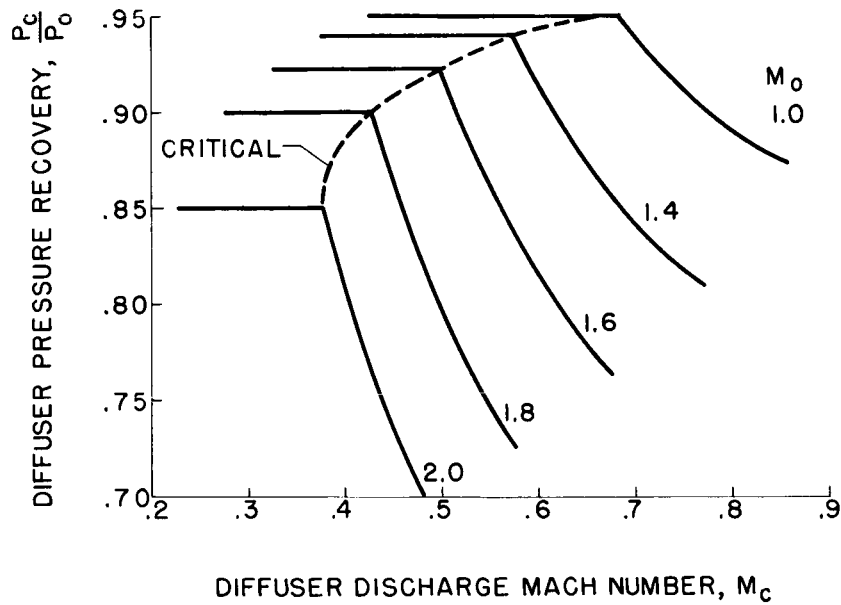


Figure 3

ENGINE-DIFFUSER MATCHING

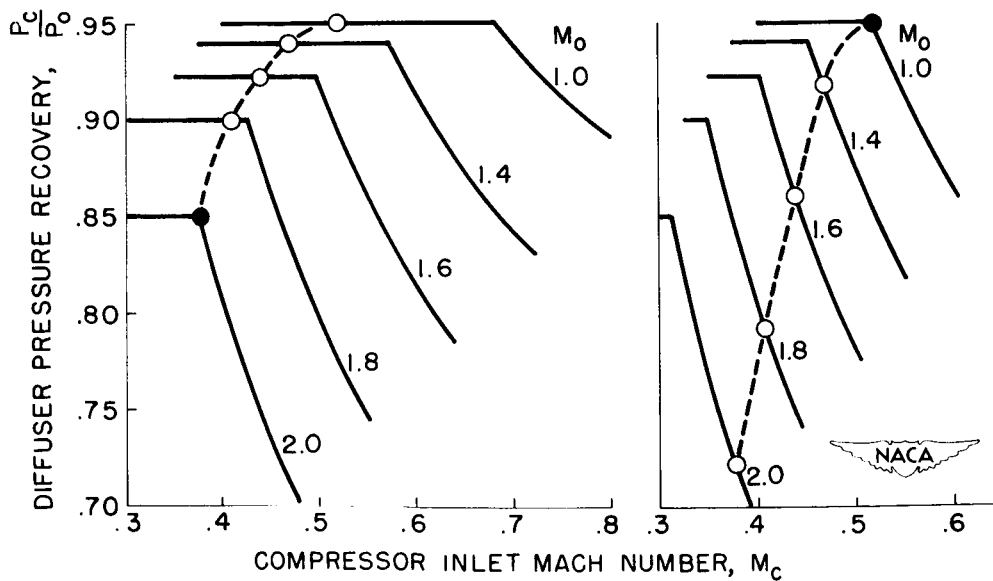


Figure 4

DECLASSIFIED

12. EFFECTS OF INLET DESIGN ON PERFORMANCE OF TURBOJET-ENGINE
INSTALLATIONS

By Roger W. Luidens and Fred T. Esenwein

CONFIDENTIAL

12. - EFFECTS OF INLET DESIGN ON PERFORMANCE OF TURBOJET-ENGINE INSTALLATIONS

By Roger W. Luidens and Fred T. Esenwein

INTRODUCTION

As pointed out in the introductory comments, the turbojet-engine-inlet matching problem has a number of aspects, such as matching over the range of supersonic Mach number, matching for take-off and low-speed operation, and matching for altitude and temperature effects. The primary purpose of this paper is to discuss the inlet matching problem over the range of supersonic Mach number up to a free-stream Mach number M_0 of 2.0, and to discuss the problems associated with take-off.

The penalties associated with mismatching an inlet and turbojet engine will appear as thrust losses associated with low pressure recoveries, or as drag penalties due to air spillage, or both. The performance of various inlet configurations will therefore be discussed in terms of a thrust parameter, which is defined as engine thrust F_n minus inlet drag D_i divided by the thrust for 100-percent pressure recovery. The analysis is made for a typical turbojet engine operating at constant engine speed in rpm, constant afterburner temperature, and having the air-flow characteristics presented in the introductory remarks.

First, the problem of matching in the supersonic speed range will be illustrated by considering the theoretical performance of a number of possible fixed- and variable-geometry inlet designs. Significant points of the analysis will then be substantiated by experimental results.

ANALYSIS

Presented in figure 1 is the variation of the thrust parameter as a function of free-stream Mach number. If the engine is assumed to have an inlet which at each flight Mach number yields the maximum pressure recovery attainable through an oblique and normal shock and a 95-percent subsonic recovery and to have zero drag, the engine performance shown by the solid curve is obtained. This pressure recovery assumption gives an 86-percent recovery at a free-stream Mach number M_0 of 2.0 and 95 percent at M_0 of 1.0 and below. This curve also represents what might be called the performance with a perfectly matched two-shock inlet. It is a reference curve and will be shown on subsequent figures.

CONFIDENTIAL



The dashed curve is the performance of a fixed-geometry inlet designed to be matched at a free-stream Mach number of 2.0. The design of the inlet is shown in the right-hand sketch. The angle of the wedge for maximum pressure recovery is 16° . The oblique and normal shocks fall at the lip of the inlet, and consequently a full free-stream tube of air enters the inlet with zero spillage. The performance of the inlet is thus at the reference value at the high Mach number.

The center sketch shows a flow configuration for a typical Mach number below design M of 1.7. The oblique shock has moved ahead of the inlet lip and the deflection of the flow through the oblique shock causes excessive spillage of air around the cowl. Because of the mass spillage, a strong shock must form in the subsonic diffuser in order to meet the engine specified diffuser discharge Mach number. Because of the restricted air flow into the inlet and the resulting low pressure recovery, the inlet performance is 20 percent less than the reference value over most of the Mach number range. Of the 20-percent loss, only about 4 percent results from additive drag due to mass spillage around the inlet. The remaining 16 percent is associated with the low pressure recovery. At subsonic Mach numbers, choking occurs at the inlet throat because of the high air-flow requirement, as shown, for example, at M of 0.85. Thus a fixed-geometry inlet designed for the high Mach number is grossly mismatched over most of the lower Mach number range.

Perhaps the inlet would be better matched to the engine requirements if it were designed for an intermediate Mach number. Such a case is shown in figure 2, where the inlet is designed for M equal to 1.5. The curves from the previous figure are also shown. As before, at the flight Mach numbers below design, severe performance penalties result for reasons discussed on figure 1. At above design flight Mach numbers, large penalties occur because the cowl area of the inlet is too small. A loss of 13 percent exists at M_0 of 2.0. From the two cases considered, it is concluded that an inlet that is mismatched because it is effectively undersize in general gives large performance losses.

This conclusion leads to consideration of an inlet which is enlarged so that it is never undersized over the range of Mach number considered. An example is shown in figure 3. The inlet is sized at M of 0.85 to avoid choking at the minimum inlet area, but retains the geometry which yields high performance at a Mach number of 2.0, that is, the 16° wedge design. This design is shown in the lower left-hand sketch. The inlet performance over the range of Mach number is shown by the dashed line. Reference performance is, of course, obtained at M_0 equal to 0.85. The operation of the inlet at supersonic speeds is shown typically at M of 2.0. The inlet is now oversize and spillage occurs behind a bow shock to meet the air flow



SECRET

required by the engine. At Mach number of 2.0, the pressure recovery is high but the inlet is spilling about 16 percent of its air capacity around the cowl. The drag due to the spillage results in the 6-percent performance loss shown. The largest loss in performance is 13 percent and occurs at M of 1.4. This loss results partly because of spillage and partly because the 16° wedge angle does not give good pressure recovery at Mach numbers in this range. Thus a fixed-geometry inlet, sized for the low Mach number condition, is mismatched because it is oversize at the higher Mach numbers. In general, then, with fixed-geometry inlets appreciable performance losses must be accepted over at least a part of the Mach number range. Therefore, it is worthwhile looking into variable-geometry inlets to see if matching can be achieved over a wide Mach number range.

A large part of the loss shown on this figure results from the high drag associated with spillage behind a bow shock. One scheme for reducing this drag is shown in figure 4. The curve from figure 3 is also presented. Instead of spilling the air behind a bow shock (left-hand sketch) the excess air is taken into the inlet and exhausted through a sonic nozzle ahead of the engine (right-hand sketch). This scheme is sometimes called a bypass system. The performance of this variable-geometry inlet is about 8 percent better than the fixed-geometry inlet over the Mach number range. It has a maximum loss in performance of 5 percent from the reference value at M of 1.4. The maximum loss occurs near 1.4 because the 16° wedge does not give good pressure recoveries at the Mach number near 1.4. This improved performance has been bought by introducing the complexity of mechanically varying part of the inlet because the size of the nozzle must, of course, be varied with flight Mach number.

A second type of variable-geometry inlet which yields good performance is shown in figure 5. The inlet is designed at the high Mach number (right-hand sketch). As previously stated, the trouble with the fixed wedge inlet was that it spilled too much air at the lower Mach numbers. This difficulty can be avoided if the wedge angle is decreased with decreasing Mach number. Fortunately, to reduce the wedge angle to the value for maximum pressure recovery at each Mach number was sufficient. A typical flow configuration is shown at M_0 of 1.6 in the center sketch. The wedge for maximum pressure recovery is 11° . In order to meet the air flow required by the engine it is still necessary to spill air around the inlet, partly behind an oblique shock and partly behind a normal shock. This air spillage results in the performance losses indicated by the dashed line in figure 5. It is a maximum of 4 percent at M of 1.3 and zero at M of 2.0 or 0.85. About the only way to avoid this spillage is to use still more complex inlets with a variable cowl. It is questionable, however, whether the added complication is warranted for the potential



gains that exist. The sketches on the figures have shown a wedge parallel to the fuselage surface; the wedge could also be normal to the surface.

Another way of obtaining good performance is to keep the wedge angle constant and translate the wedge to achieve matching over the Mach number range. The technique of translation is ideal for cone-type inlets where changing the cone angle is mechanically difficult. The performance of a translating constant angle spike is shown in figure 6. The reference curve, which is the same as that presented on previous figures, corresponds very closely to the curve that would be obtained if the optimum cone were considered at each Mach number and the drag were assumed zero. Also presented on the figure is the performance of the two fixed-geometry inlets, one designed for high Mach number and the other sized for low Mach number. They show about the same performance losses as the fixed wedge inlets and for the same reasons. The variable-geometry inlet shows a maximum loss in performance of 3 percent from the reference curve at M of 1.2. The operation of the variable-geometry inlet is shown in the sketches. The inlet is designed at M of 2.0 (right-hand sketch). At lower Mach numbers (for example M of 1.4), the cone must be retracted slightly (indicated on the sketch to scale). The spike is retracted in such a manner that mass spillage occurs only behind an oblique shock and the normal shock remains at the cowl lip. All the drag associated with bow shock spillage is thus eliminated with this design. At M_0 of 0.85, a maximum tip retraction of 40 percent of the cowl radius is required to avoid choking at the throat.

All the variable-geometry inlets discussed required continuous variation with Mach number and usually the variation was in one direction, such as decreasing wedge angle with decreasing M . So these inlets are amenable to the control systems previously discussed.

EXPERIMENTAL RESULTS

So far the matching problem has been discussed from a theoretical point of view; it remains to substantiate the analysis with experimental results.

Supersonic Matching

An experimental investigation of fixed- and variable-geometry side inlets mounted on a typical aircraft fuselage was recently made in the 8- by 6-foot supersonic tunnel; the results serve to support the analysis. The model used has already been described in the previous paper. A picture of the model installed in the 8- by 6-foot supersonic tunnel is presented as figure 7. The three types of inlet



SECRET

12-5

2235

studied are shown in figure 1 of the preceding paper; they are the ramp or wedge inlet, the normal wedge inlet, and the spike inlet. The performance of the translating cone inlet was determined by tests with the cone in several fixed positions. Similarly, the variable-ramp-type inlet was simulated by tests of two fixed-angle wedges. The present investigation was conducted with all the fuselage boundary layer removed ahead of the inlet. Representative test results at M equal to 1.5 and 2.0 are shown in figure 8 for the half-spike inlet. Presented are the model drag coefficient C_D (the drag includes fuselage drag as well as inlet drag) and inlet pressure recovery P_2/P_0 as a function of diffuser discharge Mach number M_2 , where P_2 is the diffuser-discharge total pressure and P_0 is the free-stream total pressure. The lower curves present a modified thrust parameter corresponding to these data. (This parameter includes the inlet drag and the fuselage drag, which are represented by D_f , and is therefore not directly comparable with values determined in the analysis.) The drag shows the usual drag increase with subcritical inlet operation and constant drag with supercritical operation. The pressure recoveries show the characteristic decrease with supercritical operation. Also, the peak pressure recoveries show good agreement with the values assumed in the analysis, which are indicated by the caret marks on the scale. The inlet is designed at peak thrust minus drag for a Mach number of 2.0. The design point corresponds with the intersection of the dashed line engine operating line with the M of 2.0 performance curve. At M of 1.5, it may be seen from the nature of the pressure recovery that the inlet is operating supercritically, which is in accord with the theoretical analysis. Corresponding to the supercritical inlet operation, the thrust parameter is 11 percent less than the peak value. It can be seen from the pressure recovery curve, however, that the inlet is capable of good pressure recoveries. The analysis showed that critical pressure recovery of the inlet could be matched to the engine by retracting the spike. The results for a variable-spike inlet are shown in figure 9. The data at M of 2.0 are reproduced from figure 8. The data at M equal to 1.5 are for the retracted spike. The engine operating line shows that the inlet now is operating approximately at critical condition and near the peak thrust minus drag at Mach number of 1.5. The thrust parameter has improved 9 percent over that for the fixed spike inlet previously shown.

Similar data obtained for a ramp-type inlet are summarized in figure 10 in terms of the thrust parameter as a function of free-stream Mach number. (The thrust parameter again includes fuselage drag.) If the inlet is variable-wedge-angle inlet, the thrust performance is represented by the upper solid line connecting the circle, diamond, and triangle data points, which are respectively a 14° , 6° , and 0° wedge inlet. The data at Mach number of 0.63 were obtained by running the 8- by 6-foot supersonic tunnel subsonically. (Data were

SECRET



actually obtained for the 14° wedge inlet and are extrapolated to the case of zero wedge angle by correcting for the increase in throat area that results when the wedge angle is reduced.) The performance of a fixed-geometry inlet designed for Mach number 2.0 is shown by the circles and the decrement in thrust parameter from that available for the variable-geometry inlet corresponds to the loss predicted by the analysis. Similarly, a high-compression inlet sized for a Mach number of 0.6 shows the loss in performance due to subcritical inlet operation at a Mach number of 2.0 predicted by the analysis.

Take-Off Performance

It has been shown experimentally and analytically that several variable-geometry inlets are available that give good matching over the high subsonic through supersonic speed range. The next problem is that of getting good take-off performance with inlets satisfactory for supersonic flight. There are several factors involved in this problem that cannot be easily analyzed theoretically and are best handled experimentally.

At static conditions, the inlet operates at an infinite velocity ratio and in order to get good inlet pressure recoveries the inlet should have a bellmouth or at least well-rounded lips. Also for best supersonic performance the cowl lips should be sharp. Therefore, both a blunt and sharp-lip inlet were investigated at Mach number 2.0 and at static conditions. In figure 11 are shown schlieren photographs at a Mach number of 2.0 of two inlets designed for that Mach number. These inlets are mounted on the aircraft fuselage; the fuselage boundary layer is clearly in evidence and the inlets themselves are above the boundary layer. The inlet on the right has a sharp lip. (The dashed lines show the internal contour.) For the sharp-lip inlet the shocks fall at the inlet lip, as was assumed in the "ANALYSIS." The inlet on the left is a design compromised with a blunt lip from take-off considerations. Because of the bluntness of the lip and inherent internal contraction associated with rounding it, choking occurs at the inlet throat of the inlet and strong bow shock is forced to stand ahead of the inlet, with an attendant high drag. The detached bow wave shown is not associated with the engine-air-flow requirements. The performance of the two inlets in terms of the modified thrust parameter is shown below them. An 8-percent loss results from blunting the lip of the inlet. Because the pressure recoveries for these two inlets were the same, the performance loss associated with the blunt lip is due entirely to its drag.

The blunt-lip inlet was designed for good take-off performance, whereas the sharp-lip inlet was not; therefore the performance at take-off is considered. The variation of pressure recovery with diffuser discharge Mach number is shown at static conditions in



figure 12. The dashed line is the engine operating point. (These data for zero wedge angle were also obtained by correcting data taken with the 14° wedge for the increase in throat area resulting from decreasing the wedge angle.) The pressure recovery of the blunt lip is 97 percent, almost 10 percent better than the sharp-lip inlet. In terms of thrust, the blunt-lip inlet results in the engine producing 95 percent of its rated thrust, and the sharp-lip inlet, 15 percent less thrust. The good performance of the blunt-lip inlet is obtained at the expense of an 8-percent loss at Mach number 2.0. The performance of the sharp-lip inlet can be improved at take off by using auxiliary inlets. With this modification good performance can be obtained at both take off and supersonic speeds. The take-off problems associated with the half-spike inlet are similar to those for the wedge inlet.

SUMMARY

In summarizing this discussion of the turbojet-inlet matching problem, we should appreciate that the matching problem varies with the type of turbojet engine and mode of engine operation, and with the flight plan and limitations of the airplane. Each problem must be considered on its own merits. For the present analysis, fixed-geometry inlets showed thrusts of 13 percent to 20 percent less than the maximum possible over most of the Mach number range from 0.8 to 2.0; whereas variable-geometry inlets, such as the variable wedge or translating spike, showed performance close to the maximum over the same Mach number range. Blunting the cowl lip of a variable-geometry inlet penalized its performance 8 percent at Mach number 2.0 but improved its performance 15 percent at take off as compared with the sharp-lip inlet. The performance of the sharp-lip inlet could probably be improved at take off by use of auxiliary inlets. In general, then, the designer is faced with the problem of weighing the aerodynamic performance penalties of fixed inlets against the mechanical complexity of variable-geometry inlets, which show performance advantages.

DECLASSIFIED

FIXED WEDGE INLET

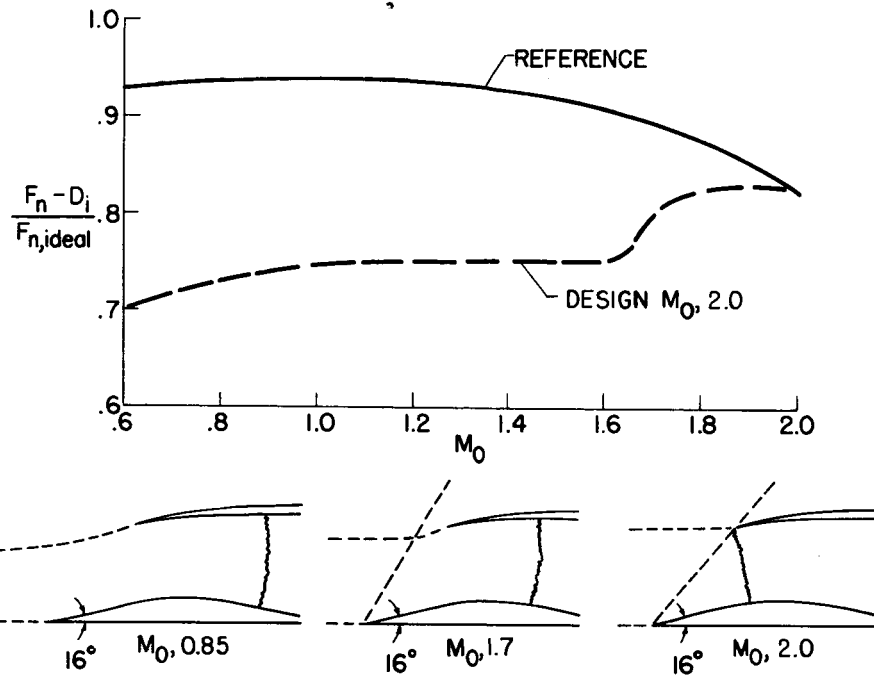


Figure 1

FIXED WEDGE INLET

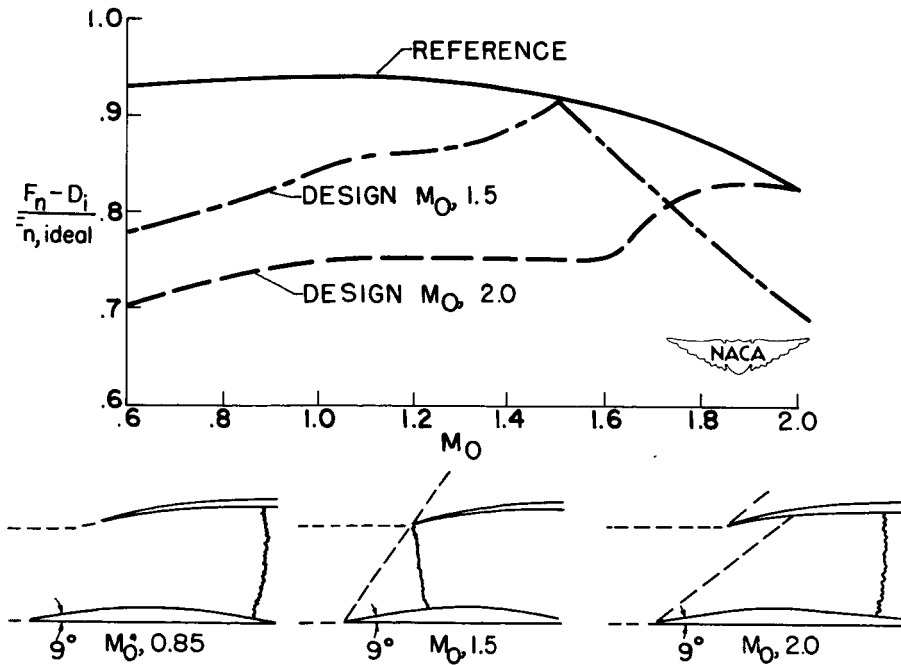


Figure 2

03710 [REDACTED]

FIXED WEDGE INLET

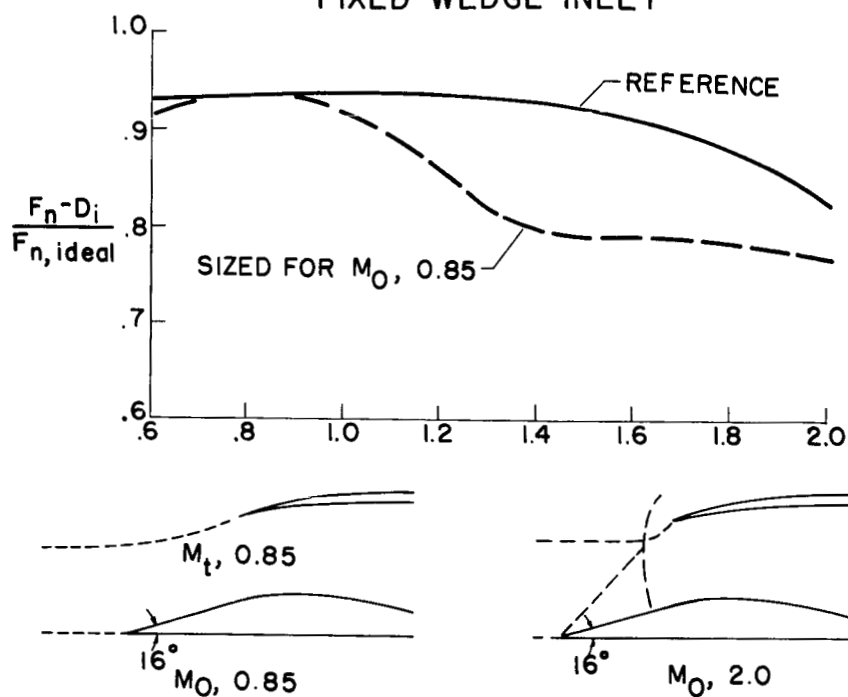


Figure 3

FIXED WEDGE INLET

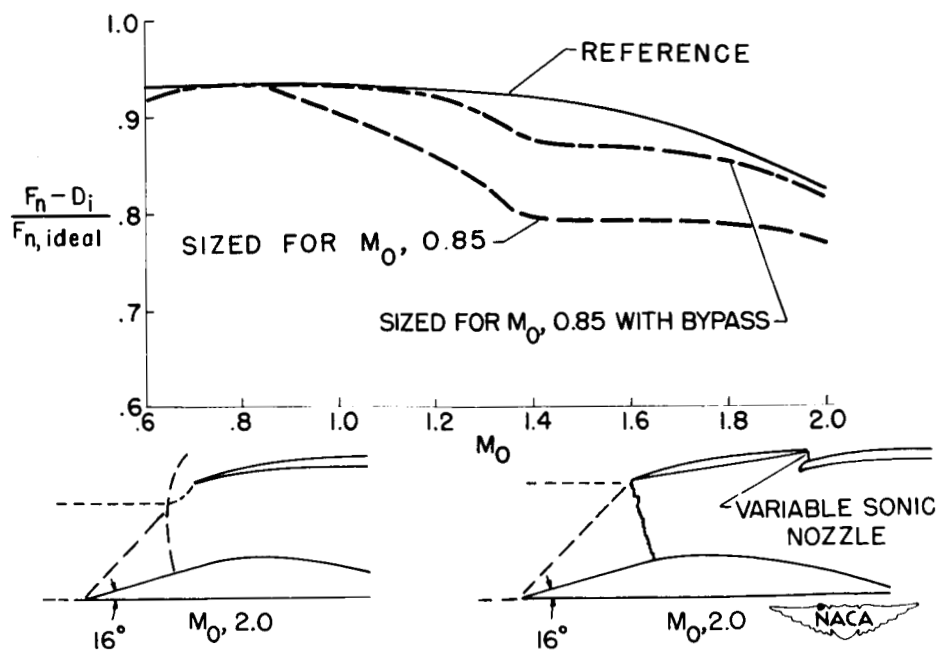


Figure 4

[REDACTED]

CONFIDENTIAL

VARIABLE WEDGE INLET

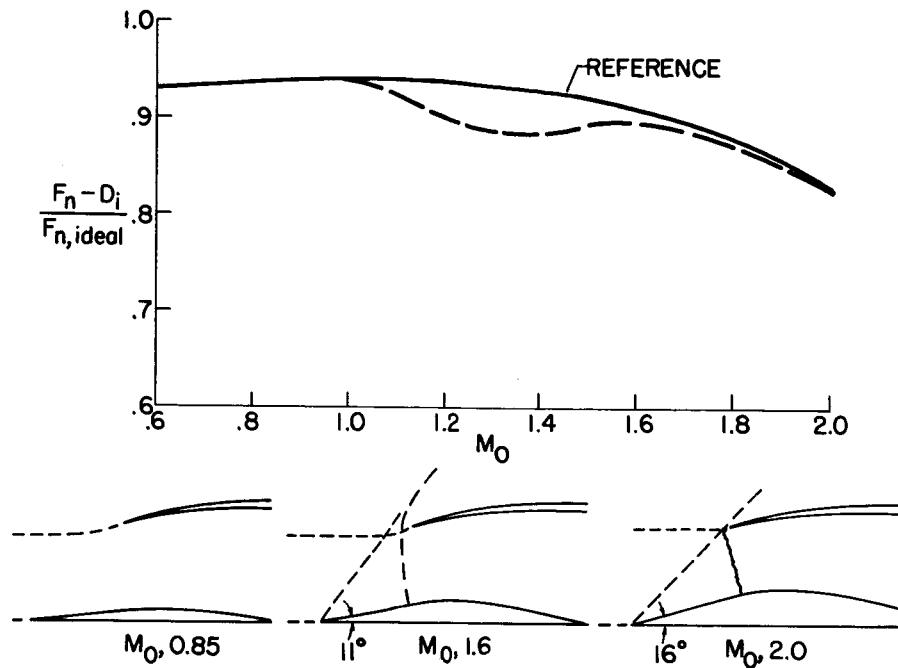


Figure 5

SPIKE INLETS

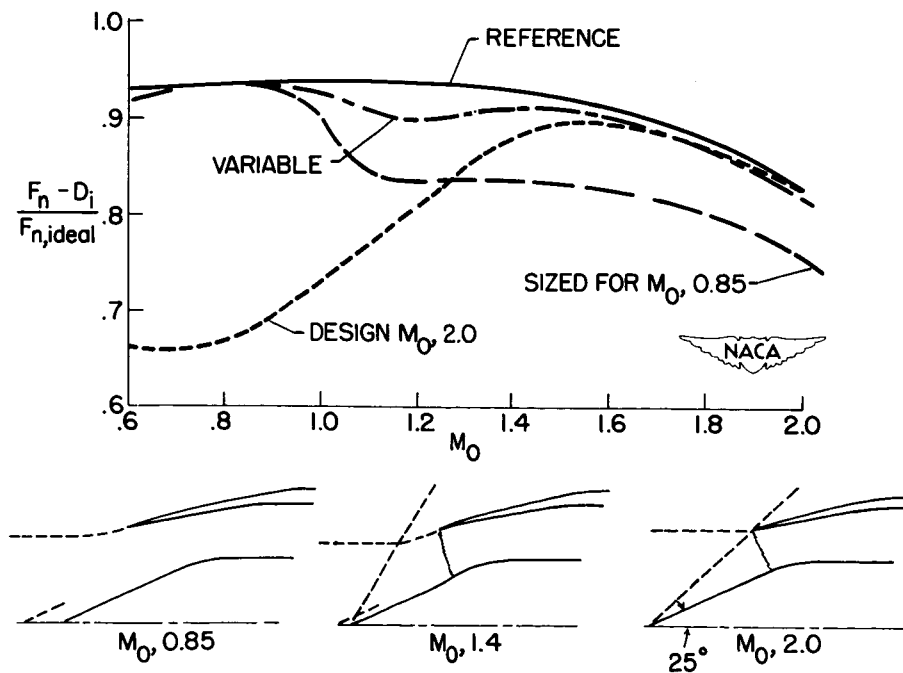


Figure 6



FIXED SPIKE (M_0 , 2.0) INLET

× INLET SIZED FOR $M_0, 0.85$
 < ASSUMED P_2/P_0

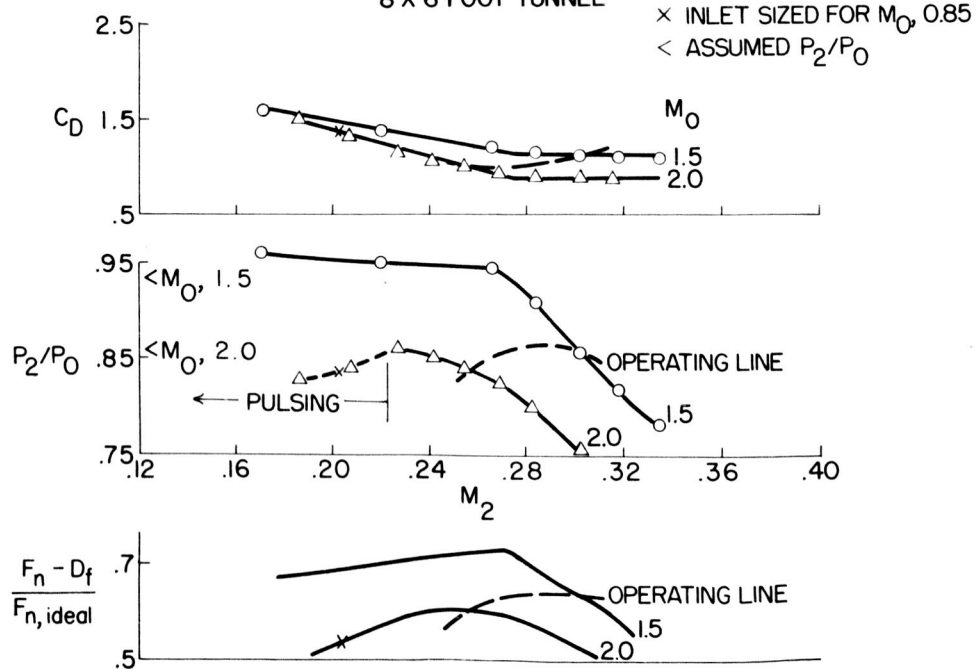


Figure 8

DECLASSIFIED

VARIABLE SPIKE INLET 8 X 6 FOOT TUNNEL

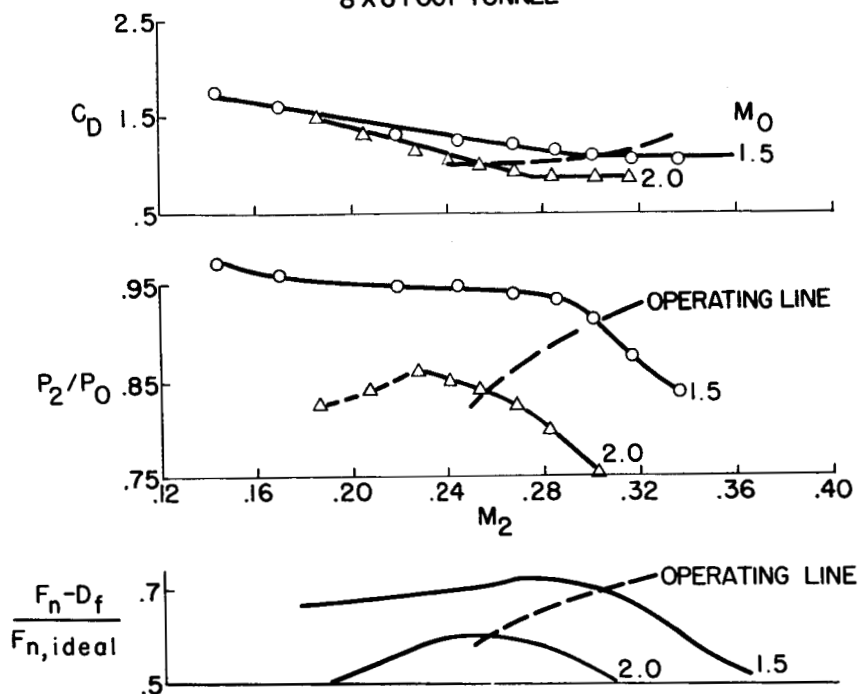


Figure 9

WEDGE INLETS 8 X 6 FOOT TUNNEL

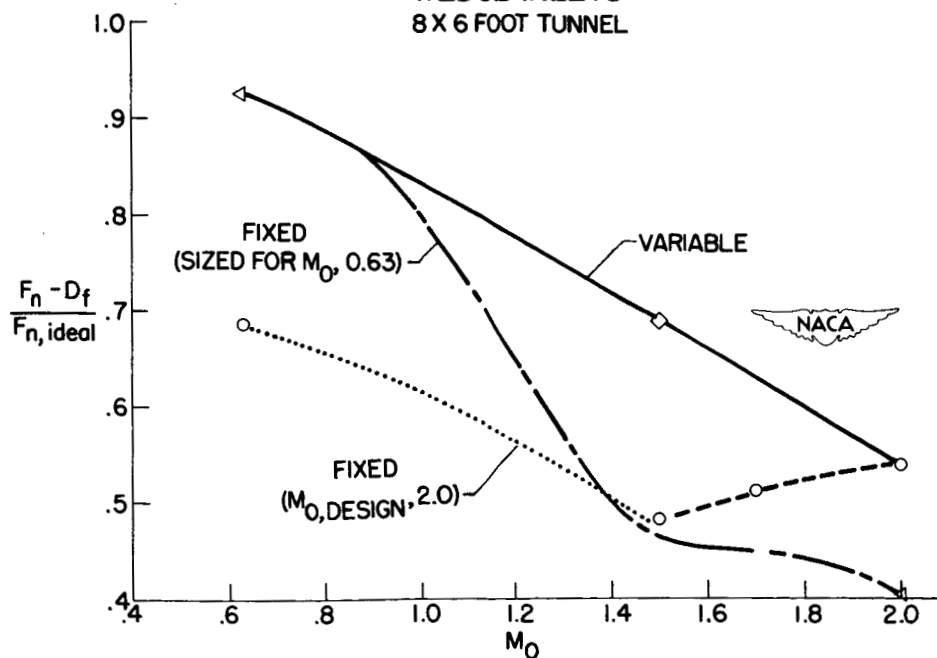
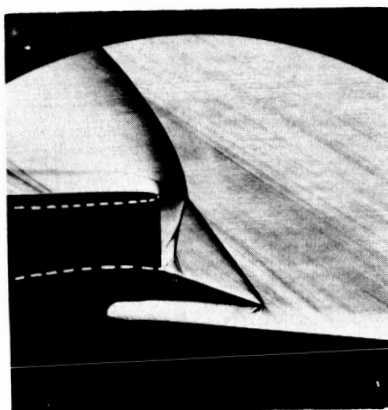


Figure 10

037100000000

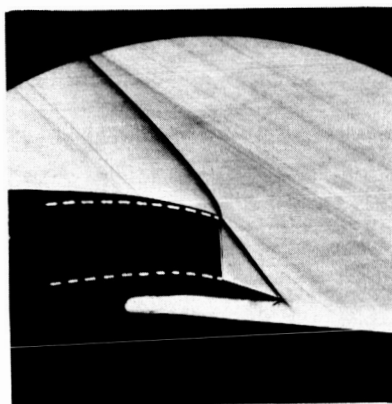
SCHLIEN PHOTOGRAPHS

$M_0, 2.0$



$$\frac{F_n - D_f}{F_{n, ideal}} = 0.54$$

BLUNT LIP INLET



$$\frac{F_n - D_f}{F_{n, ideal}} = 0.59$$

SHARP LIP INLET



Figure 11

WEDGE INLET AT $M_0, 0.0$; SEA LEVEL; DESIGN $M_0, 2.0$
WEDGE ANGLE, 0°

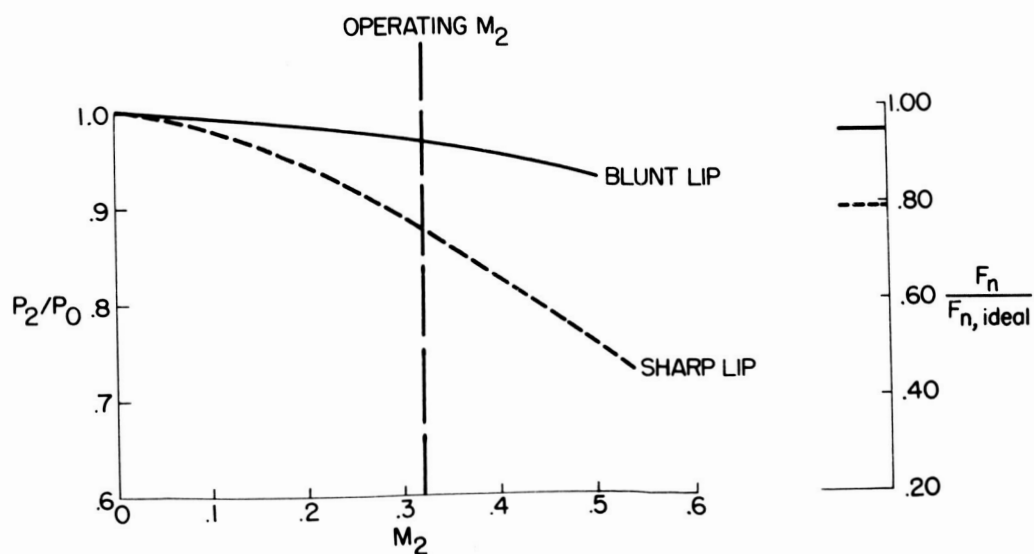


Figure 12

DO NOT REPLY

13. COMMENTS IIc

SECRET

13. - COMMENTS IIc

By Demarquis D. Wyatt

Now that some of the inlet problems of the turbojet engine installation have been considered, some of the exit problems will be examined. It is known that the engine jet must be discharged efficiently and, as was pointed out in the paper by Gabriel and the subsequent comments, a really efficient discharge nozzle cannot exist at supersonic flight speeds without some divergence or expansion to utilize the high nozzle pressure ratios in this flight regime. Secondly, unless transpiration cooling is applied, an efficient cooling-air system with a simple method of pumping the cooling airflow must be provided for afterburning engines. The quantities of cooling air that must be handled have been indicated by Mr. Fleming in the first section.

There may be many methods of solving these two exit problems of efficient nozzles and adequate cooling systems, and all methods should be explored. Recent research has indicated, however, that through the use of properly designed ejectors an adequate simultaneous solution may be achievable.

A preliminary research program conducted on small-scale cylindrical shroud ejectors and reported in reference 1 has given much physical insight into the behavior of ejectors suitable for high-speed aircraft. Figure 1 shows a typical performance curve for such an ejector without secondary airflow. The ejector pressure ratio, or total pressure in the annulus surrounding the primary nozzle divided by the ambient static pressure outside the exit, is plotted in figure 1 as a function of the nozzle pressure ratio, or total pressure in the nozzle divided by ambient static pressure.

For low nozzle pressure ratios the primary jet does not expand enough to intercept the shroud walls (left-hand sketch) and the ejector pressure ratio is wholly determined by viscous entrainment considerations. When the nozzle pressure ratio reaches a critical value which depends on the ejector diameter ratio (ratio of shroud diameter to nozzle diameter), the jet abruptly attaches to the shroud wall probably as a result of a Coanda effect (middle sketch). At the point of interception the jet is supersonic, and the ejector annulus surrounding the nozzle therefore becomes isolated from ambient conditions. The ejector pressure ratio becomes abruptly divorced from the viscous entrainment value and reaches a new value established by other considerations.

Since the expanding jet intercepts the shroud at a point relatively close to the primary nozzle exit, a low value of viscous shear on the jet boundary would be anticipated. If the shear is assumed negligible, the

SECRET




jet boundary is a constant-pressure boundary and the ejector pressure in the annulus should have the same value. If it is assumed that one-dimensional flow is reached in the shroud at a station near the point of jet interception, the static pressure across the shroud becomes equal to the pressure on the jet boundary and the ejector pressure. The equations of conservation of mass and momentum between the primary nozzle-exit plane and this one-dimensional shroud plane can then be solved to determine the Mach number at the one-dimensional plane and the ejector pressure. When the nozzle pressure ratio is increased above the critical value, the secondary pressure ratio remains a constant fraction of the nozzle pressure ratio as shown by both theoretical and experimental curves at high nozzle pressure ratios.

The critical value of nozzle pressure ratio is theoretically determined from the criterion that the shroud discharge pressure must be at least equal to the ambient pressure. The maximum pressure rise across the expanded flow (and therefore the minimum nozzle pressure ratio satisfying the postulated flow) will be obtained by a normal shock wave at the supersonic Mach number in the assumed one-dimensional shroud plane. The agreement between the theoretical critical nozzle pressure ratio so calculated and the experimental value is excellent for the configuration illustrated. Of course, the real flow in the shroud is more complicated than the assumed flow; in particular, the normal shock pressure rise can be obtained only by a series of branched shocks extending over a considerable finite distance. Therefore, for shorter shroud configurations the agreement between theoretical and experimental critical nozzle pressure ratios is not so good as for the case illustrated.

The ejector without secondary flow is of little interest in the practical airplane application; therefore, the characteristics of the same configuration with varying amounts of secondary flow (fig. 2) will next be examined. Included on figure 2 are the nonflow case from figure 1 and values of reduced-ejector-flow to nozzle-flow ratios of 4 and 12 percent (τ is the ratio of the ejector total temperature to the nozzle total temperature).

An increase in ejector pressure is observed for a given nozzle pressure as the weight flow through the ejector passage is allowed to increase. This phenomenon can be anticipated from physical reasoning. As the nozzle pressure ratio is increased, the primary jet expands. The expansion of the primary jet is now cushioned by the ejector airflow, however, and, if negligible mixing is assumed, the primary jet can never intercept the shroud walls. As the primary jet expands, the flow area available for the ejector flow decreases and the ejector flow accelerates. A critical nozzle pressure ratio is again reached, this time resulting in choking of the ejector flow at some station in the shroud, designated on figure 2 as the control plane.



DECLASSIFIED

The ejector pressure after the critical nozzle pressure ratio is reached is obviously not the pressure at the control plane but some higher pressure corresponding to the effusion between the primary nozzle exit plane and the control plane. If it is assumed that the primary jet expands isentropically and that there is no mixing between the two jets, the equations of conservation of mass and momentum can again be set up and solved between the primary nozzle exit plane and the control plane to yield the ejector pressure ratio. This pressure ratio is now a function of both the ejector diameter ratio and the corrected weight flow ratio.

Since the ejector flow is choked at the critical nozzle pressure ratio, further increases in nozzle pressure should result in the ejector pressure remaining at a constant fraction of the nozzle pressure. This expectation is confirmed by the experimental data, which are in good qualitative agreement with the theoretical variation predicted from the analysis outlined in the preceding paragraph. It has not yet been possible to predict the critical nozzle pressure ratio with secondary flow.

With this physical picture of the ejector performance, the thrust characteristics of the ejector configuration will be examined. For the cylindrical ejector, the gross thrust can be calculated across a momentum plane at the primary nozzle exit from experimentally determined pressures and weight flows. The thrusts so calculated for the configuration of figure 2 are presented in figure 3. The thrusts have been divided by the thrust from an ideal convergent-divergent nozzle handling the primary weight flow.

The general trend of ejector thrust is that anticipated from the airflow performance curves of figure 2. At low nozzle pressure ratios the thrust is reduced below the ideal value as a result of low annulus passage pressures induced by the viscous entrainment of the secondary fluid. When the primary jet either attaches to the shroud wall for the no-flow case, or chokes the secondary flow passage for operation with secondary flow, a discontinuous decrease in thrust accompanies the sudden decrease in annulus pressure. Increases in nozzle pressure above the critical value raise the general pressure level in the annulus and result in a steady rise in thrust.

It will be noted that at high nozzle pressure ratios or at high ejector air flows the gross thrust from the ejector configuration may approach or even exceed the ideal gross thrust from the isolated engine air flow. Part of this high gross thrust comes from the additional mass flow handled in the ejector, but much of the thrust arises from the confinement of the primary jet by the ejector shroud and the resultant physical analogy of the ejector to a convergent-divergent nozzle.

0371030

Inasmuch as the ejector performance is very dependent on the diameter ratio and length of shroud, the air flow and thrust characteristics of different ejector designs will show considerable variation. Since part of the gross thrust is obtained as a result of ejector air flow, the net thrust remaining after consideration of the free-stream momentum term will be very dependent on the ejector design geometry and the source of the secondary flow. An extensive experimental investigation of the air-flow and thrust characteristics of ejector having made variations in design details is currently being conducted at this laboratory. The results of this program are discussed in the next paper in relation to supersonic airplane performance.

REFERENCE

1. Kochendorfer, Fred D., and Rousso, Morris D.: Performance Characteristics of Aircraft Cooling Ejector Having Short Cylindrical Shrouds. NACA RM 51E01, 1951.

DECLASSIFIED

2235-13

EJECTOR WITHOUT SECONDARY FLOW

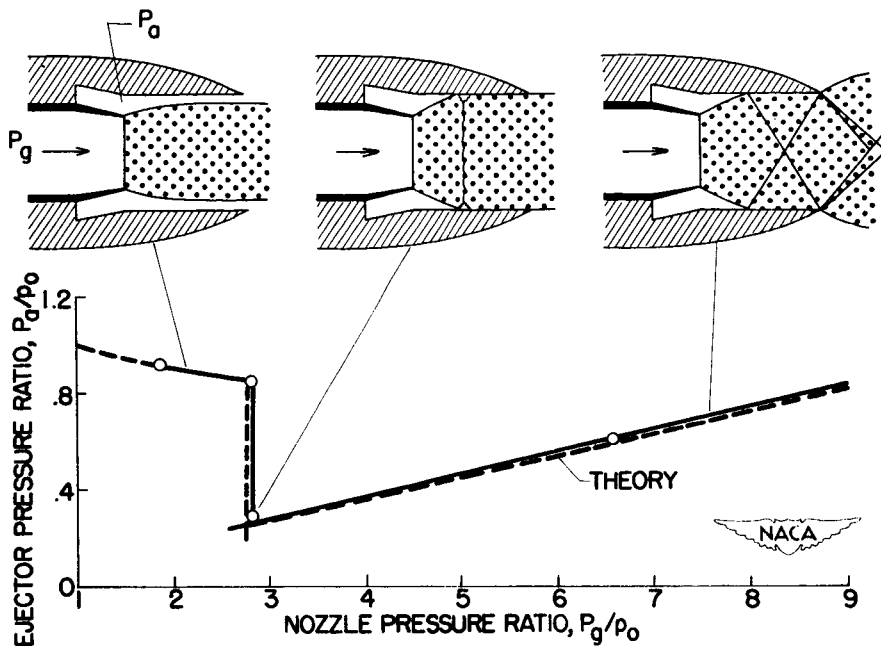


Figure 1

EJECTOR WITH SECONDARY FLOW

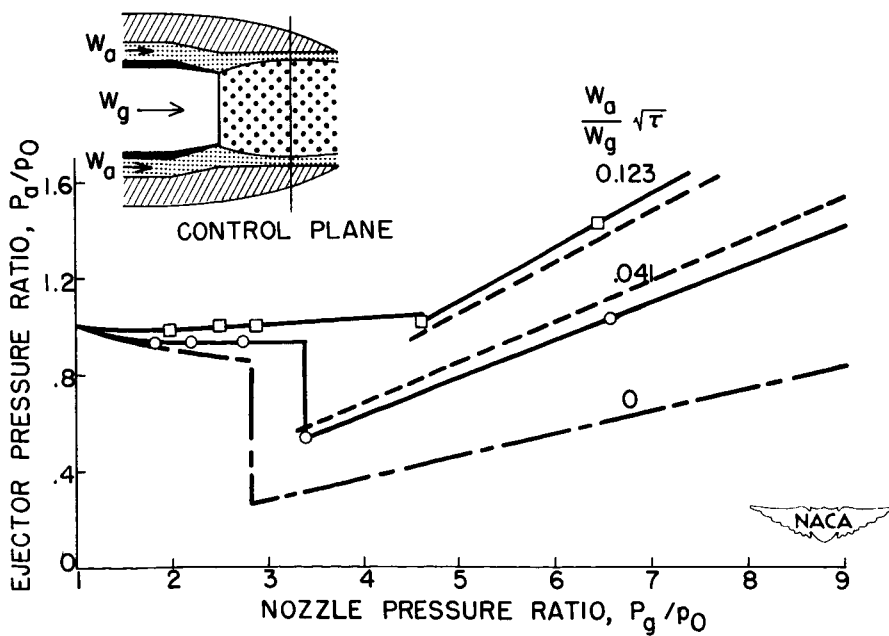


Figure 2

031710-030

2235-13

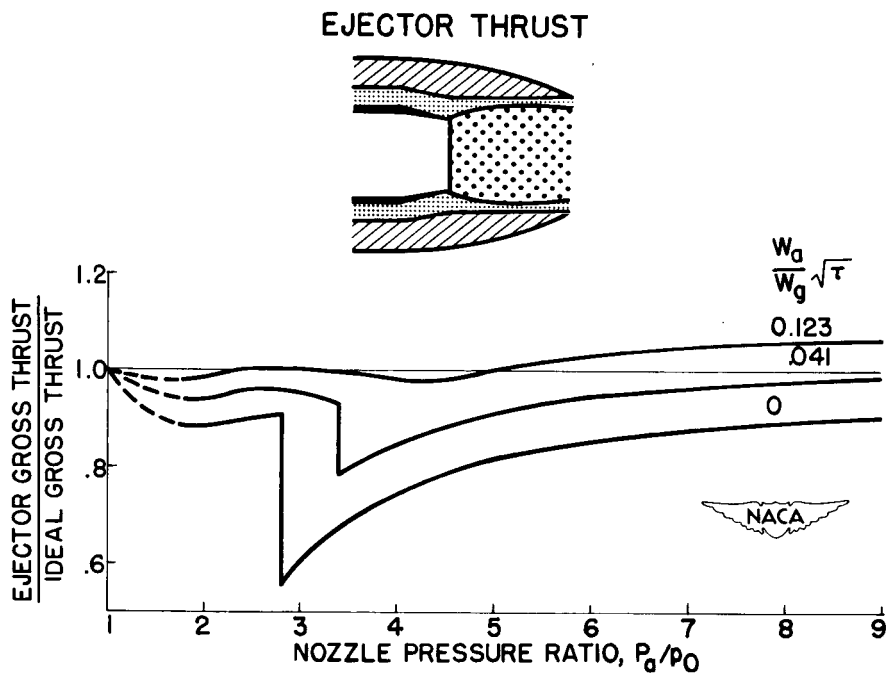


Figure 3

DECLASSIFIED

14. THRUST CHARACTERISTICS OF AN EJECTOR PUMP

By H. Dean Wilsted

[REDACTED]

SECRET

14. THRUST CHARACTERISTICS OF AN EJECTOR PUMP

By H. Dean Wilsted

INTRODUCTION

An experimental investigation of ejector performance was conducted at the NACA Lewis laboratory. Sufficient data are available at present to allow a preliminary examination of the ejector thrust problem. The purpose of this paper is to discuss the penalties and gains in thrust obtainable with an ejector installation.

EXPERIMENTAL APPARATUS

The thrust and pumping characteristics were evaluated on the research apparatus schematically shown in figure 1. Primary air can be supplied to the primary nozzle of the ejector through the internal piping system, and secondary air, through the annulus surrounding this pipe. The ejector, consisting of the primary nozzle and the shroud, may be discharged either to atmospheric pressures or into an altitude chamber. The entire rig is hinged as a pendulum, and the system is made flexible by metal bellows connecting the stationary piping and movable piping on both the secondary and primary flow systems. Ejector thrust is measured by a thrust device located on the center line of the ejector. Pressure instrumentation and temperature instrumentation are used to measure pressures and temperatures in both the secondary and primary streams, just upstream of the primary nozzle. For all configurations investigated, the primary nozzle exit diameter was 4 inches.

RANGE OF EXPERIMENTAL VARIABLES

The experimental investigation being conducted on this apparatus covers a range of ejector configurations and operating conditions. The range of these variables, together with nomenclature and symbols, is presented in figure 2. A sketch of an ejector consisting of the primary nozzle and the ejector shroud is schematically shown at the top of the figure. The ratio of shroud exit diameter D_s to nozzle exit diameter D_p is being varied from about 1.05 to 1.60. The ratio of spacing between the nozzle exit and shroud exit, denoted by S , to the nozzle exit diameter D_p is being varied from 0.4 to 2.0. The nozzle pressure ratio P_g/P_0 , is being varied from 1.5 to 10, and the secondary pressure ratio, or ejector pressure ratio P_a/P_0 , from the minimum that



the ejector will pump (values as low as 0.4 have been obtained) to a maximum of 4.0. Now these variables produce ratios of cooling-air flow to nozzle-air flow from 0 to about 1.0. These operating conditions have been extended to increase the usefulness of the data of reference 1.

PUMPING CHARACTERISTICS

An essential requirement of all ejectors is that they provide sufficient mass flow for cooling in any particular installation. The pumping characteristics of all ejectors are similar, and a typical map is shown in figure 3. Ejector pressure ratio P_a/p_0 is plotted against nozzle pressure ratio P_g/p_0 for constant values of weight-flow ratio. The weight-flow ratio has been corrected to a ratio of cooling-air to primary nozzle-air temperatures (T_g/T_a) of 4.0 by the method described in reference 2. The marked similarity between the performance of the conical ejector and the cylindrical ejector described in the introductory comments can be seen. In the region where the jet has not yet attached to the shroud wall (A to B), there is little effect on the shroud pressure. At point C where the jet attaches itself to the shroud wall, there is a large decrease in pressure within the shroud, or an over-expansion of the gases to a pressure below ambient pressure. An increase in primary pressure ratio beyond the choke point, of course, produces a linear rise in shroud pressure with increasing nozzle pressure.

THRUST CHARACTERISTICS

Note the similarity of the pumping characteristics shown in figure 3 to the thrust characteristics shown in figure 4. The ratio of ejector gross thrust to gross thrust is plotted against nozzle pressure ratio, and again curves of constant weight-flow ratio corrected to a temperature ratio of 4.0 are shown. The same characteristics are shown as were shown by the pumping characteristic curve. With an increase in weight-flow ratio, there is a large increase in the gross thrust ratio, which is much larger than would be expected from the small increase in mass flow alone.

EFFECT OF SHROUD DIAMETER ON THRUST CHARACTERISTICS

The data of figure 4 are for a given configuration. Figure 5 shows what happens when the shroud exit diameter is changed. The ratio of ejector gross thrust to nozzle gross thrust is plotted against nozzle pressure ratio. Data are shown for several values of the ratio of shroud exit diameter to nozzle exit diameter. If it is assumed that the ejector is without secondary cooling air flow and the nozzle pressure ratio is just sufficient to attach the jet to the shroud wall, then



suppose the ejector shroud is moved outward, that is, its diameter is increased. The jet would detach itself and a larger pressure ratio would be required to again make the jet attach to the wall. This change is shown in figure 5, for as the diameter ratio is increased, there is a progressive increase in the nozzle pressure ratio at which the attachment occurs. For the larger diameter ratio ejectors, it is expected that there would be a greater expansion within the shroud, reducing the internal pressure. This phenomenon is also shown by these data, for as the diameter ratio is increased, the thrust ratio progressively decreases, indicating a greater overexpansion of the gases within the shroud. These data are for the case without secondary flow. If data had been plotted for any low constant weight-flow ratio, the curves would have been essentially parallel to those shown. These data are also for approximately optimum spacing conditions; that is, as the shroud diameter was increased, the spacing between the nozzle exit and the shroud exit was also increased.

EFFECT OF SPACING ON NET THRUST

Obviously, the ejector performance of interest is that produced under flight conditions, that is, this optimization of spacing must be examined on a net-thrust basis taking into account the inlet momentum of engine air and cooling air. The inlet momentum and the cooling-air requirements are both functions of the flight plan. The flight characteristics of various ejectors in a given flight plan and in a given cooling installation were therefore investigated. It has been shown that an interceptor-type airplane, to obtain maximum combat time, would require an afterburner operating to temperatures as great as 3500° R. Assuming use of a 3500° R afterburner and the cooling requirements previously presented shows that about 4 percent as much air is required for cooling as is consumed by the engine itself. Each ejector considered must then supply this minimum flow for all operating conditions. Generally, the ejector will supply more air than will be needed and the duct losses and ejector pumping characteristics must be matched. When this match is accomplished and the gross thrust values are corrected for inlet momentum of engine air and cooling air, results such as those in figure 6 are obtained.

In this figure is plotted the ratio of ejector net thrust to convergent nozzle net thrust. Note that these are net thrust values and not gross thrust values. The net-thrust ratio is plotted against spacing ratio; that is, the distance between the nozzle exit and the shroud exit is progressively increased. This configuration had a diameter ratio of 1.1. For spacing ratios below or above the ratios giving maximum thrust ratio, there is a large loss in thrust. Data are shown for flight Mach number M_0 of 0, 0.9, and 1.4. For this range of operating conditions, the optimum spacing ratio, as indicated by the dashed curve, did




not vary greatly with the changing flight conditions. It would be possible to obtain almost optimum conditions with a fixed configuration ejector. For example, at a spacing ratio of 0.9 and starting at take-off conditions, the thrust would drop slightly to 0.9 flight Mach number and beyond that would increase with flight Mach number. At a flight Mach number of 1.4, a 6-percent increase in thrust over that obtainable from a convergent nozzle is indicated. This improvement in thrust ratio is the result of a more nearly isentropic expansion of the primary gases within the ejector shroud than that possible from the underexpanded convergent nozzle.

These data are for a small diameter ratio. Data are shown for the large diameter ratios in figure 7, where the diameter ratio is 1.6 and the thrust ratio is again plotted against spacing ratio. The flight Mach numbers shown are 0, 0.5, and 0.9 at sea-level flight conditions and 0.8, 1.4, and 2.0 at 35,000-foot-altitude flight conditions. The optimum or peak thrust value, that is, the optimum spacing ratio, varies over a wide range with the changing operating conditions. This variation might be associated with larger weight flows with changing spacing ratio, but it was found that for all operating conditions except the 0 and 0.5 flight Mach numbers the cooling duct was choked at the exit and the cooling-air-flow ratio was therefore constant with changing spacing ratio. There can be, then, no correlation between the optimum spacing ratio and the weight-flow ratio. It was actually found that this optimum spacing again is associated with the pressures in the ejector shroud. For example, at a spacing ratio of 2.0, as the flight Mach number is increased there is a reduction in net thrust ratio which is associated with the overexpansion of the jet. At a Mach number of 1.4, the thrust ratio is 0.75, showing a 25-percent loss in net thrust. As the flight Mach number is increased to 2.0, there is a large increase in thrust over that obtained at a Mach number of 1.4. The operating point has continued beyond the overexpansion range in the ejector performance map and into a range where the nozzle of the ejector is giving a more nearly isentropic expansion of the primary gas stream. The primary factors in ejector thrust performance have been shown to be: (1) the magnitude of the overexpansion in the shroud at the lower nozzle pressure ratios and (2) the ability of the configuration to approach an isentropic expansion at the higher pressure ratios.

EFFECT OF DIAMETER RATIO ON NET THRUST

The effect of diameter ratio under flight conditions can be investigated by using the optimum spacings such as those obtained from a plot of the type shown in figure 6. Data showing the effect of diameter ratio on net thrust are shown in figure 8. Data are shown for flight Mach numbers of 0.8, 1.4, and 2.0. The maximum thrust values are obtained at ejector diameter ratios that are rather small. As yet, there are no data

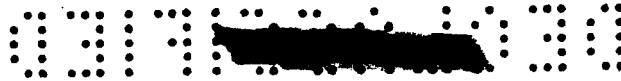


for diameter ratios below 1.1, but for the 1.4 flight Mach number, a peak in this curve can be expected at a diameter ratio between 1.0 and 1.1. This peak will occur because as the diameter is decreased the shroud is also retracted to maintain optimum spacing, and therefore the thrust ratio would approach unity as the diameter ratio neared unity. Also, for the higher flight Mach numbers where the pressure ratios are much higher, a peak in the curve would occur at some higher ejector diameter ratio in order to accomplish the complete expansion of the gases within the shroud. If advantage were taken of such a change in peak thrust values, it would be necessary to have a variable-area ejector. This may not be true and it remains to find what happens when the data are obtained in this region.

At a Mach number of 2, thrust ratios as high as 1.08 or an 8-percent improvement in thrust over that available from a convergent nozzle has been reached. This value is the highest obtained in this analysis. It is possible, however, that higher values may be obtained when additional data are available. With regard to maximum or peak values of thrust, the importance of using a supersonic nozzle on the supersonic airplane received considerable emphasis. The variable-area ejector may be a partial answer to the problem of a variable-area supersonic nozzle.

VARIABLE-SPACING EJECTOR

Obviously there are many variations in ejector configuration that can be made. One is the variable-spacing ejector. In figure 9 is shown net-thrust ratio plotted against flight Mach number. The data of this figure are for a diameter ratio of 1.1 with optimum spacing ratio. Also shown is the range over which it is possible to cool the afterburner when taking air from the boundary-layer air scoop and using only the ram that is there available to pump the air through the ducting system. Obviously you would expect some loss in thrust from the losses in the inlet diffuser and the losses in ducting. However, because of the heating in the cooling duct, there is sufficient increase in the momentum to just about offset the losses in the ducting system. With a variable-spacing ejector, it would therefore be possible to operate with the ejector to a Mach number of 0.3 where the boundary-layer air in itself can provide the necessary cooling. At this point, the ejector shroud could be retracted and the cooling air supplied by the boundary-layer air scoop ram energy. In the region where the ejector can provide a higher thrust (above a flight Mach number of 0.9), the ejector shroud can again be used to obtain the highest possible values of net-thrust ratio. The losses associated with this method of operation would be on the order of 3 or 4 percent below 0.3 flight Mach number, and gains as high as 3 or 10 percent may be possible at a flight Mach number of 2.0. Possible advantages in flight are thus seen for the variable spacing



ejector. The type of ejector to be used in any given installation, that is, whether it should be a fixed or a variable configuration, will have to be based on an analysis such as has been described herein. Of course, additional performance data are essential. These data are being obtained as rapidly as possible.

SUMMARY

It has been shown that thrusts greater than the thrust obtainable from convergent nozzles can be achieved with ejectors. These gains are obtained from a more nearly isentropic expansion of the primary nozzle gases than is possible with the underexpanded convergent nozzle. At a flight Mach number of 2, improvements over the net thrust obtainable from a convergent nozzle should exceed 8 percent.

In order to obtain the greatest thrust at supersonic flight speeds and at the same time keep the overexpansion losses to a minimum at subsonic speeds, ejectors having small diameter ratios should be used.

REFERENCES

1. Huddleston, S. C., Wilsted, H. D., and Ellis, C. W.: Performance of Several Air Ejectors with Conical Mixing Sections and Small Secondary Flow Rates. NACA RM E8D23, 1948.
2. Wilsted, H. D., Huddleston, S. C., and Ellis, C. W.: Effect of Temperature on Performance of Several Ejector Configurations. NACA RM E9E16, 1949.



REF ID: A66000

EJECTOR EXPERIMENTAL APPARATUS

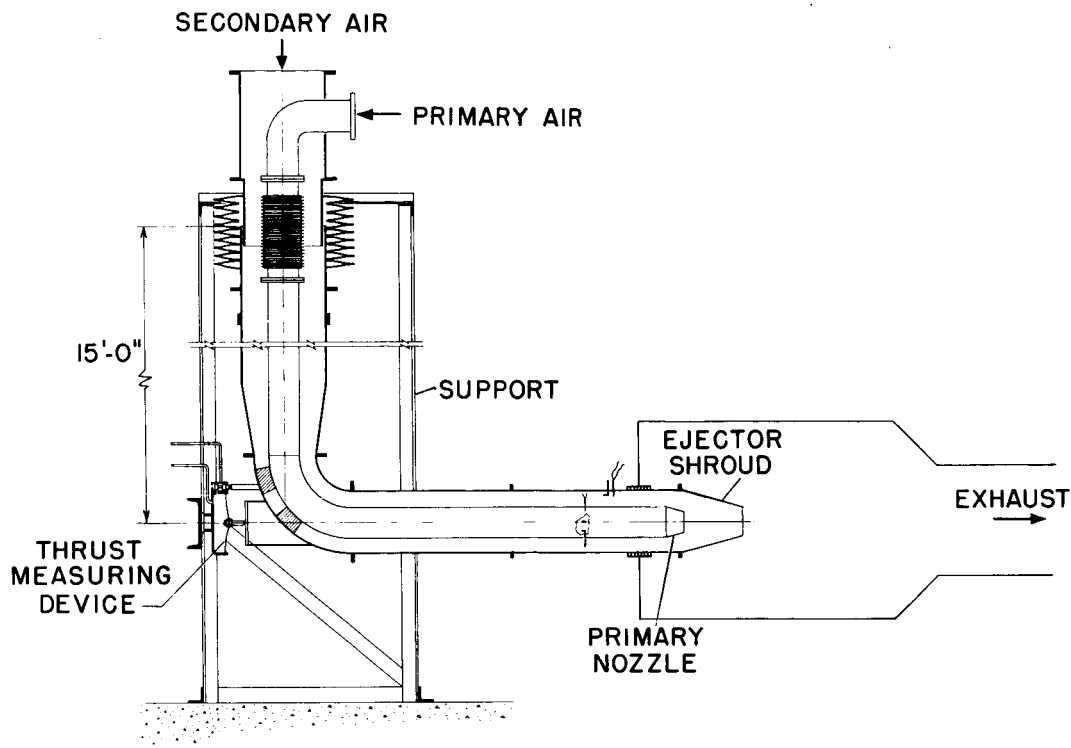
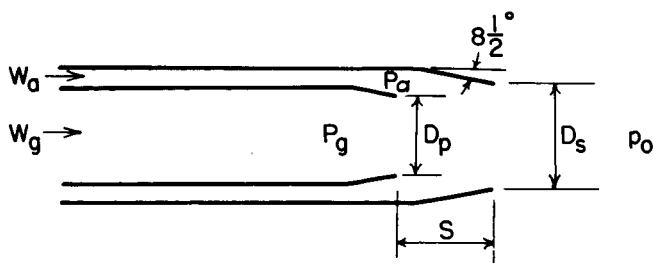


Figure 1

RANGE OF EXPERIMENTAL VARIABLES



SHROUD EXIT DIAMETER, $\frac{D_s}{D_p}$	NOZZLE EXIT DIAMETER	1.05 TO 1.60
SPACING, $\frac{S}{D_p}$	NOZZLE EXIT DIAMETER	0.4 TO 2.0
NOZZLE PRESSURE RATIO, $\frac{P_g}{P_0}$		1.5 TO 10.0
EJECTOR PRESSURE RATIO, $\frac{P_a}{P_0}$		MIN. (0.4) TO 4.0
COOLING-AIR FLOW, $\frac{W_a}{W_g}$	NOZZLE-AIR FLOW	0 TO 1.0



Figure 2

03713C [REDACTED] 34

EJECTOR PUMPING CHARACTERISTICS

(W_a/W_g CORRECTED TO $T_a/T_g = 4.0$)

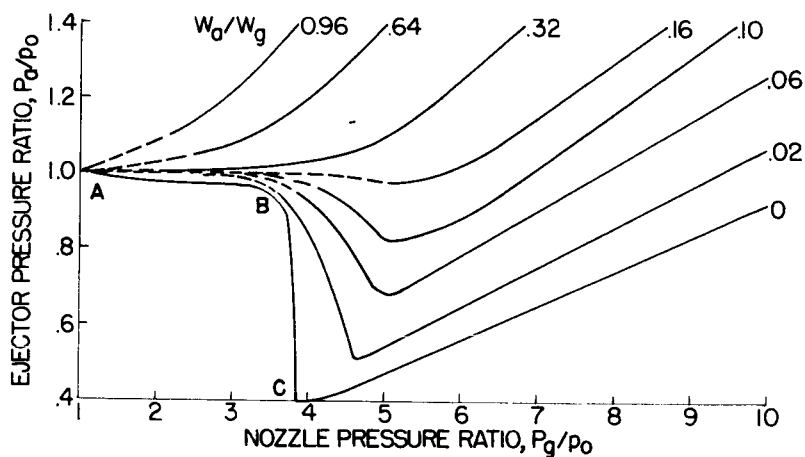


Figure 3

EJECTOR GROSS THRUST CHARACTERISTICS

(W_a/W_g CORRECTED TO $T_a/T_g = 4.0$)

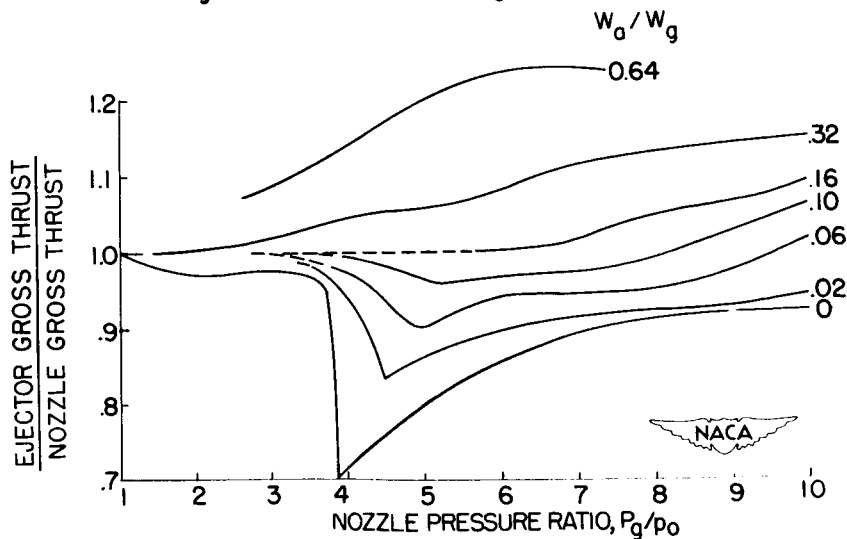


Figure 4

[REDACTED]

REF ID: A68018

EFFECT OF SHROUD DIAMETER ON THRUST CHARACTERISTICS

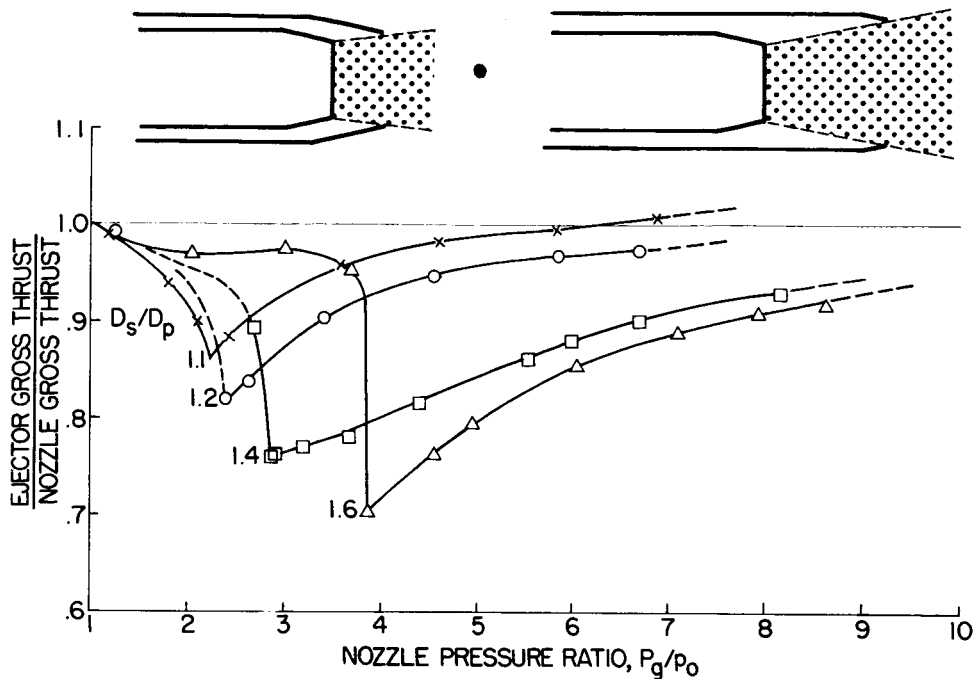


Figure 5

EFFECT OF SPACING ON NET THRUST

$D_s/D_p, 1.1$

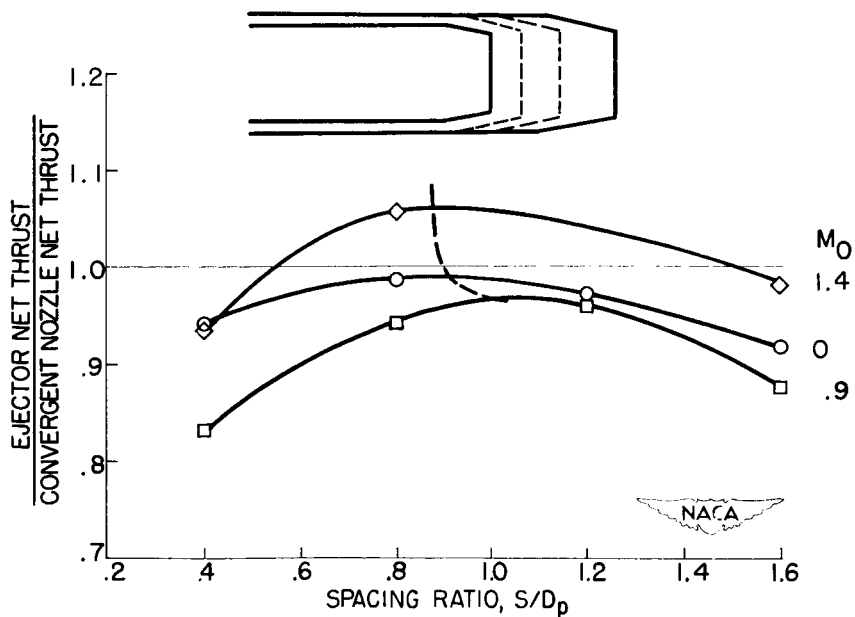


Figure 6

CONFIDENTIAL

EFFECT OF SPACING ON NET THRUST

$D_s/D_p, 1.6$

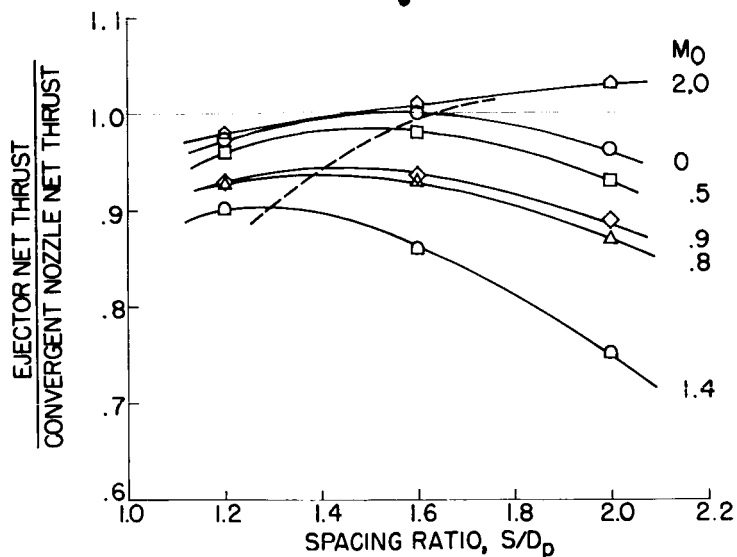


Figure 7

EFFECT OF DIAMETER RATIO ON NET THRUST (OPTIMUM SPACING)

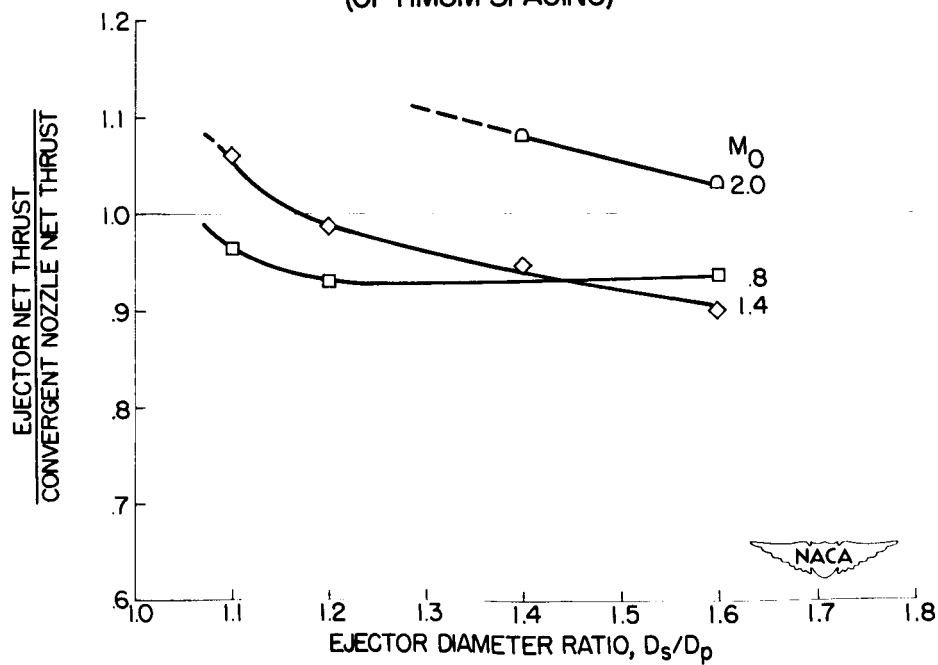


Figure 8

NACA

DECLASSIFIED

USE OF VARIABLE-SPACING EJECTOR $D_s/D_p, 1.1$

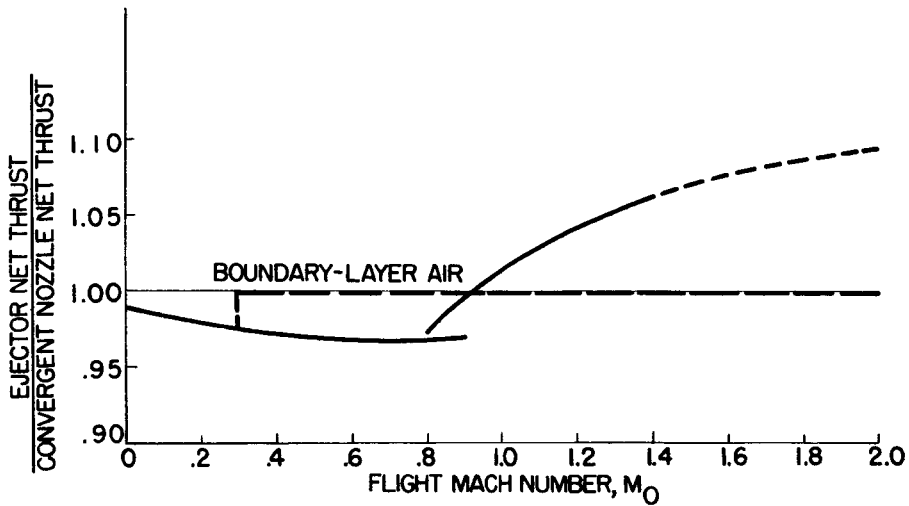


Figure 9